This is to certify that the
thesis entitled

FUNCTIONALIZED SURFACES FOR SELECTIVE CAPTURE OF BIOMOLECULES

presented by

Elizabeth A. Igrisan

has been accepted towards fulfillment
of the requirements for the

M.S. degree in Chemistry

Major Professor's Signature

08/21/2009

Date

FUNCTIONALIZED SURFACES FOR SELECTIVE CAPTURE OF BIOMOLECULES

By

Elizabeth A. Igrisan

A THESIS

Submitted to
Michigan State University
in partial fulfillment of the requirements
for the degree of

MASTER OF SCIENCE

Chemistry

2009

ABSTRACT

FUNCTIONALIZED SURFACES FOR SELECTIVE CAPTURE OF BIOMOLECULES

By

Elizabeth A. Igrisan

This thesis describes the synthesis of several functional surfaces for isolation of phosphopeptides, glutathione-S-transferase (GST), and glycopeptides. Gold surfaces modified with ZrO_2/poly(styrene sulfonate) films selectively capture phosphorylated peptides from an unpurified protein digest. Substrates prepared by heating an array of TiO_2 nanoparticles also enrich phosphopeptides, and these plates selectively recover ~70% of a synthetic H_5 phosphopeptide (125 fmol) in the presence of 1 pmol of nonphosphopeptide mixture. On-plate capture is attractive for high recoveries prior to analyses by matrix-assisted laser desorption/ionization mass spectrometry (MALDI-MS).

In efforts to create surfaces that bind GST-tagged proteins, gold substrates modified with poly(acrylic acid) or poly(2-hydroxyethyl methacrylate) (PHEMA) brushes were derivatized with reduced glutathione in a variety of methods. These polymer brushes should have much higher binding capacities than monolayer films. Unfortunately the immobilized glutathione did not bind GST, perhaps because of residual glutathione in the sample. PHEMA brushes were also functionalized with 3-aminophenylboronic acid (APBA) to create surfaces that capture glycopeptides. The APBA-modified films bind small amounts of simple *cis*-diol-containing carbohydrates, and initial studies show that glycopeptide enrichment on these polymer brushes improves the MALDI-MS signal-to-noise ratio for some glycopeptides present in a digest of horseradish peroxidase. However, signals are weak and nonspecific binding occurs.

TABLE OF CONTENTS

LIST OF TABLES

Chapter Two: Metal Oxide-Modified Plates for Analysis of Phosphopeptides by MALDI-MS

Chapter Four: Enrichment of Glycopeptides Using Aminophenylboronic Acid-Derivatized Polymer Brushes

LIST OF FIGURES

Chapter One: Introduction

Chapter Two: Metal Oxide-Modified Plates for Analysis of Phosphopeptides by MALDI-MS

Chapter Four: Enrichment of Glycopeptides Using Aminophenylboronic Acid-Derivatized Polymer Brushes

LIST OF ABBREVIATIONS

ACN..... acetonitrile

ADP..... adenosine diphosphate

APBA.....3-aminophenylboronic acid

ATP.....adenosine triphosphate

ATRP..... atom transfer radical polymerization

BAC..... bromoacetyl chloride

BIBB..... bromoisobutyryl bromide

bpy.....2,2'-bipyridine

BSA.....bovine serum albumin

α-CHCA.....α-cyano-4-hydroxycinnamic acid

CID.....collision-induced dissociation

Con A.....concanvalin A

DHB.....2,5-dihydroxybenzoic acid

D/I..... desorption/ionization

DMAP.....4-dimethylaminopyridine

DMF.....*N*,*N*'-dimethylformamide

DTT.....dithiothreitol

EDC..... *N*-(3-dimethylaminopropyl)-*N*'-ethylcarbodiimide hydrochloride

ER..... endoplasmic reticulum

ESI..... electrospray ionization

FAB.....fast atom bombardment

FD..... field desorption

FTIR..... Fourier transform infrared

GalNAc..... *N*-galactosamine

GlcNAc..... *N*-glucosamine

GSH..... reduced glutathione

GST..... Glutathione-S-Transferase

IDA..... iminodiacetate

IMAC..... immobilized metal affinity chromatography

LbL..... layer-by-layer

LD..... laser desorption

LIT..... linear ion trap

MALDI..... matrix-assisted laser desorption/ionization

MOAC..... metal oxide affinity chromatography

MPA..... mercaptopropionic acid

MS..... mass spectrometry

MS/MS..... tandem mass spectrometry

MUA..... mercaptoundecanoic acid

MUD..... mercaptoundecanol

m/z..... mass-to-charge ratio

ND..... nanodiamond

NHS..... *N*-hydroxysuccinimide

NP..... nanoparticle

NTA..... nitrilotriacetic acid

PAA..... poly(acrylic acid)

PAH..... poly(allylamine hydrochloride)

PDMS.....polydimethylsiloxane

PEM..... polyelectrolyte multilayer

PHEMA..... poly(2-hydroxyethyl methacrylate)

phos b.....phosphorylase b

PNGase F..... protein-*N*-glycanase F

PSS.....poly(sodium 4-styrene sulfonate)

PTBA..... poly(*tert*-butyl acrylate)

PTM..... post-translational modification

QIT.....quadrupole ion trap

RNase B..... ribonuclease B

SA..... succinic anhydride

SALDI.....surface-assisted laser/desorption ionization

SAM.....self-assembled monolayer

SEM..... scanning electron microscopy

S/N..... signal-to-noise ratio

tBOC..... *t*-butyl-dicarbonate

TEA.....triethylamine

TFA.....trifluoroacetic acid

THAP..... 2',4',6'-trihydroxyacetophenone

TOF.....time-of-flight

WGA.....wheat germ agglutinin

Chapter One: Introduction

1.1 Outline

The focus of this thesis is the development of functional surfaces for selective capture and enrichment of analytes, specifically digested proteins with post-translational modifications (PTMs), prior to their analysis by matrix-assisted laser desorption/ionization mass spectrometry (MALDI-MS). Figure 1.1 demonstrates the enrichment process. To put the research in perspective, this chapter first discusses surface modifications and some of their applications (section 1.2). Subsequent sections describe the significance of two PTMs of proteins, phosphorylation and glycosylation, as well as the primary method for their characterization, MS (sections 1.3 and 1.4). Although MS is the leading technique for phosphoprotein and glycoprotein analysis, challenges in the detection of proteins or peptides with PTMs have led to the development of methods for enriching these species prior to analysis. Section 1.5 provides an overview of several enrichment techniques for phosphopeptides and glycopeptides. The research discussed in this thesis primarily focuses on the modification of MALDI sample plates to provide rapid, high-throughput on-plate enrichment with minimal sample loss and sample handling. Section 1.6 gives an overview of this research.

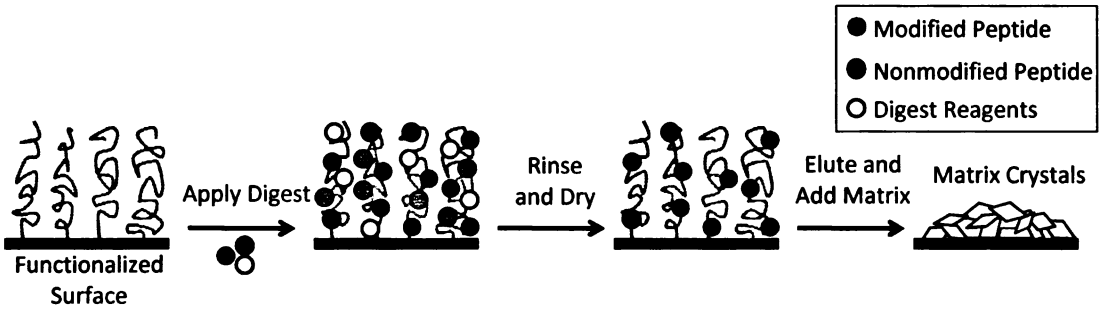

Figure 1.1: Schematic diagram of the enrichment of modified peptides from a protein digest spotted on a functionalized surface. Nonmodified peptides and digest reagents are rinsed away, and bound modified peptides are eluted and allowed to crystallize with a matrix. The analyte can be analyzed directly on the plate using MALDI-MS. Figure adapted from Dunn et al.[1]

1.2 Surface Modification

1.2.1 Polymer Grafting

Modification of solid supports with thin organic films allows tailoring of surfaces for a variety of applications, including protein isolation. One common modification involves grafting polymer brushes on a solid substrate, and either chemisorption or physisorption can link the brushes to the surface. The polymer films described in this thesis contain a covalent linkage to an alkanethiol self-assembled monolayer (SAM), which is adsorbed to a gold-coated substrate. In general, polymer films can be "grafted to" or "grafted from" a surface (Figure 1.2), and this thesis includes both forms of grafting. Grafting of poly(acrylic acid) (PAA) films to a gold-coated surface (Chapter 3) occurs by covalently linking polymer chains to a surface. However, the "grafting to" method typically yields thinner films with lower chain densities than the "grafting from" strategy. This is due to limited access to reactive sites after grafting even a low density of chains to the surface. The chains lie predominantly parallel to the substrate, thus covering sites for further grafting. As an alternative, grafting of poly(2-hydroxyethyl

methacrylate) (PHEMA) can occur by growth of the polymer chains from initiators immobilized on a gold-coated surface (Chapters 3 and 4). This grafting method allows thicker films to form because small monomers can continue to diffuse to the reactive sites as the polymer grows. In "good" solvents, the growing polymer chains also swell, which facilitates diffusion of small molecules in the film. Therefore, polymer films can be easily derivatized for a variety of applications including the rapid capture of biomolecules.

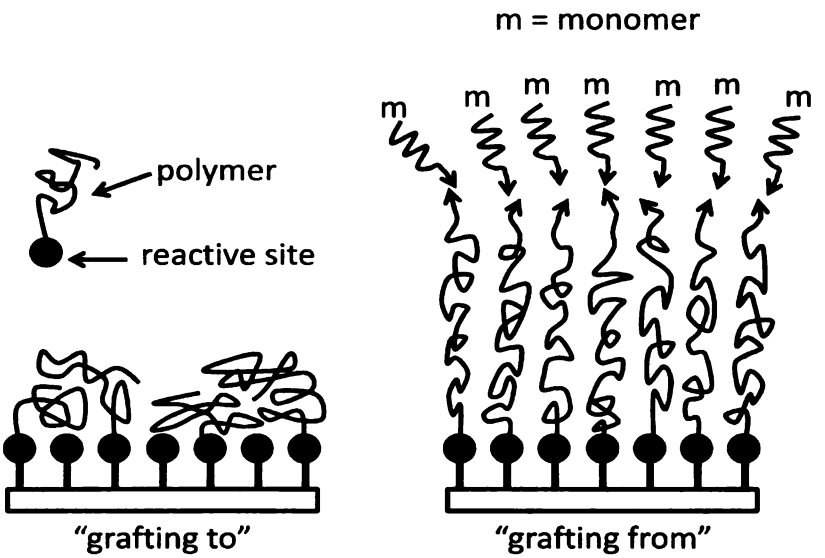

Figure 1.2: Schematic diagram comparing "grafting to" versus "grafting from" methods for growing films on surfaces. Figure adapted from Bruening et al.[2]

Many polymerization techniques are applicable to growth of polymers from surfaces, including free radical polymerization, anionic polymerization, cationic polymerization, controlled radical polymerization, and atom transfer radical polymerization (ATRP). This thesis focuses on the use of surface-initiated ATRP to rapidly grow PHEMA films from gold-coated substrates. Derivatization of the brushes with reduced glutathione or aminophenylboronic acid (APBA) aims at developing

surfaces for the capture of glutathione-s-transferase (GST)-tagged proteins or glycopeptides, respectively.

Matyjaszewski and Sawamoto introduced ATRP in 1995.[3,4] This technique is a particularly appealing form of polymerization due to its controlled growth of polymers that results in a narrow molecular weight distribution.[5] Surface initiated ATRP often generates uniform brushes, and the use of commercially available initiators and transition metal catalysts is also attractive.[6] The controlled growth of polymer brushes in ATRP occurs because the rate of activation of dormant halogen-terminated chain ends by the oxidation of copper (I) is significantly slower than the reverse reaction (Figure 1.3). This results in a low radical concentration that favors polymerization over termination and gives a fairly constant rate of polymerization.[5]

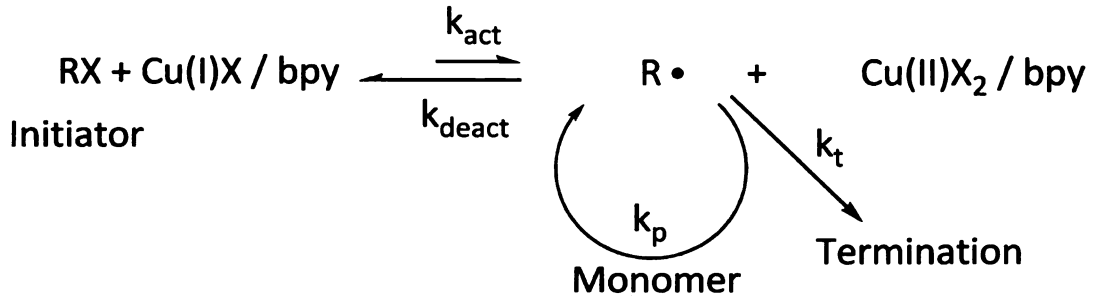

Figure 1.3: Scheme of the mechanism for transition metal-catalyzed ATRP, adapted from Matyjaszewski.[5] k_{act}, k_{deact}, k_p, and k_t represent the rate constants for activation, deactivation, polymerization, and termination, respectively.

1.2.2 Polyelectrolyte Multilayers

Solid supports can also be modified by layer-by-layer (LbL) adsorption,[7,8,9] which in one of its simplest forms involves exposing a substrate to alternating polyanion and polycation solutions, with rinsing with H_2O after adsorption of each "layer" (Figure 1.4). The application of many adsorption steps yields thicker films, and virtually any charged

substrate can be modified in this fashion. The ionic strength, pH, and polyion concentration in the solution also affect the thickness and stability of the film,[7] and the polyelectrolyte multilayer (PEM) films can terminate with either a polycation or polyanion, including charged nanoparticles. Because of the versatility of LbL adsorption, a number of studies attempted to employ PEM films in applications such as catalysis, drug delivery, and sensing.[2,7,10,11]

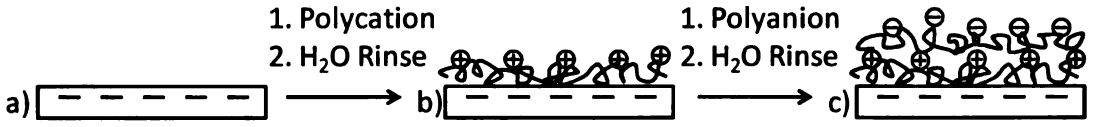

Figure 1.4: Schematic diagram of a negatively charged substrate before (a) and after adsorption of a polycation and rinsing with H_2O (b), and after subsequent adsorption of a polyanion and a second rinsing with H_2O (c). Repetition of the process yields multilayer films. Figure adapted from Bruening et al.[2]

1.3 Post-Translational Modifications of Proteins

1.3.1 Protein Phosphorylation

Protein phosphorylation is a reversible post-translational modification (PTM) regulated by kinases and phosphatases in eukaryotic cells. Although phosphorylation is just one of hundreds of PTMs, it is a key regulatory mechanism and plays an essential role in several cellular functions, including membrane transport, gene expression, and apoptosis.[12,13,14,15,16,17,18] In 1955, Fischer and Krebs first recognized the significance of protein phosphorylation and dephosphorylation as a regulatory mechanism in the cell,[19] and many studies focused on this PTM since the early 1990s when Liu and coworkers determined that the drug Cylcosporin specifically inhibits the protein phosphatase PP2B to make organ transplantation possible.[20]

In eukaryotic cells, protein phosphorylation can occur at the hydroxyl groups of the amino acid residues serine (S), threonine (T), and tyrosine (Y) when adenosine triphosphate (ATP) donates its gamma phosphate to the amino acid residue and becomes adenosine diphosphate (ADP) (Figure 1.5).[21] Reversible protein phosphorylation is an enzymatically regulated process, where kinases catalyze the addition of a phosphate group and phosphatases catalyze dephosphorylation (Figure 1.6). Upon phosphorylation, the protein may undergo conformational changes that change its activity, so phosphorylation of a protein can, in a sense, "turn on" a regulatory pathway, which can then be "turned off" by dephosphorylation.[22]

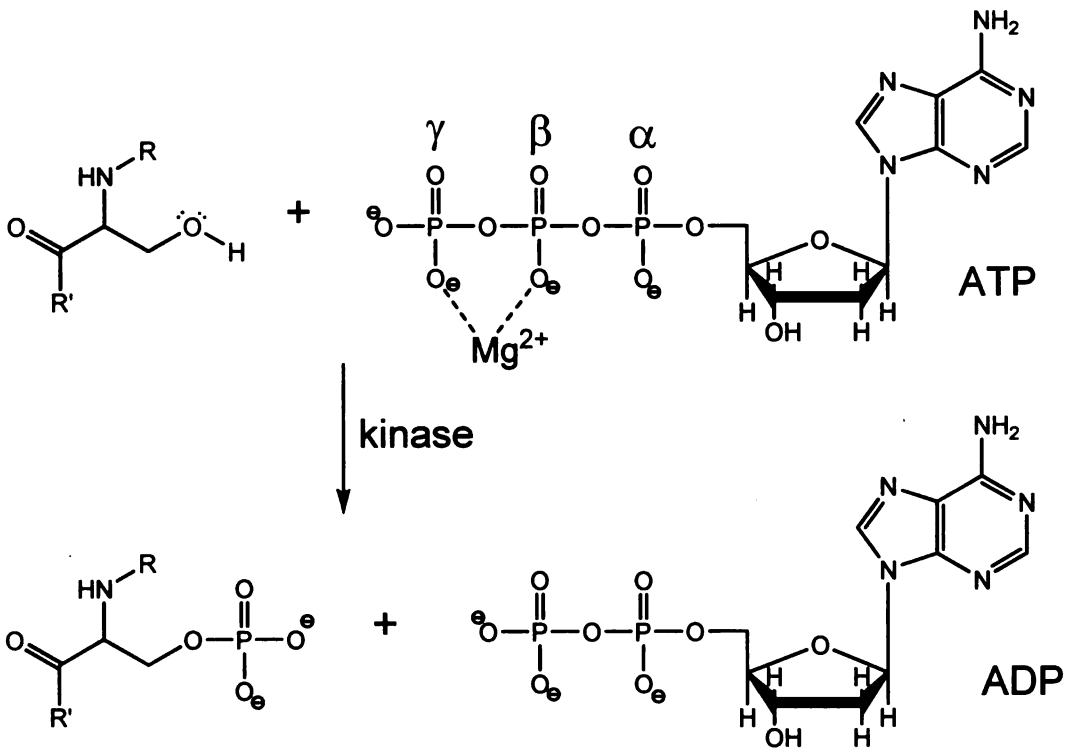

Figure 1.5: Kinase-catalyzed phosphorylation of serine by ATP, adapted from Walsh.[21]

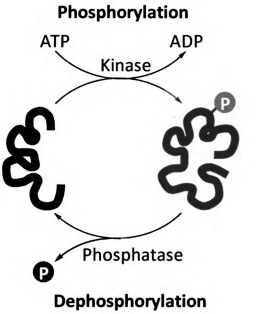

Figure 1.6: Cartoon showing reversible protein phosphorylation and the conformational change of the protein upon addition of the phosphate group.

Because phosphorylation plays a major role in several regulatory mechanisms, abnormal phosphorylation of proteins either leads to or results from numerous types of diseases, including diabetes, muscular dystrophy, and various forms of cancer.[23,24] Therefore, the identification and analysis of phosphorylation processes is essential for understanding cellular regulation and for the advancement of pharmaceutical targets.[25] However, the amount of a particular phosphorylated protein in the cell is low relative to the amount of nonphosphorylated proteins, and a protein often contains multiple serine, threonine, and tyrosine residues. Both of these facts make identification of phosphorylation sites challenging. Even so, such identifications can sometimes be made using mass spectrometry, which is discussed in section 1.4.

1.3.2 Protein Glycosylation

Protein glycosylation is a common post-translational modification that occurs in eukaryotic cells. Processing of the core oligosaccharides of the glycan moiety of the glycoprotein begins in the endoplasmic reticulum (ER) and further trimming and modification of the glycoprotein occurs once moved to the Golgi complex.[26,27] Figure 1.7, adapted from Nelson,[22] shows a simplified scheme of the synthesis of the core oligosaccharide on an *N*-linked glycoprotein. Synthesis begins on the cytosolic surface of the ER, where monosaccharide units are added individually to dolichol phosphate. After addition of two *N*-acetylglucosamines (GlcNac, step a) and five mannose units (step b), the oligosaccharide in the figure is translocated across the ER membrane and into the lumen (step c), where more monosaccharide units can be added (not shown here). The core oligosaccharide is then transferred from dolichol phosphate to an asparagine (Asn) residue on the growing polypeptide chain with the assistance of the oligosaccharyltransferase enzyme complex (step d),[26] yielding an *N*-linked glycoprotein (e). The fully translated protein is then released from the mRNA (step f) and the dolichol phosphate is translocated back to the cytosolic surface of the ER (step g) and a phosphate group is released (step h). The glycoprotein is further modified within the ER and in the Golgi complex, with the assistance of several enzymes. Processing of the glycan moiety within the ER produces relatively uniform glycoproteins, as any alterations administered in the ER are common among all glycoproteins. Most structural diversity between glycoproteins is not introduced until the biomolecules are in the Golgi complex.[26]

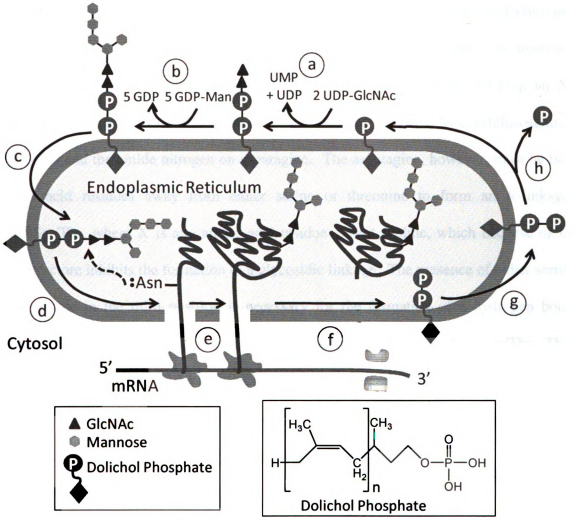

Figure 1.7: Schematic diagram showing the synthesis of the core oligosaccharide of a glycoprotein, where the oligosaccharide moiety is built up by the successive addition of monosaccharide units, (a) and (b), which occurs on the cytosolic face of the ER. The oligosaccharide is translocated across the ER membrane and into the lumen (c) and additional monosaccharide units can be added while inside the lumen (not shown here). The core oligosaccharide is transferred from the dolichol phosphate to an Asn residue of the protein (d), forming an *N*-linked glycoprotein (e). The fully translated protein is released from the mRNA (f) and the dolichol phosphate is translocated (g) and a phosphate is removed (h). The glycoprotein is further modified within the ER and in the Golgi complex. Figure adapted from Nelson.[22]

The glycan moiety of a glycoprotein attaches to the polypeptide chain through either an *N*- or *O*-linkage (Figure 1.8). An oligosaccharide can attach its anomeric carbon to the hydroxyl group on either a serine or threonine residue, forming an *O*-glycosidic

linkage. Figure 1.8a shows an *O*-linkage between *N*-acetylgalactosamine (GalNAc) and the hydroxyl group on serine. An oligosaccharide can alternatively attach its anomeric carbon to the amide nitrogen on an asparagine or glutamine residue, forming an *N*-glycosidic linkage.[22] Figure 1.8b shows an *N*-linkage between *N*-acetylglucosamine (GlcNAc) and the amide nitrogen on asparagine. The asparagine, however, must be two amino acid residues away from either serine or threonine to form an *N*-linkage, AsnXSer/Thr, where X is any amino acid residue except proline, which because of its ring structure inhibits the formation of a glycosidic linkage. The presence of either serine or threonine in the third position is necessary for the formation of a hydrogen bond between the carbonyl group on either Asn/Gln and the hydroxyl group on Ser/Thr. This facilitates the formation of the glycosidic linkage by decreasing the dissociation constant of the amide nitrogen.[28]

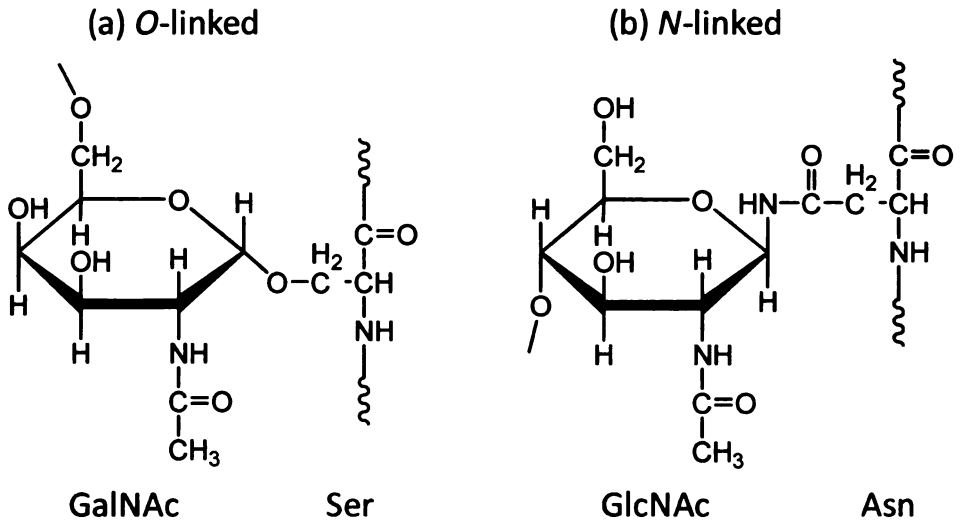

Figure 1.8: Structures of a) *N*-acetylgalactosamine *O*-linked to the hydroxyl group of serine and b) *N*-acetylglucosamine *N*-linked to the amide nitrogen of asparagine. Figure adapted from Nelson et al.[22]

The glycan moiety of the glycoprotein assists in the folding and conformational stability of the individual protein, whereas the entire glycoprotein plays a significant role in protein recognition, the immune system, and cell-to-cell recognition.[26,27,29,30,31] Protein glycosylation is enzymatically controlled, as discussed above, which means that the monosaccharide units comprising the oligosaccharide can be easily modified if the enzyme or reactant concentration is altered. This variation in oligosaccharide structure may alter the function and activity of the glycoprotein, which can potentially lead to disease.[26,27] Thus, it is not surprising that abnormal glycosylation of proteins plays a key role in several diseases, including diabetes, liver disease, and various forms of cancer.[32,33,34,35] The identification and analysis of protein glycosylation is, therefore, essential for understanding cellular regulation and these diseases. Unfortunately, determination of glycosylation sites presents a challenge similar to that associated with the identification of phosphorylation sites, namely the low abundance of glycoproteins and peptides relative to that of nonglycoproteins and peptides. Additionally, the oligosaccharides attached to the protein can contain various monosaccharide units, and this diversity complicates analysis of protein glycosylation. Nevertheless, mass spectrometry (Section 1.4) is a useful tool for glycoprotein analysis.

1.4 Mass Spectrometry for Characterization of Phosphoproteins/Phosphopeptides and Glycoproteins/Glycopeptides

Throughout the recent decades, mass spectrometry (MS) has become the premier method for protein sequencing and for the identification of phosphorylation and glycosylation sites. First introduced in 1897 by Sir Joseph J. Thomson,[36] MS has developed into a tool that is useful for a wide range of applications. Although there are

several types of mass spectrometers, all instruments have the general design described in Figure 1.9. Ions analyzed by MS must be in the gas phase; however, the analyte may be introduced into the instrument in the liquid, gas, or solid phase. The ionization source converts the analyte into gas-phase ions, and the mass analyzer separates the ions based on their mass-to-charge ratios (*m/z*). The detector then "counts" these ions, and a computer processes the data to give a mass spectrum.

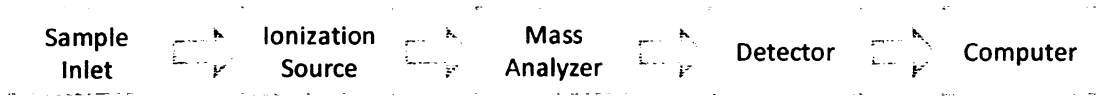

Figure 1.9: Schematic diagram of a mass spectrometer.

1.4.1 Ionization Sources

The ionization source and mass analyzer are the two most important components of the mass spectrometer. Initially designed by Arthur J. Dempster in 1918, electron ionization (EI) was one of the first ionization methods developed and remains the most common form of ionization for organic molecules. While the development of the EI source was a major advancement for mass spectrometry, this ionization method limits samples to those that are volatile and thermally stable. This ionization method is not conducive to the analysis of large biomolecules, such as proteins and peptides, because vaporization of these molecules is challenging without extensive thermal degradation. These challenges were overcome in the late 1970s and early 1980s with the development of desorption/ionization (D/I) techniques that first included field desorption (FD) and laser desorption (LD), which are able to produce gas-phase ions from condensed-phase samples. While these D/I methods greatly expanded the range of compounds open to analysis by mass spectrometry, field desorption and laser desorption have limited use

today.[37] FD involves heating of the sample on the probe with an electric field as high as 10^8 V/cm and requires an experienced operator.[37] LD involves a pulsed laser focused on a solid target, which rapidly heats the analyte causing it to desorb and ionize. Unfortunately, the use of LD is limited to compounds with molecular weights of approximately 500 Daltons (Da), as any analyte over this mass will fragment.[37] This mass limitation was overcome with the development of fast atom bombardment (FAB) by Barber and Bordoli in the early 1980s,[38,39] in which a high energy beam of neutral atoms or molecules is focused on the sample.[37] Unfortunately FAB is an insensitive ionization method and has been superseded by matrix-assisted laser desorption/ionization (MALDI) and electrospray ionization (ESI). MALDI is related to laser desorption in that a pulsed laser is used to desorb and ionize the analyte, but MALDI incorporates a matrix to aid in this process. Although ESI is not a desorption/ionization method, it is capable of ionizing non-volatile analytes and has overcome mass and sensitivity limitations. As soft ionization techniques, MALDI and ESI have revolutionized mass spectrometry and its applications to biomolecule analysis. These techniques are further discussed below.

1.4.1.1 Matrix-Assisted Laser Desorption/Ionization

The principle of MALDI was developed in the late 1980s by Hillenkamp and Karas, who discovered that the energy required to ionize alanine decreases 10-fold in the presence of tryptophan.[40] This concept was adapted from Tanaka, who originally demonstrated that an inorganic cobalt nanopowder, mixed with glycerol, provided rapid heating necessary to desorb and ionize the analyte,[41] and has since been applied to MALDI, where the compound of interest is mixed with a matrix prior to analysis. The matrix consists of a small organic molecule that strongly absorbs light at the wavelength

of the laser. Common matrices include 2,5-dihydroxybenzoic acid (DHB), α-cyano-4-hydroxycinnamic acid (α-CHCA), and trihydroxyacetophenone (THAP). A solution with a 1:1000 molar ratio of analyte to matrix crystallizes on a MALDI sample plate, which is typically made of stainless steel and occasionally coated with gold. After evaporation of the solvent and crystallization of the matrix-analyte mixture, a pulsed laser, usually a nitrogen laser at 337 nm, is fired at the sample, as depicted in Figure 1.10, and the matrix sublimes due to rapid heating by the laser. The energy absorbed by the matrix transfers to the analyte molecule (M), causing the analyte molecule to desorb and ionize with the matrix. MALDI is a soft ionization technique, so singly-charged intact ions form with minimal fragmentation, as described in Karas' "lucky survivors" model,[42] and peaks present in a MALDI mass spectrum typically correspond to a singly protonated species, $[M+H]^+$. Signals due to sodium adducts, $[M+Na]^+$, also commonly appear in MALDI mass spectra. MALDI is a useful ionization technique for large, non-volatile, and thermally labile species, including proteins and peptides, polymers, carbohydrates, and inorganic compounds.[37] Additionally, sample preparation is simple and MALDI exhibits a relatively high tolerance to contaminants such as salts and buffers. MALDI is the ionization technique used for all MS experiments described in this thesis.

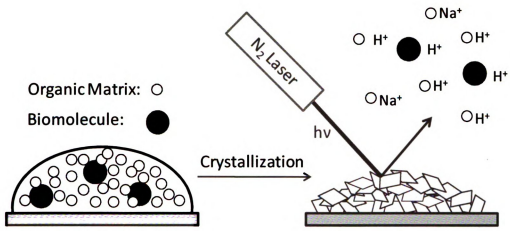

Figure 1.10: Schematic diagram of the ionization of a MALDI sample, where the organic matrix is present in a much higher quantity than the analyte. After co-crystallization of the biomolecule and matrix, a pulsed laser is fired at the sample and the matrix and analyte are both desorbed and ionized.

1.4.1.2 Electrospray Ionization

Another technique that has greatly expanded biomolecule analysis is electrospray ionization (ESI). Developed in the late 1980s, ESI is unique in that ionization occurs under atmospheric pressure and ions often form as multiply-charged species. Ions form due to the application of an electric field (3-6 kV) to a solution passing through a capillary tube with a flux of 1-10 μL/min.[37] This electric field causes charge to accumulate at the surface of the solution at the end of the capillary, and highly charged droplets form as the solution breaks free. These charged droplets pass through an inert gas, typically nitrogen, which removes any remaining solvent. Charge accumulates on the surface of the droplet and Coulombic explosions result due to charge repulsion. Secondary droplets continue to break down until only individual ions remain, many of which may be multiply-charged. ESI is widely used for analysis of proteins and synthetic polymers, and even small polar molecules.[37]

1.4.2 Mass Analyzers Compatible with MALDI

1.4.2.1 Time-of-Flight Mass Analyzer

MALDI is a pulsed ionization method, producing ions in bundles, and the time-of-flight (TOF) mass analyzer analyzes packets of ions at a time. Hence, the TOF analyzer is highly compatible with a MALDI source. The TOF analyzer separates ions based on the time required to travel through a field-free region from the ion source to the detector. Bundles of ions are ejected from the source and a potential is applied across an electrode and extraction grid, through which the ions pass, causing them to accelerate toward the flight tube. Accelerated ions with the same charge achieve the same kinetic energy, and because kinetic energy (E_k) is proportional to mass (m) and the square of velocity (v) (Equation 1.1), ions with different masses have different characteristic velocities. Therefore, in TOF analyzers ions are separated based on velocity, and mass-to-charge ratios are determined by measuring the time required for the ions to pass from the source to the detector. This is described by Equation 1.3, which states that the mass-to-charge ratio (m/z) is directly proportional to the product of the charge on an electron (e = 1.67 x 10^{-19} C), the accelerating voltage (V), and the square of the time (t), divided by the square of the distance traveled by the ion (d). The length of the flight tube is typically 1 to 2 m. As described by Equation 1.3, the ion with the smallest m/z value will have the smallest flight time and will, therefore, reach the detector first.

Equation 1.1: $E_k = \frac{1}{2}mv^2 = zeV$

Equation 1.2: $v = \frac{d}{t}$

Equation 1.3: $\frac{m}{z} = \frac{2eVt^2}{d^2}$

Since its first use as a mass analyzer in the 1950s by Wiley and McLaren, several developments such as the use of an electrostatic reflector and delayed pulsed extraction greatly improved the resolution of TOF analyzers. In addition to improvements in mass resolution, TOF measurements are attractive for analysis because mass spectra can be collected quite rapidly, making TOF a high-throughput technique. The mass range of TOF is, in principle, unlimited. Karas and coworkers showed that even a protein as large as 300 kDa can be examined.[43]

1.4.2.2 Linear Ion Trap Mass Analyzer

All mass spectrometry experiments described in this thesis were conducted using a Thermo vMALDI LTQ XL instrument that contains a linear ion trap (Figure 1.11). The vMALDI source, where v stands for vacuum (170 mTorr), houses the sample plate, a fiber optic cable connected to the N_2 laser, a camera, and a modified quadrupole (Q00). In this particular instrument, the N_2 laser (337 nm) irradiates the sample at an incident angle of ~30° and the diameter of the laser spot is about 80-120 μm. The RF quadrupole (Q0) and octapole (Q1) are located after the source and guide ions into the linear ion trap. Before the RF quadrupole and octapole is the Q00 quadrupole, which increases the translational kinetic energy of the ions. The RF quadrupole creates a downhill potential

gradient to guide the ions and then the octapole also increases the translation kinetic energy of the ions. Helium is used as the bath gas, at 10^{-3} Torr, in the linear ion trap to collisionally cool the ions, as well as for collision-induced dissociation (CID) for tandem mass spectrometry experiments. Using the parameters discussed above, the upper *m/z* value for this instrument is 4000.

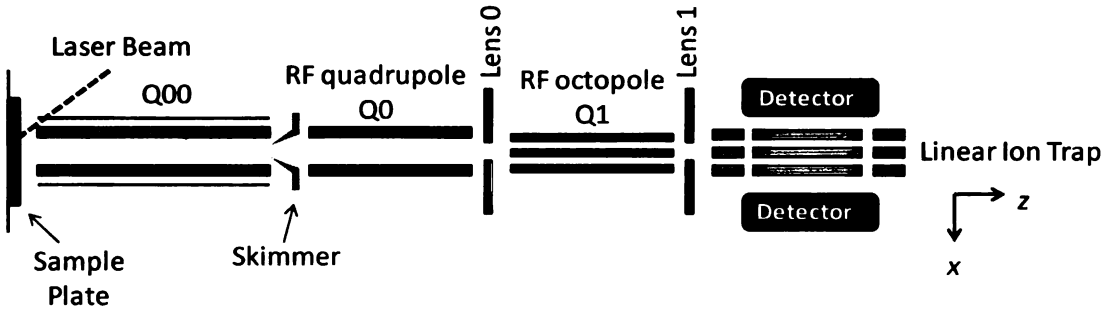

Figure 1.11: Schematic diagram of the Thermo vMALDI LTQ XL instrument with a linear ion trap. Figure is redrawn from Garrett and coworkers.[44]

The quadrupole ion trap (QIT), also known as the Paul trap, was developed by Wolfgang Paul in the 1960s. In independent studies in 1993, Schwartz and Jonscher first coupled the MALDI source and quadrupole ion trap to one another.[45,46] Two-dimensional (2D) quadrupole ion trap mass analzyers, or linear ion traps (LIT), are similar to three-dimensional (3D) QITs, except 2D analyzers confine ions in the radial dimension (*xy* plane) of the quadrupole via application of an RF potential, while a DC potential confines ions in the axial dimension at the ends of the trap.[37] Briefly, the Thermo 2D ion trap consists of four parallel hyperbolic rods, which are divided into three sections (Figure 1.12). Upon entering the LIT along the *z*-axis, ions are collisionally cooled with an inert gas (He) and oscillate in the *xy* plane due to the RF potential applied to the rods, while moving along the *z*-axis in between the end electrodes. A DC voltage is applied to the ends of the quadrupole to prevent the ions from exiting the LIT.[37] Ions

have stable trajectories when q is less than 0.908 in the LIT for a given V_{RF} range (Figure 1.13), which is described in Equation 1.4, where $\Omega = 2v\pi$, which is the applied RF frequency (v = 1.2 MHz), V_{RF} is the magnitude of RF voltage (ramped from zero to 10 kV), and r_0 is the distance from the center of the trap to the end (r_0 = 4.12 mm).[37,47] Ions below the mass range are lost because they have unstable trajectories.[37] The major advantage of the linear ion trap over the Paul ion trap is that the LIT has a much higher trapping efficiency. This 2D trap has an efficiency of 55-70%, while the Paul trap only has 5% trapping efficiency.[37] The LIT is capable of storing more ions because space charge effects are minimal compared with the Paul ion trap since ions are focused along the *xy* plane instead of in all three directions.

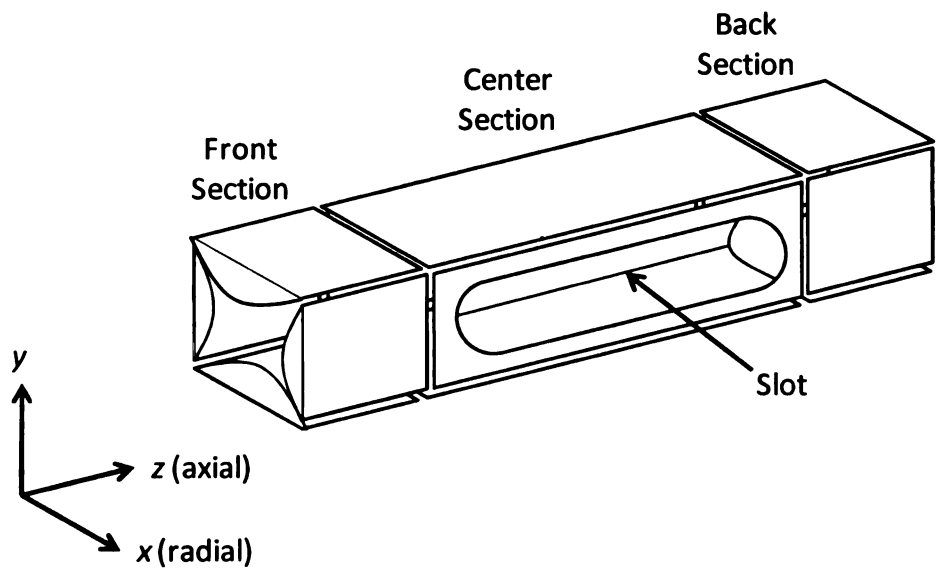

Figure 1.12: Schematic diagram of a Thermo linear ion trap. Ions are trapped in the center section of the 2D LIT, and the front and back sections are necessary to minimize distortion of the electric field of the center section. This improves trapping efficiency. Ions are radially ejected through two slots (30 x 0.25 mm) in the exit rods in the center section. Figure adapted from de Hoffmann et al.[37]

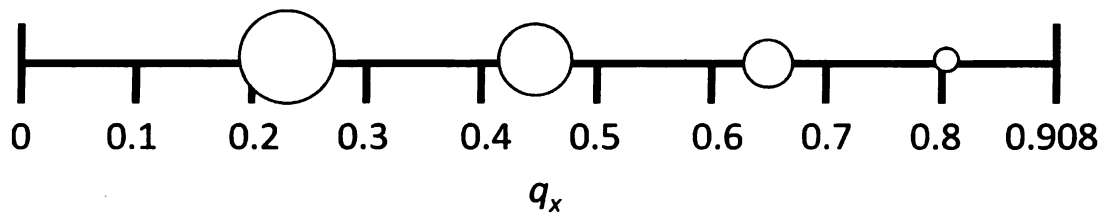

Figure 1.13: In the LIT, ions have stable trajectories when q is less than 0.908. Circles represent ions in the stable region and the size of the circles corresponds to the relative size of m/z values. For the a-q stability diagram, see either de Hoffmann et al. or Douglass et al.[37,47]

Equation 1.4: $$q = \frac{4zeV_{RF}}{mr_0^2\Omega^2}$$

Equation 1.5: $$\beta = [a + (q^2/2)]^{1/2}$$

Equation 1.6: $$f = \beta v / 2$$

Ions are expelled radially from the trap through two slots (30 x 0.25 mm) in the exit rods using resonance ejection (Figure 1.12). An ion in the linear ion trap oscillates at a secular frequency specific to its m/z value. When an RF voltage at a particular frequency is applied along the z-axis, the oscillations of ions in the trap with the corresponding secular frequency will begin to increase. The secular frequency f of an ion is related to the applied voltage through the β term in Equations 1.5 and 1.6, where a is zero in the LIT. Therefore, f is directly proportional to V_{RF}. Equation 1.5 is applicable only for $q < 0.4$. If the amplitude of the applied voltage is large enough, the oscillations of the ions will be so great that they will be destabilized and ejected from the trap.[37] Two detectors are used in the Thermo LIT to ensure that all ions are expelled from the trap and are detected.

Tandem-in-time mass spectrometry (MS/MS), including multistage tandem mass spectrometry (MS^n, where n>2), is easily performed in the linear ion trap. First, ions with a specific *m/z* value are selected and all other ions are ejected from the trap (isolation). These isolated precursor ions are then fragmented via the application of a low amplitude resonance excitation voltage which increases the kinetic energy of the ions and causes them to collide with the helium gas present in the trap (where q is 0.25). The collisions convert kinetic energy to internal energy and cause the ions to fragment. Finally, the product ions are expelled from the linear ion trap by resonance ejection.[37]

1.4.3 Challenges in Phosphopeptide and Glycopeptide Detection by Mass Spectrometry

Although mass spectrometry is now the premier tool for analysis of both phophopeptides and glycopeptides, there are several challenges in detecting these species. In most eukaryotic cells, the amount of phosphorylated protein is low relative to the amount of nonphosphorylated protein,[48,49,50] and the same challenge exists for glycosylated protein.[51] The structural diversity of glycoproteins also makes it difficult to determine the monosaccharide units that make up a glycan.[52] Phosphorylation may decrease the ionization efficiency of some species in the presence of nonphosphopeptides, and this becomes increasingly challenging as the number of phosphorylation sites increases.[53,54] However, recent studies suggest that phosphopeptides have similar ionization efficiencies as nonphosphopeptides.[55]

1.5 Enrichment Techniques for Phosphopeptides and Glycopeptides Prior to MS Analysis

As discussed above, phosphopeptides and glycopeptides are present in low amounts relative to other peptides present in a sample, making analysis by mass spectrometry challenging. A number of recently developed techniques aid in the detection of phosphorylated and glycosylated peptides by selectively capturing these species to overcome their low abundance. The sections below provide a brief summary of the most widely used enrichment methods for both phosphopeptides and glycopeptides. For more thorough descriptions of enrichment techniques, refer to recent reviews by Dunn et al and Thingholm et al for phosphorylated peptides[56,57] and Ito et al, Liu et al, and Mechref et al for glycosylated peptides.[58,59,60]

1.5.1 Enrichment Methods for Phosphorylated Peptides Prior to MS Analysis

Phosphopeptide enrichment techniques can be broadly grouped into immunoprecipitation, affinity chromatography, and chemical derivatization or covalent binding. Immunoprecitation is limited to tyrosine phosphorylation and certain motifs for serine and threonine phosphopeptides,[61] so covalent binding and affinity chromatography are more general techniques. Although covalent binding may allow higher enrichment specificities than affinity chromatography, the majority of the covalent procedures require multiple steps.[62,63,64] Hence, affinity chromatography is the most widespread method for phosphopeptide enrichment. Typical forms of affinity methods include immobilized metal affinity chromatography (IMAC) and, more recently, metal oxide affinity chromatography (MOAC). These two techniques are similar in that phosphopeptides selectively bind to a resin, while rinsing removes unbound species,

including impurities. Finally, elution yields concentrated analyte, and the phosphopeptides can be analyzed via mass spectrometry. Figure 1.14 shows this general process. Although IMAC and MOAC may not provide the specificity of covalent binding, they are relatively simple, rapid enrichment techniques and are useful for numerous applications.

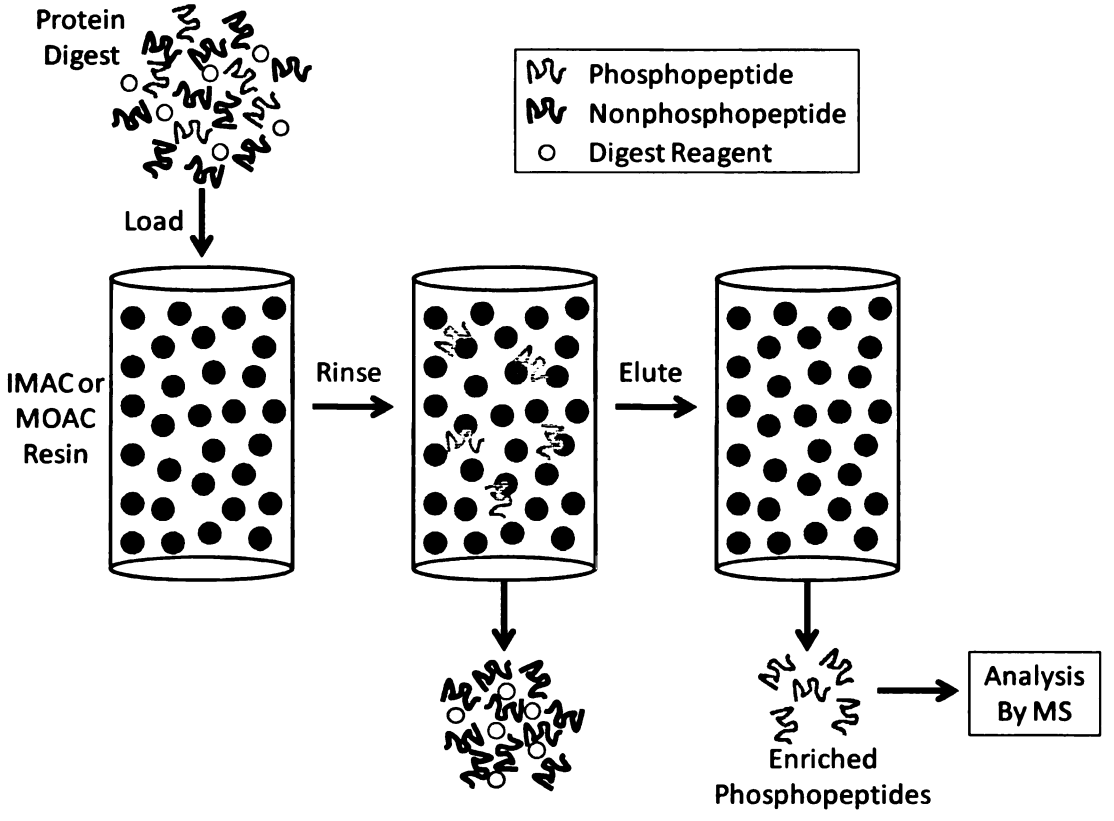

Figure 1.14: Schematic diagram showing the general procedure for enrichment of phosphopeptides using IMAC or MOAC in a column format. The column packing is different for each method, but both techniques involve loading the sample onto a column, rinsing to remove any contaminants, and elution of enriched phosphopeptides. The analyte can then be analyzed with MS. Figure adapted from Dunn et al.[56]

1.5.1.1 Immobilized Metal Affinity Chromatography

Immobilized metal affinity chromatography (IMAC) was introduced in 1975 by Porath[65] and relies on the interaction between immobilized metal-ligand complexes and a

specific functional group, in this case, phosphate. The two most common metal-binding ligands in IMAC are iminodiacetate (IDA) and nitrilotriacetate (NTA) (Figure 1.15). These ligands strongly complex metal ions such as Fe(III), Ga(III), Zr(IV), and Al(III). Hochuli and coworkers first applied NTA to IMAC in 1987 because of its strong complexing ability.[66] This tetradentate ligand should bind metal ions more strongly than IDA, which is a tridentate ligand. Therefore, NTA more effectively prevents metal leaching than IDA.

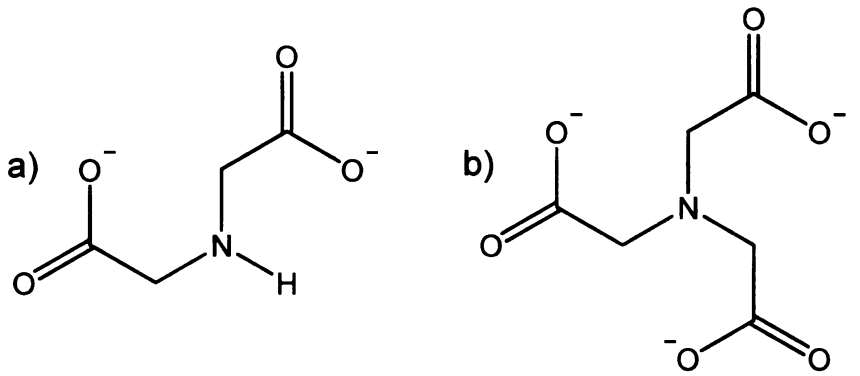

Figure 1.15: Structures of a) iminodiacetate (IDA), and b) nitrilotriacetate (NTA).

Unfortunately, binding of acidic residues to metal ion complexes results in significant adsorption of nonphosphopeptides. Methyl esterification of the carboxyl groups on glutamic and aspartic acid can sometimes overcome this challenge,[67] but this introduces an additional step in the enrichment process. Additionally, because derivatization is usually less than 100%, esterification complicates mass spectra. The most critical challenge with IMAC is the potential sample loss due to multiple rinsing and elution steps on the column (Figure 1.14), and some commercial methods even require additional rinsing steps. To overcome this challenge, several groups developed techniques to enrich sample directly on a MALDI plate.

In 1993, Hutchins and coworkers introduced surface-enhanced affinity capture in on-plate capture of a glycoprotein, which was analyzed directly with MALDI-TOF-MS.[68] Two years later, Brockman and coworkers derivatized a MALDI target with a self-assembled monolayer (SAM) for the specific capture of biomolecules.[69] After incubation of the sample, the plate was rinsed, and matrix was added directly to the plate prior to analysis by MALDI-TOF-MS.[69] These works, along with many others, lead to the development of on-plate enrichment using IMAC in 2005. Using gold MALDI targets as substrates, Shen and coworkers derivativized SAMs with NTA and then formed the Ga(III)-ligand complex.[70] The Ga(III)-NTA-SAM-derivatized MALDI plates allowed successful enrichment of synthetic phosphopeptides. Our group recently used MALDI plates coated with poly(2-hydroxyethyl methacrylate) (PHEMA) brushes derivatized with Fe(III)-NTA to enrich phosphopeptides prior to MS analysis.[71] The high capacity of polymer brushes relative to monolayers greatly enhances enrichment efficiency.

1.5.1.2 Metal Oxide Affinity Chromatography

Metal oxide affinity chromatography (MOAC) has recently become one of the most successful methods for enriching phosphopeptides. Sano, Pinske, and Larsen were among the first to introduce titanium dioxide resins for enrichment of phosphorylated peptides.[72,73,74,75] Although titanium dioxide is probably the most widely used metal oxide, zirconium dioxide is also capable of enriching phosphorylated peptides and it has been reported that it has a higher binding affinity toward phosphate than carboxylate anions.[76,77] The isoelectric points of TiO_2 and ZrO_2 are approximately 6 and 7, respectively,[78,79] so at low pH both of these metal oxides are positively charged and are able to selectively adsorb phosphopeptides. Other metal oxides, including aluminum

oxide (Al_2O_3), niobium oxide (Nb_2O_5), and aluminum hydroxide ($Al(OH)_3$), have also been used for the selective enrichment of phosphorylated peptides.[80,81,82]

In MOAC, proteolytic digests are typically loaded onto a column packed with a metal oxide resin, such as TiO_2, and the loading solution usually contains either acetic acid or trifluoroacetic acid to minimize unwanted binding of acidic peptides. Pinske and coworkers loaded their samples in 0.1 M acetic acid, rinsed the column with 0.1 M acetic acid in 80% acetonitrile, and eluted the phosphopeptides by increasing the pH to 9.0 with ammonium bicarbonate.[73] However, some residual nonspecific binding of nonphosphopeptides containing acidic residues occurred. Derivatization of the acidic residues using *O*-methyl esterification, resulted in little nonspecific affinity for the TiO_2.[73]

Larsen and coworkers used a 0.1% TFA loading buffer and a rinsing solution containing 2,5-dihydroxybenzoic acid (DHB) to minimize nonspecific adsorption.[72] TFA is much more acidic than acetic acid and this loading solution has a pH of 1.9, compared with 2.7 for acetic acid. The lower pH in the loading solution protonates acidic residues more effectively and therefore aids in preventing nonspecific adsorption to the TiO_2 resin. These studies also used an ammonium hydroxide solution at pH 10.5 to elute phosphopeptides, which resulted in higher recoveries compared with a pH 9.0 elution. This method allowed identification of 20 phosphopeptides in a MALDI-MS spectrum of 500 fmol of α-casein digest along with essentially no signals from nonphosphopeptides.[72] Larsen and coworkers also examined the ability of other acids to reduce binding of nonphosphorylated peptides to TiO_2 resins. They determined that 2,5-DHB, salicylic acid and phthalic acid exhibit the greatest ability to inhibit binding of nonphosphorylated

peptides, followed by benzoic acid, cyclohexane carboxylic acid, phosphoric acid, TFA, and acetic acid.[72] When binding to the TiO_2 surface, salicyclic acid creates a chelating bidentate structure, compared with the bridging bidentate complex formed between phosphate and TiO_2 (Figure 1.16). As a result of these differences, Larsen suggests that DHB, which is similar to salicylic acid, competes for binding sites with nonphosphopeptides and not with phosphopeptides.[72]

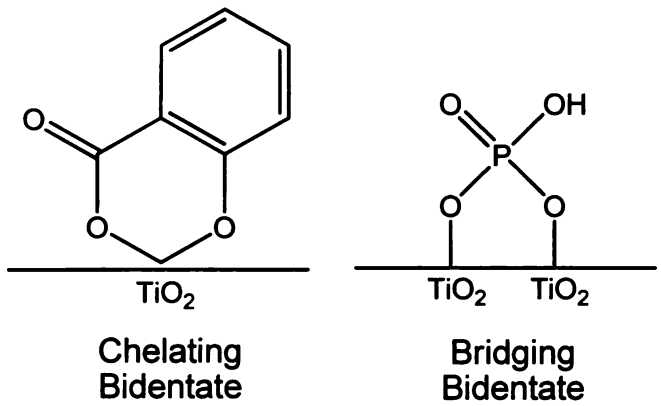

Figure 1.16: Schematic diagram comparing the chelating bidentate structure of salicylic acid on TiO_2 with the bridging bidentate complex formed between phosphate and titanium dioxide. Figure adapted from Larsen et al.[72]

As with IMAC, work with metal oxides has primarily occurred on columns where potential sample loss is an issue due to multiple rinsing and elution steps. On-plate techniques have also been applied to enrichment methods using metal oxides. Lin and coworkers immobilized TiO_2-coated gold nanoparticles on a glass slide for on-plate enrichment of phosphopeptides and analysis by MALDI-TOF-MS (Figure 1.17).[83] More recently, Ekstr□m and coworkers prepared polymer MALDI plates with channels packed with TiO_2 for the selective enrichment of one pmol to 100 fmol of β-casein digest.[84] The wash, rinse, elution, and matrix solutions were pulled through the channels using a vacuum and the sample was flipped over for MALDI-MS analysis as the matrix

crystallized on the rear side of the plate. Other titanium dioxide on-plate enrichment techniques include work by Qiao et al, where an array of TiO_2 nanoparticles was prepared on a stainless steel MALDI target by heating an array of 2 μL drops of a 100 mg/mL TiO_2 suspension on the plate at 400 °C for 1 h.[85] Tan et al affixed TiO_2-coated magnetic nanoparticles to a stainless steel MALDI target by holding a magnet to the rear side of the plate while the sample was loaded, incubated, rinsed, and mixed with matrix.[86]

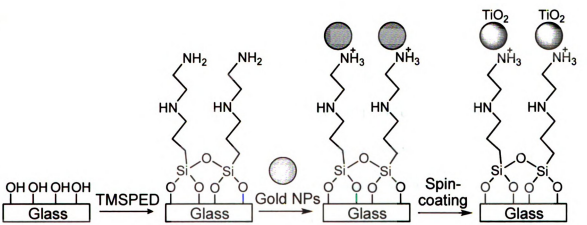

Figure 1.17: Schematic diagram showing the immobilization of a thin film of *N*-[3-(trimethoxysilyl)propyl]ethylenediamine (TMSPED) on glass, attachment of gold nanoparticles (NPs) to the film, and coating of the nanoparticles with TiO_2. In the TiO_2 coating step, a solution of titanium isopropoxide is spin-coated on the surface, followed by annealing to give TiO_2 nanoparticles. The figure is adapted from Lin et al.[83]

A number of studies also examined the use of magnetic beads for capturing phosphopeptides in solution. Magnetic beads are attractive for enrichment because they can simply be collected in an external magnetic field, and they have a high surface area to volume ratio that gives a high binding capacity. In 2005, magnetic nanoparticles were first coated with metal oxides for phosphopeptide enrichment.[87,88,89] Typically, coating of the Fe_3O_4 beads with SiO_2 occurs using either sodium silicate or tetraethyl orthosilicate, and subsequent formation of the metal oxide employs titanium butoxide,

zirconium butoxide, or aluminum isopropoxide for either titania, zirconia, or alumina-coated beads, respectively. To enrich a phosphopeptide sample, a proteolytic digest in TFA is mixed with magnetic beads (~25 μg) in a microcentrifuge tube and incubated for as little as 30 s. The beads are typically rinsed with an acetonitrile/TFA solution, and a magnet is used to hold the beads to the wall of the tube while the solution is decanted. Matrix solution that contains phosphoric acid to elute the phosphopeptides can be mixed with the beads and then spotted to the MALDI target for direct MS analysis, or beads can be directly spotted on the MALDI plate without addition of matrix, which is attractive as no elution step is necessary. Without matrix, surface-assisted laser desorption/ionization (SALDI) MS is used,[87] but this technique generally yields lower signals than MALDI. In addition to metal oxide coatings, magnetic nanoparticles can also be modified with IMAC materials. Xu and coworkers functionalized magnetic nanoparticles with Fe(III)-IDA in 2006 and used these beads for phosphopeptide enrichment prior to MALDI-TOF/TOF-MS analysis.[90] The development of on-plate enrichment methods and the use of modified magnetic particles has the potential to improve the analysis of phosphopeptides by reducing sample handling and sample loss.

1.5.2 Enrichment Methods for Glycoproteins/Glycopeptides Prior to MS Analysis

Lectin affinity chromatography and reversible covalent binding are the two main methods for enrichment of glycoproteins and glycopeptides prior to analysis by mass spectrometry, with lectin affinity chromatography being more common. While both of these techniques provide selective enrichment of glycopeptides, lectin chromatography is a highly specific form of separation.[90] These two types of enrichment are briefly described below.

1.5.2.1 Lectin Affinity Chromatography

Lectins are proteins that have a high affinity for certain carbohydrates, and these proteins are categorized based on the monosaccharide to which they bind most strongly. Hence, lectin affinity chromatography separates proteins based on their glycan moiety. Typically, serum glycoproteins are digested using trypsin, loaded onto a column containing one or more immobilized lectins bound to a support, and rinsed. Finally, bound peptides are eluted and deglycosylated using protein-*N*-glycanase F (PNGase F).[91] Deglycosylation is often necessary because the glycan moiety typically has a very large molecular weight that precludes MS detection in some cases because the *m/z* value is past the upper limit of many mass analyzers.

Although a vast amount of work has been accomplished using lectins immobilized in columns,[92,93,94] multiple rinsing and elution steps increase the possibility of sample loss, as with IMAC and MOAC columns for phophopetide isolation (Figure 1.14). Even Top Tips (Glygen), pipet tips loaded with lectins such as concanavalin A on agarose, require several washings and multiple elutions prior to analysis by MALDI-TOF-MS.[95] Recent methods address these issues and aim to minimize sample handling and loss. One of these techniques that involves the establishment of lectin microarrays was recently reviewed by Hu et al.[96] In these methods, lectins are immobilized on a solid support, such as gold or polydimethylsiloxane (PDMS), through either covalent bonding or physical adsorption, and the glycopeptide sample can be directly applied to the microarray. Wong and coworkers covalently immobilized lectins in an array on a PDMS substrate and spotted glycoproteins directly on the microarray. Following sample incubation, matrix was added to the microarray, which was then affixed to a MALDI

target for analysis by MALDI-TOF-MS.[97] Microarrays are advantageous because different lectins can be immobilized on each spot of the plate to simultaneously enrich different glycoproteins from the same sample.

Magnetic particles can also be modified for glycoprotein analysis. Sparbier and coworkers demonstrated that magnetic beads functionalized with concanavalin A (Con A) and wheat germ agglutinin (WGA), the two most commonly employed lectins, are capable of enriching glycosylated proteins.[98,99] Glycoprotein samples were incubated for 1 h, washed, and eluted under acidic conditions, and the particles were held in place using an external magnetic field, while the supernatant was decanted. Proteins were digested with trypsin following elution and were then analyzed using MALDI-TOF-MS. The authors show that these modified beads specifically bind glycoproteins based on the functionality of the particles.[99] These magnetic particles significantly decrease sample handling and potential sample loss, which are challenges with column lectin affinity chromatography.

1.5.2.2 Covalent Binding Enrichment Methods

Several covalent binding techniques exist for glycosylated peptide enrichment, and some of these methods have been applied to modified magnetic beads. Two common modifications of particles for binding glycosylated peptides include functionalization with hydrazide and boronic acid groups. In 2003, Zhang and coworkers used hydrazide functionalized particles to enrich *N*-linked glycosylated peptides.[100] In this work, a glycoprotein sample was oxidized using sodium periodate, which converts *cis*-diol groups on the glycan moiety to aldehydes (Figure 1.18). The oxidized monosaccharide was then coupled with hydrazide groups immobilized on a resin, forming a covalent

hydrazone bond, and nonglycoproteins were removed by rinsing. The covalently bound glycoprotein was then digested with trypsin, leaving glycosylated peptides bound to the resin whereas nonglycosylated peptides were rinsed away. The α-amino groups on the immobilized glycopeptides were isotopically labeled while bound to the resin, and then the formerly *N*-linked glycopeptides were cleaved from the oligosaccharide chain using PNGase F (Figure 1.18). The released peptides were identified and quantified using either microcapillary high-performance liquid chromatography electrospray ionization (μLC-ESI) MS/MS or by μLC separation followed by MALDI MS/MS analysis. This enrichment technique, however, is only applicable toward *N*-linked glycoproteins as PNGase F cleaves the bond between the innermost GlcNAc and asparagine residues of the glycan group from *N*-linked glycoproteins,[101] and there is no comparable enzyme for *O*-linked glycoproteins. Zhang and coworkers demonstrate that hydrazide-functionalized beads are capable of selective capture of *N*-linked glycoproteins, as essentially all peaks present in the mass spectra were due to expected *N*-linked glycopeptides.[100] Since this work, separation of glycopeptides using hydrazide chemistry has become increasingly popular. Hydrazide chemistry is an effective enrichment technique for the identification and quantification of glycopeptides, both by itself, as well as coupled to other separation methods such as lectin affinity chromatography.[102,103,104,105,106]

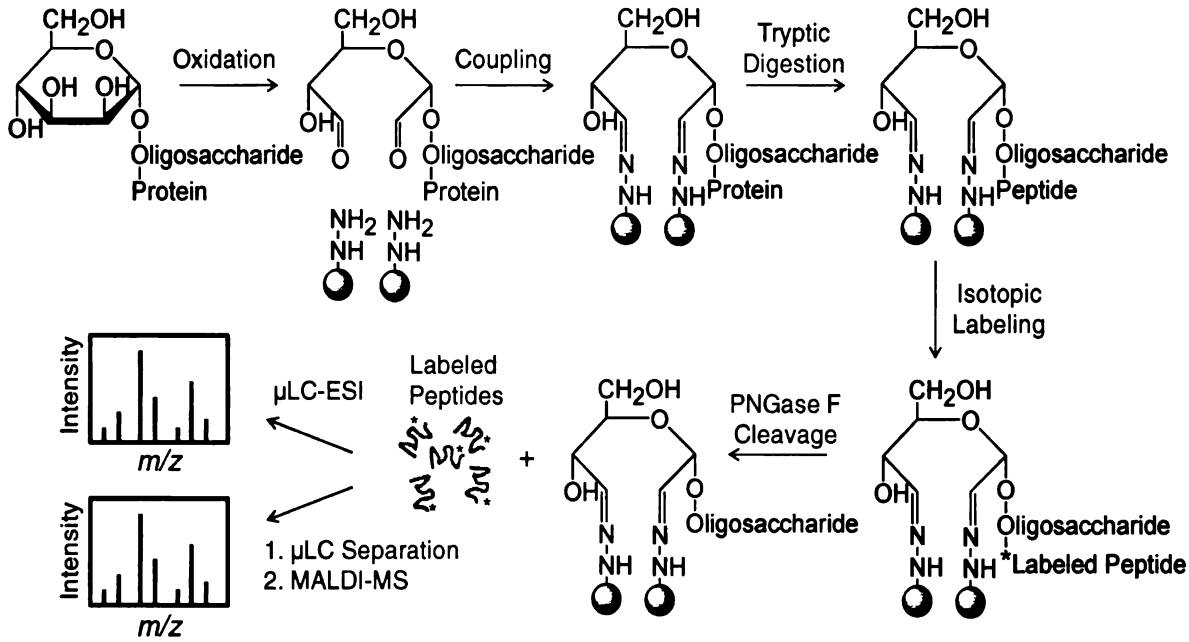

Figure 1.18: Schematic diagram showing the oxidation of *cis*-diol-containing glycoprotein with sodium periodate, coupling with hydrazide-functionalized beads, and then tryptic digestion of the protein, yielding glycopeptides covalently bound to the magnetic particles. Glycopeptides bound to the resin are isotopically labeled and then cleaved using PNGase F to give formerly *N*-linked isotopically labeled peptides prior to analysis by either ESI or MALDI. Figure adapted from Zhang et al.[100]

In addition to hydrazide-functionalized supports, boronic acid-derivatized resins can selectively and rapidly enrich glycosylated peptides prior to MS analysis. The affinity of boronic acid groups for *cis*-diol-containing compounds was discovered in the late 1940s,[107,108,109] and this chemistry is applicable to glycopeptide enrichment because essentially all carbohydrate groups in glycopeptides contain one, if not multiple, *cis*-diol groups. The covalent interaction between boronic acid and *cis*-diols is relevant to both *N*-linked and *O*-linked glycopeptides, so this method is essentially applicable to all glycoproteins. Figure 1.19 shows the equilibria for the formation of the boronate ester from phenylboronic acid and a general *cis*-diol.

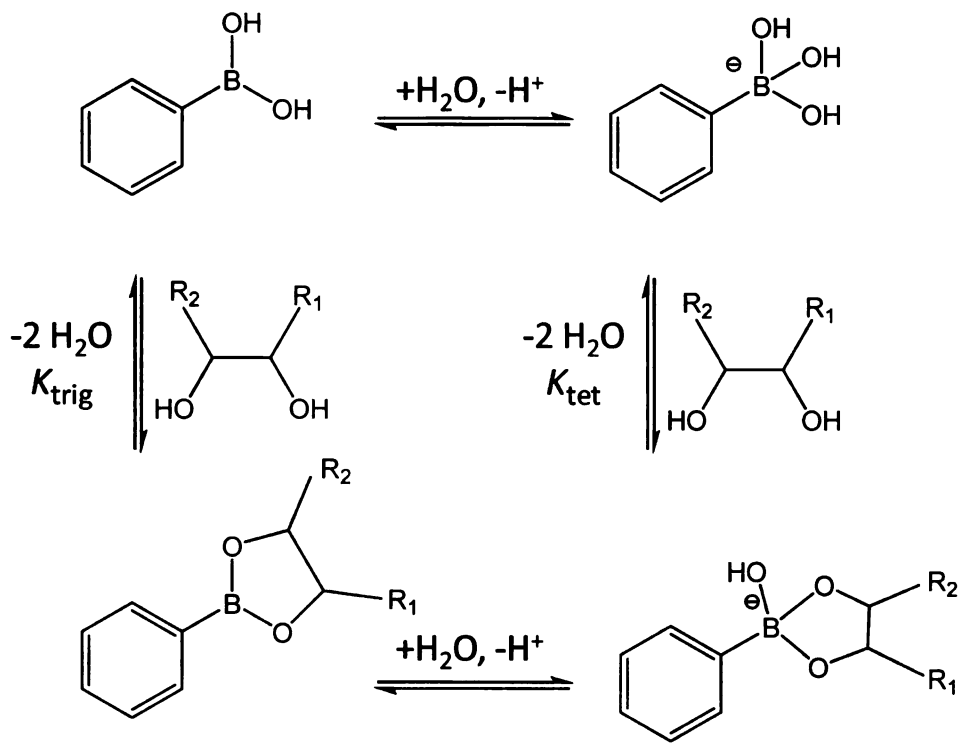

Figure 1.19: Relevant equilibria for the formation of a boronate ester from phenylboronic acid and a *cis*-diol. The boronate ester may exist in both trigonal and tetrahedral forms. K_{trig} and K_{tet} are the equilibrium constants for the formation esters from the trigonal and tetrahedral forms of phenylboronic acid, respectively. Figure adapted from Yan et al.[110]

While a *cis*-diol-containing compound can bind to phenylboronic acid in either the tetrahedral or trigonal forms, the equilibrium constant is higher for formation of the tetrahedral form, $K_{tet} > K_{trig}$.[110,111] The pK_a of the boronic acid and of the boronate ester formed, as well as the pH of the solution and the type of buffer used and its concentration, will all affect the binding between boronic acid and the *cis*-diol-containing compound.[110,111] The optimal pH for binding can be estimated by simply averaging the p$K_{a,acid}$ and p$K_{a,diol}$.[110] While this predicted pH may be helpful, the actual optimal pH will depend on the reaction conditions. In general, compounds containing *cis*-diols most effectively bind to boronic acids under basic conditions and are released by lowering the pH.

In recent years, the interaction between boronic acid and *cis*-diol groups has been exploited for the enrichment of glycosylated proteins and peptides. In addition to their work in 2005 and 2006 involving the immobilization of lectins on beads, Sparbier and coworkers also used commercially available phenylboronic acid-functionalized beads for glycoprotein enrichment.[98,99] Glycoprotein samples were incubated under slightly basic conditions (pH 8.5) for 1 h at room temperature under gentle shaking, and bound glycoproteins were eluted under acidic conditions and analyzed using MALDI-TOF/TOF-MS. Sparbier et al demonstrated that these phenylboronic acid-functionalized beads are capable of selective enrichment of glycopeptides. The authors also showed that while beads containing immobilized phenylboronic acid, Con A, and WGA are all able to capture glycopeptides, each material has its individual binding profile.[98,99]

In a similar method, Zhou and coworkers synthesized aminophenylboronic acid-functionalized magnetic nanoparticles and incubated them with tryptically digested proteins under slightly alkaline conditions (pH 8.5) for 90 min.[112] The nanoparticles were rinsed, and bound peptides were eluted under acidic conditions and analyzed by MALDI-QIT-TOF MS. The authors showed that signals (and signal to noise) due to glycopeptides significantly increased after enrichment compared with conventional MALDI analysis.[112] Yeap and coworkers functionalized nanodiamond (ND) with succinic anhydride and subsequent reaction with aminophenylboronic acid and then enriched intact proteins, including ovalbumin and ribonuclease B (RNase B).[113] Glycoproteins were incubated with the ND in phosphate buffer for 3 h at either pH 7.4 or 9, and the ND powder was separated by centrifugation. After removal of the supernatant, matrix solution was mixed with the ND prior to spotting on the sample plate, and these

samples were air-dried and analyzed by MALDI-TOF MS. The glycosylated proteins ovalbumin and RNase B were identified in separate experiments and bovine serum albumin (BSA), a nonglycosylated protein, was not present in mass spectra when succinic anhydride was used as a "spacer" between the ND particle and aminophenylboronic acid.[113]

Most recently, Xu and coworkers used mesoporous silica for selective enrichment of glycopeptides.[114] In this work, aminophenylboronic acid was immobilized within the pores of the silica (Figure 1.20). A glycopeptide sample in ammonium bicarbonate was added to a suspension of boronic acid-functionalized silica and was incubated for just 15 min with shaking. The supernatant was decanted after centrifugation, and the beads were washed with ammonium bicarbonate, which was again decanted after centrifugation. A solution containing TFA and acetonitrile was used to elute the glycopeptides (30 min) from the silica. After centrifugation, the eluent and matrix were spotted onto a MALDI target for analysis by MALDI-QIT MS. This boronic acid-functionalized material was capable of enriching 23 fmol of tryptically digested horseradish peroxidase (HRP) with little nonspecific binding.[114]

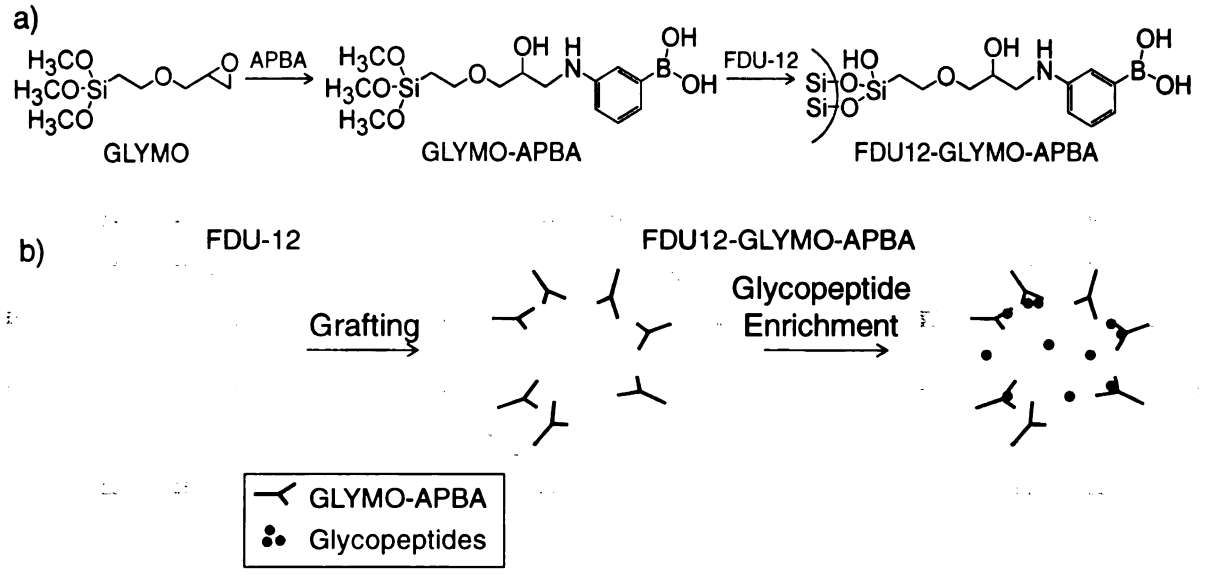

Figure 1.20: Schematic diagram of a) reaction between (3-glycidyloxypropyl)trimethoxysilane (GLYMO) and 3-aminophenylboronic acid (APBA) to form GLYMO-APBA, followed by attachment to mesoporous silica FDU-12; and b) grafting of GLYMO-APBA to mesoporous silica, then enrichment of glycopeptides within the silica pore. Figure adapted from Xu.[114]

1.6 Research Overview

This thesis focuses on the design and fabrication of various modified MALDI plates for the direct enrichment of biomolecules prior to MALDI-MS analysis. On-plate enrichment techniques can potentially reduce sample handling, preparation time, and sample loss. Chapter Two describes deposition of TiO_2 nanoparticles on a gold-coated substrate modified with a bilayer of polyelectrolytes and on-plate enrichment of phosphorylated peptides using the modified substrate. The chapter includes a comparison of the enrichment performance of these plates with substrates containing TiO_2 nanoparticles immobilized by simple heating. The MALDI plates with TiO_2 particles immobilized by heating showed a phosphopeptide recovery of 69%. Chapter Three presents methods for the synthesis of polymer brushes derivatized with reduced glutathione, with the intention of specifically binding GST-tagged proteins. Chapter Four

describes the derivatization of thicker poly(2-hydroxyethyl methacrylate) brushes with aminophenylboronic acid. These polymer-modified plates are examined for the specific on-plate enrichment of glycosylated peptides from an unpurified glycoprotein digest. Finally, Chapter Five summarizes the conclusions of this work and suggests future directions.

1.7 References

[1] Dunn, J. D.; Igrisan, E. A.; Palumbo, A. M.; Reid, G. E.; Bruening, M. L. "Use of High-Capacity Polymer Brushes Immobilized on MALDI Plates for the Analysis of Phosphopeptides by MS," Poster Presented at the 55th ASMS Conference, June 4-7, 2007, Indianapolis, IN.

[2] Bruening, M. L.; Dotzauer, D. M.; Jain, P.; Ouyang, L.; Baker, G. L. *Langmuir* **2008**, *24*, 7663-7673.

[3] Kamigaito, M.; Sawamoto, M.; Higashimura, T. *Macromolecules* **1995**, *28*, 5671-5675.

[4] Wang, S.; Matyjaszewski, K. *Journal of the American Chemical Society* **1995**, *117*, 5614-5615.

[5] Matyjaszewski, K.; Xia, J. *Chemical Reviews* **2001**, *101*, 2921-2990.

[6] Matyjaszewski, K.; Spanswick, J. *Materials Today* **2005**, *8*, 26-33.

[7] Ai, H.; Jones, S. A.; Lvov, Y. M. *Cell Biochemistry and Biophysics* **2003**, *39*, 23-43.

[8] Bertrand, P.; Jonas, A.; Laschewsky, A.; Legras, R. *Macromolecular Rapid Communications* **2000**, *21*, 319-348.

[9] Decher, G. *Science* **1997**, *277*, 1232-1237.

[10] Hammond, P. T. *Advanced Materials* **2004**, *16*, 1271-1293.

[11] Johnston, A. P. R.; Cortez, C.; Angelatos, A. S.; Caruso, F. *Current Opinion in Colloid & Interface Science* **2006**, *11*, 203-209.

[12] Hunter, T. *Cell.* **2000**, *100*, 113-127.

[13] Duronio, V. *Biochemical Journal.* **2008**, *415*, 333-344.

[14] Palfrey, H. C.; Alper, S. L.; Greengard, P. *Journal of Experimental Biology.* **1980**, *89*, 103-115.

[15] Sombroek, D.; Hofmann, T. G. *Cell Death and Differentiation.* **2009**, *16*, 187-194.

[16] Stamm, S. *Journal of Biological Chemistry.* **2008**, *283*, 1223-1227.

[17] Turner, K. M.; Burgoyne, R. D.; Morgan, A. *Trends in Neurosciences.* **1999**, *22*, 459-464.

[18] Whitmarsh, A. J.; Davis, R. J. *Cellular and Molecular Life Sciences* **2000**, *57*, 1172-1183.

[19] Fischer, E. H.; Krebs, E. G. *Journal of Biological Chemistry* **1955**, *216*, 121-132.

[20] Liu, J.; Farmer, J. D.; Lane, W. S.; Friedman, J.; Weissman, I.; Schreiber, S. L. *Cell* **1991**, *66*, 807-815.

[21] Walsh, C. T. *Posttranslational Modification of Proteins*; Roberts and Company: Englewood, CO, **2006**, 35-36.

[22] Nelson, D. L.; Cox, M. M. *Principles of Biochemistry*; W. H. Freeman and Company: New York, NY, **2005**, 228-230, 1069-1071.

[23] Cohen, P. *European Journal of Biochemistry* **2001**, *268*, 5001-5010.

[24] Yu, L.; Issaq, H. J.; Veenstra, T. D. *Proteomic Clinical Applications* **2007**, *1*, 1042-1057.

[25] McConnell, J. L.; Wadzinski, B. E. *Molecular Pharmacology* **2009**, *75*, 1249-1261.

[26] Helenius, A.; Aebi, M. *Carbohydrates and Glycobiology* **2001**, *291*, 2364-2369.

[27] Rudd, P. M.; Dwek, R. A. *Critical Reviews in Biochemistry and Molecular Biology* **1997**, *32*, 1-100.

[28] Rao, V.S.R.; Qasba, P.K.; Balaji, P.V.; Chandrasekaran, R. *Conformation of Carbohydrates*; Harwood Academic Publisher: Amsterdam, Netherlands, **1998**, 131.

[29] Durand, G.; Seta, N. *Clinical Chemistry* **2000**, *46*, 795-805.

[30] Paulson, J. C. *Trends in Biochemical Sciences* **1989**, *14*, 272-276.

[31] Varki, A. *Glycobiology* **1993**, *3*, 97-130.

[32] Coffman, F. D. *Critical Reviews in Clinical Laboratory Sciences* **2008**, *45*, 531-562.

[33] Dias, W. B.; Hart, G. W. *Molecular Biosystems* **2007**, *3*, 766-772.

[34] Saldova, R.; Wormald, M. R.; Dwek, R. A.; Rudd, P. M. *Disease Markers* **2008**, *25*, 219-232.

[35] Turner, G. A. *Clinica Chimica Acta* **1992**, *208*, 149-171.

[36] Griffiths, I. W. *Rapids Communications in Mass Spectrometry* **1997**, *11*, 2-16.

[37] de Hoffmann, E.; Stroobant, V. *Mass Spectrometry: Principles and Applications*; John Wiley & Sons: West Sussex, **2007**, 29-40, 43-55.

[38] Barber, M.; Bordoli, R. S.; Sedgewick, R. D.; Tyler, A. N. *Journal of the Chemical Society, Chemical Communications* **1981**, 325-327.

[39] Barber, M.; Bordoli, R. S.; Sedgewick, R. D.; Tyler, A. N. *Nature* **1981**, *293*, 270-275.

[40] Karas, M.; Bachmann, D.; Hillenkamp, F. *Analytical Chemistry* **1985**, *57*, 2935-2939.

[41] Tanaka, K.; Waki, H.; Ido, Y.; Akita, S.; Yoshida, Y.; Yoshida, T. *Rapid Communications in Mass Spectrometry* **1988**, *2*, 151-153.

[42] Karas, M.; Glückmann, M.; Schäfer, J. *Journal of Mass Spectrometry* **2000**, *35*, 1-12.

[43] Karas, M.; Ingendoh, A.; Bahr, U.; Hillenkamp, F. *Biomedical and Environmental Mass Spectrometry* **1989**, *18*, 841.

[44] Garrett, T. J.; Yost, R. A. *Analytical Chemistry* **2006**, *78*, 2465-2469.

[45] Schwartz, J. C.; Bier, M. E. *Rapid Communications in Mass Spectrometry* **1993**, *7*, 27-32.

[46] Jonscher, K.; Currie, G.; McCormack, A. L.; Yates, J. R. *Rapid Communications in Mass Spectrometry* **1993**, *7*, 20-26.

[47] Douglass, D. J.; Frank, A. J.; Mao, D. M. *Mass Spectrometry Reviews* **2005**, *24*, 1-29.

[48] Kratzer, R.; Eckerstrom, C.; Karas, M.; Lottspeich, F. *Electrophoresis* **1998**, *19*, 1910-1919.

[49] Stensbalk, A.; Anderson, S.; Jensen, O. N. *Proteomics* **2001**, *1*, 207-222.

[50] Zeller, M.; Koenig, S. *Analytical and Bioanalytical Chemistry* **2004**, *378*, 898-909.

[51] Ullmer, R.; Plematl, A.; Rizzi, A. *Rapic Communications in Mass Spectrometry* **2006**, *20*, 1469-1479.

[52] Medzihradszky, K. F. *Methods in Enzymology* **2005**, *405*, 116-138.

[53] Liao, P. C. Leykam, J.; Andrews, P. C.; Gage, D. A.; Allison, J. *Analytical Biochemistry* **1994**, *219*, 9-20.

[54] Craig, A. G.; Hoeger, C. A.; Miller, C. L. Goedken, T.; Rivier, J. E.; Fischer, W. H. *Biological Mass Spectrometry* **1994**, *23*, 519-528.

[55] Steen, H.; Jebanathirajah, J. A.; Rush, J.; Morrice, N.; Kirschner, M. W. *Molecular & Cellular Proteomics* **2006**, *5*, 172-181.

[56] Dunn, J. D.; Reid, G. E.; Bruening, M. L. *Mass Spectrometry Reviews* **2009** DOI 10.1002/mas.20219.

[57] Thingholm, T. E.; Jensen, O. N.; Larsen, M. R. *Proteomics* **2009**, *9*, 1-18.

[58] Ito, S.; Hayama, K. Hirabayashi, J. *Methods in Molecular Biology*; Humana Press: Clifton, N.J. **2009**, *534*, 195-203.

[59] Liu, X.; Ma, L.; Li, J. *Analytical Letters* **2008**, *41*, 268-277.

[60] Mechref, Y.; Madera, M.; Novotny, M. V. *Methods in Molecular Biology*; Humana Press: Clifton, N.J. **2008**, *424*, 373-396.

[61] Schmidt, S. R.; Schweikart, F.; Andersson, M. E. *Journal of Chromatography B* **2007**, *849*, 154-162.

[62] Bodenmiller, B.; Mueller, L. N.; Pedrioli, P. G.; Pflienger, D. *Molecular Biosystems* **2007**, *3*, 275-286.

[63] Tao, W. A.; Wollscheid, B.; O'Brien, R.; Eng, J. K. *Nature Methods* **2005**, *2*, 591-598.

[64] Zhou, H.; Watts, J. D.; Aebersold, R. *Nature Biotechnology* **2001**, *19*, 375-378.

[65] Porath, J.; Carlsson, J.; Olsson, I.; Belfrage, G. *Nature* **1975**, *258*, 598-599.

[66] Hochuli, E.; Dobeli, H.; Schacher, A. *Journal of Chromatography* **1987**, *411*, 177-184.

[67] Ficarro, S. B.; McCleland, M. L.; Stukenberg, P. T.; Burke, D. J.; Ross, M. M.; Shabanowitz, J.; Hunt, D. F.; White, F. M. *Nature Biotechnology* **2002**, *20*, 301-305.

[68] Hutchins, T. W.; Yip, T. *Rapid Communications in Mass Spectrometry* **1993**, *7*, 576-580.

[69] Brockmann, A. H.; Orlando, R. *Analytical Chemistry* **1995**, *67*, 4581-4585.

[70] Shen, J. W.; Ahmed, T.; Vogt, A.; Wang, J. Y.; Severin, J.; Smith, R.; Dorwin, S.; Johnson, R.; Harlan, J.; Holzman, T. *Analytical Biochemistry* **2005**, *345*, 258-269.

[71] Dunn, J. D.; Igrisan, E. A.; Palumbo, A. M.; Reid, G. E.; Bruening, M. L. *Analytical Chemistry* **2008**, *80*, 5727-5735.

[72] Larsen, M. R.; Thingholm, T. E.; Jensen, O. N.; Roepstorff, P.; Jorgensen, T. J. D. *Molecular & Cellular Proteomics* **2005**, *4*, 873-886.

[73] Pinske, M. W. H.; Uitto, P. M.; Hilhorst, M. J.; Ooms, B.; Heck, A. J. R. *Analytical Chemistry* **2004**, *76*, 3935-3943.

[74] Sano, A.; Nakamura, H. *Analytical Sciences* **2004**, *20*, 565-566.

[75] Sano, A.; Nakamura, H. *Analytical Sciences* **2004**, *20*, 861-864.

[76] Blackwell, J. A.; Carr, P. W. *Journal of Chromatography* **1991**, *549*, 43-57.

[77] Blackwell, J. A.; Carr, P. W. *Journal of Chromatography* **1991**, *549*, 59-75.

[78] Vassileva, E.; Proinova, I.; Hadjiivanov, K. *Analyst* **1996**, *121*, 607-612.

[79] Renger, C.; Kuschel, P.; Kristoffersson, A.; Clauss, B.; Oppermann, W.; Sigmund, W. *Journal of Ceramic Processing Research* **2006**, *7*, 106-112.

[80] Wang, Y. B.; Chen, W. Wu, J. S.; Guo, Y. L; Xia, X. H. *Journal of American Society of Mass Spectrometry* **2007**, *18*, 1387-1395.

[81] Ficarro, S. B.; Parikh, J. R.; Blank, N. C.; Marto J. A. *Analytical Chemistry* **2008**, *80*, 4606-4613.

[82] Wolschin, F.; Wienkoop, S.; Weckwerth, W. *Proteomics* **2005**, *5*, 4389-4397.

[83] Lin, H. Y.; Chen, C. T.; Chen, Y. C. *Analytical Chemistry* **2006**, *78*, 6873-6878.

[84] Ekstr□m, S.; Wallman, L.; Helldin, G.; Nilsson, J.; Marko-Varga, G.; Laurell, T. *Journal of Mass Spectrometry* **2007**, *42*, 1445-1452.

[85] Qiao, L.; Roussel, C.; Wan, J.; Yang, P.; Girault, H. H.; Liu, B. *Journal of Proteome Research* **2007**, *6*, 4763-4769.

[86] Tan, F.; Zhang, Y.; Wang, J.; Wei, J.; Qin, P.; Cai, Y.; Qian, X. *Rapid Communications in Mass Spectrometry*, **2007**, *21*, 2407-2414.

[87] Chen, C. T.; Chen, Y. C. *Analytical Chemistry* **2005**, *77*, 5912-5919.

[88] Chen, C. T.; Chen, W. Y.; Tsai, P. J.; Chien, K. Y.; Yu, J. S.; Chen, Y. C. *Journal of Proteome Research* **2007**, *6*, 316-325.

[89] Lo, C. Y.; Chen, W. Y.; Chen, C. T.; Chen, Y. C. *Journal of Proteome Research* **2007**, *6*, 887-893.

[90] Xu, S. Y.; Zhou, H. J.; Pan, C. S.; Fu, Y.; Zhang, Y.; Li, X.; Ye, M. L.; Zou, H. F. *Rapid Communications in Mass Spectrometry* **2006**, *20*, 1769-1775.

[91] Drake, R. R.; Schwegler, E. E.; Malik, G.; Diaz, G.; Block, T.; Mehta, A.; Semmes, O. J. *Molecular & Cellular Proteomics* **2006**, *5*, 1957-1967.

[92] Geng, M.; Zhang, X.; Bina, M.; Regnier, F. *Journal of Chromatography B: Biomedical Sciences and Applications* **2001**, *752*, 293-306.

[93] Kaji, H.; Saito, H.; Yamauchi, Y.; Shinkawa, T.; Taoka, M.; Hirabayashi, J.; Kasai, K.; Takahashi, N.; Isobe, T. *Nature Biotechnology* **2003**, *21*, 667-672.
[94] Xiong, L.; Regnier, F. E. *Journal of Chromatography B: Analytical Technologies in the Biomedical and Life Sciences* **2002**, *782*, 405-318.

[95] Kubota, K.; Sato, Y.; Suzuki, Y.; Goto-Inoue, N.; Toda, T.; Suzuki, M.; Hisanaga, S.; Suzuki, A.; Endo, T. *Analytical Chemistry* **2008**, *80*, 3693-3698.

[96] Hu, S.; Wong, D. T. *Proteomics: Clinical Applications* **2009**, *3*, 148-154.

[97] Wong, D.; Hu, S. WIPO Patent WO/**2007**/082057.

[98] Sparbier, K.; Koch, S.; Kessler, I.; Wenzel, T.; Kostrzewa, M. *Journal of Biomolecular Techniques* **2005**, *16*, 407-413.

[99] Sparbier, K.; Wenzel, T.; Kostrzewa, M. *Journal of Chromatography B* **2006**, *840*, 29-36.

[100] Zhang, H.; Li, X.; Martin, D.; Aebersold, R. *Nature Biotechnology* **2003**, *21*, 660-666.

[101] Maley, F.; Trimble, R. B.; Tarentino, A. L.; Plummer, T. H. *Analytical Biochemistry* **1989**, *180*, 195-204.

[102] Cao, J.; Shen, C.; Wang, H.; Shen, H.; Chen, Y.; Nie, A.; Yan, G.; Lu, H.; Liu, Y.; Yang, P. *Journal of Proteome Research* **2009**, *8*, 662-672.

[103] Chen, R.; Jiang, X.; Sun, D.; Han, G.; Wang, F. Ye, M.; Wang, L.; Zou, H. *Journal of Proteome Research* **2009**, *8*, 651-661.

[104] McDonald, C. A.; Yang, J. Y.; Marathe, V.; Yen, T.; Macher, B. A. *Molecular & Cellular Proteomics* **2009**, *8*, 287-301.

[105] Mirzaei, H.; Baena, B. Barbas, C. Regnier, F. *Proteomics* **2008**, *8*, 1516-1527.

[106] Zhou, L.; Beuerman, R. W.; Chew, A. P.; Koh, S. K.; Cafao, T. A.; Urrets-Zavalia, E. A.; Urrrets-Zavalia, J. A.; Li, S. F. Y.; Serra, H. M. *Journal of Proteome Research* **2009**, *8*, 1992-2003.

[107] Boeseken, J. *Advanced Carbohydrate Chemistry* **1949**, *4*, 189-210.

[108] Sugihara, J. M.; Bowman, C. M. *Journal of the American Chemical Society* **1958**, *80*, 2443-2246.

[109] Lorand, J. P.; Edwards, J. O. *Journal of Organic Chemistry* **1959**, *24*, 769-774.

[110] Yan, J.; Springsteen, G.; Deeter, S.; Wang, B. *Tetrahedron* **2004**, *60*, 11205-11209.

[111] James, T. D. *Topics in Current Chemistry* **2007**, *277*, 107-152.

[112] Zhou, W.; Yao, N.; Yao, G.; Deng, C.; Zhang, X.; Yang, P. *Chemical Communications* **2008**, 5577-5579.

[113] Yeap, W. S.; Tan, Y. Y.; Loh, K. P. *Analytical Chemistry* **2008**, *80*, 4659-4665.

[114] Xu, Y.; Wu, Z.; Zhang, L.; Lu, H.; Yang, P.; Webley, P.; Zhao, D. *Analytical Chemistry* **2009**, *81*, 503-508.

Chapter 2: Metal Oxide-Modified Plates for Analysis of Phosphopeptides by MALDI-MS

2.1 Introduction

Reversible phosphorylation of proteins within cells of both prokaryotic and eukaryotic organisms is an essential regulatory mechanism.[1] Although it is just one of hundreds of post-translational modifications (PTMs), protein phosphorylation is responsible for regulating numerous cellular functions, including membrane transport, gene expression, and apoptosis.[2,3,4,5,6,7] Abnormal phosphorylation has been identified as either the cause or consequence of several diseases, including diabetes, muscular dystrophy, and various forms of cancer.[8,9] Therefore, the identification of phosphorylation sites, as well as the quantification of phosphorylated species, is necessary to understand these biochemical processes and diseases. Mass spectrometry, particularly with electrospray ionization (ESI) and matrix-assisted laser desorption/ionization (MALDI), has become the premier tool for the identification and quantification of phosphorylated proteins and peptides. Both of these forms of mass spectrometry use soft ionization techniques that allow minimal fragmentation and therefore the identification of the intact biomolecule.

Despite the advantages of mass spectrometry, the low abundance of phosphorylated peptides and proteins relative to nonphosphorylated species makes detection challenging.[10,11,12] However, a number of recently developed techniques that isolate phosphorylated peptides from nonphosphorylated peptides make detection by mass spectrometry more feasible. Some of these methods include immobilized metal affinity chromatography (IMAC), reversible covalent binding, and metal oxide affinity

chromatography (MOAC).[13,14] While IMAC is one of the most commonly used phosphopeptide enrichment techniques, acidic amino acid residues, including aspartic acid and glutamic acid, also have some affinity for IMAC resins, which results in the non-specific binding of nonphosphorylated species.[15] Recently developed metal oxide resins exhibit strong affinities for phosphorylated species, and under appropriate conditions, the non-specific binding of acidic residues to metal oxides is minimal. In most enrichment methods with either metal oxides or IMAC, enrichment occurs in a microcolumn.[16,17,18] Unfortunately, the column-based methods often decrease throughput, as the sample must be loaded onto the column, rinsed to remove any unbound species, and then eluted to collect the analyte. The column eluate is finally either analyzed by ESI-MS or mixed with matrix and spotted on a target and analyzed by MALDI-MS.

This chapter describes two on-plate enrichment techniques where samples are spotted on a modified MALDI plate and rinsed to remove impurities prior to addition of matrix and subsequent analysis. Both methods utilize metal oxide-modified plates for selective capture of phosphorylated peptides. These on-plate enrichment techniques allow for essentially no sample loss as the enriched phosphopeptides are analyzed directly on the modified substrate and do not need to be transferred to a conventional MALDI target, as is necessary with microcolumns.

The first on-plate enrichment technique utilizes MALDI substrates modified by the electrostatic layer-by-layer (LbL) adsorption of polyelectrolytes and metal oxides, either TiO_2 or ZrO_2 nanoparticles (Figure 2.1). LbL deposition of polyelectrolytes and nanoparticles was used previously for a variety of applications and is a simple method for

substrate modification.[19,20,21] Gold-coated substrates were modified with these polyelectrolyte/metal oxide layers, and an unpurified protein digest was added to the plate and allowed to incubate for 1 h. The positively charged nanoparticles directly interact with the phosphorylated peptides.

The second method is similar to work by Qiao and coworkers,[22] in which an array of sintered TiO_2 nanoparticles is prepared on a modified MALDI target by heating the TiO_2-covered plate to 400 °C. Here, we add 1 to 2 μL of a TiO_2 suspension to wells of a modified MALDI plate and heat the plate by ramping from room temperature to 400 °C in a nitrogen-filled furnace. With these plates, we examine the recovery of a synthetic phosphorylated peptide from an excess of nonphosphorylated peptide and compare these results with recoveries from commercially available enrichment materials. The recovery of this synthetic peptide using the TiO_2-modified MALDI plates is comparable to and even higher than several commercially available IMAC and metal oxide materials.

2.2 Experimental

2.2.1 Materials

Chicken egg ovalbumin, bovine serum albumin (BSA), rabbit phosphorylase b (phos b), and pig esterase were purchased from Sigma and digested using sequencing grade modified trypsin from Promega. Other digest reagents include: Tris-HCl (Invitrogen), urea (J. T. Baker), 1,4-dithio-DL-threitol (BioChemika), ammonium bicarbonate (Columbus Chemical), and iodoacetamide (Sigma). Gold-coated silicon wafers (Silicon Quest International) were prepared by sputter coating the Si wafers with 20 nm of chromium, followed by 200 nm of gold. The sputter coating was performed by Lance Goddard Associates, Foster City, CA. The reagents used for the fabrication of

polyelectrolyte/metal oxide modified plates include 3-mercaptopropionic acid (Aldrich), poly(allylamine hydrochloride) (M_w 70,000 Da, Sigma), poly(sodium 4-styrene sulfonate) (M_w 70,000 Da, Sigma), titanium (IV) oxide (particle size, ~100 nm, Aldrich), and zirconium (IV) oxide (Aldrich). Titanium (IV) oxide used for modifying the MALDI plate by heating was received from Evonik Degussa (Piscataway, NJ) as a gift. Reagents for enrichment include trifluoroacetic acid (Aldrich), phosphoric acid (Aldrich), HPLC grade acetonitrile (EMD), glacial acetic acid (Spectrum) and 2,5-dihydroxybenzoic acid (Aldrich). Deionized water was obtained using a Millipore purification system (Milli-Q, 18 MΩcm). HPLC grade methanol (Sigma), isopropyl alcohol (EMD), and ammonium hydroxide (Columbus Chemical) were used to clean the conventional stainless steel MALDI plate according to Thermo Scientific's deep cleaning procedure in which the plate was first thoroughly rinsed with isopropanol and methanol, and then sonicated for 30 min in a solution consisting of 451 mL of acetonitrile, 451 mL of water, and 108 mL of ammonium hydroxide. After sonication, the plate was rinsed with water and methanol, and then dried under a stream of N_2 gas. Finally, HPLC grade hexane (J. T. Baker) was rubbed over the plate using a cotton swab, followed by rinsing with hexane to create a hydrophobic surface. The plate was dried under a stream of N_2 gas and stored in nitrogen-filled glove bag while not in use.

For synthesis of H_5 and D_5 peptides, sequenal grade trifluoroacetic acid (TFA) was purchased from Pierce (Rockford, IL) and N-α-Fmoc-protected amino acids and Wang resins that were derivatized with Fmoc-protected amino acides (100-200 mesh) were obtained from EMD Biosciences (San Diego, CA). D_{10}-propionic anhydride was purchased from CDN Isotopes (Pointe-Claire, Quebec, Canada) and propionic anhydride

was obtained from Sigma Aldrich (St. Louis, MO). Reagent grade *N,N'*-dimethylformamide (DMF), purchased from Spectrum Chemicals (Gardena, CA), was dried with 4-Å molecular sieves.

2.2.2 Protein Digestion

For the tryptic digestion of protein samples, twenty 100 μg samples of each protein were separately dissolved in 20 μL of 6 M urea containing 50 mM tris-HCl. To measure out 100 μg of a protein, 2 mg of protein was first dissolved in 1 mL of deionized water, and twenty 100 μL aliquots were prepared and dried separately using a SpeedVac. For the digestion of a nonphosphorylated protein mixture, 100 μg of each protein, BSA, phos b, and esterase, were combined in one Eppendorf tube and dissolved in 20 μL of the urea/tris-HCl solution. To reduce any disulfide linkages, 5 μL of 10 mM 1,4-dithio-DL-threitol (DTT) was added to each sample, and the protein solutions were heated in a water bath at ~65°C for 1 h. After cooling the sample to room temperature, 160 μL of 50 mM ammonium bicarbonate and 10 μL of 100 mM iodoacetamide were added to each protein solution, and the samples were placed in the dark for 1 h. Finally, 10 μL of 0.5 μg/μL modified trypsin was added to each sample prior to incubation for ~16 hours at 37 °C. For the digestion of the nonphosphorylated protein mix, the volumes of ammonium bicarbonate, iodoacetamide, and trypsin solutions were tripled. The digestion reaction was finally quenched with the addition of 11 μL of glacial acetic acid. Samples were dispensed into Eppendorf tubes in 22 μL aliquots and stored in a -70 °C freezer until further use.

2.2.3 Labeled Phosphopeptide Synthesis

The labeled phosphopeptide synthesis protocol is the same as described previously.[23] Briefly, the synthetic peptides, CH_3CH_2CO-LFTGHPEpSLEK (H_5 peptide) and CD_3CD_2CO-LFTGHPEpSLEK (D_5 peptide), were prepared using manual stepwise Fmoc-based solid-phase peptide synthesis on Fmoc-Lys(boc)-Wang resins (0.05 mol). Fmoc amino acids (0.25 mmol) were preactivated by thorough mixing with O-(benzotriazol-1-yl)-*N*,*N*,*N*',*N*',-tetramethyluronium tetrafluoroborate (0.25 mmol), 1-hydroxybenzotriazole hydrate (0.25 mmol), and *N*,*N*-diisopropylethylamine (0.38 mmol) in DMF, then coupled with the peptidyl resin for 15 min. For phosphoamino acid incorporation, Fmoc-Ser(PO(OBzl)OH-OH) was used and was coupled as described above, except a 3-fold excess of *N*,*N*-diisopropylethylamine was used. Fmoc removal was carried out using a 30% piperidine solution in DMF for 25 min with shaking. N-terminal acetylation was achieved after the final Fmoc deprotection step by the addition of 0.25 mmol of *N*,*N*-diisopropylethylamine and either 0.17 mmol of d_{10}-propionic anhydride or 0.17 mmol of propionic anhydride in DMF in the resin while shaking for 15 min. The side-chain protecting groups and resin were cleaved from the peptide with 2.5% triisopropylsilane and 2.5% water in trifluoroacetic acid for 2 h. The resulting peptides were precipitated in diethyl ether and redissolved in 25% aqueous acetic acid, then lypholized, and purified by Reverse Phase-High Performance Liquid Chromatography (RP-HPLC) using an Aquapore RP-300 column (4.6 mm; Perkin Elmer, Wellesley, MA) and a linear gradient elution with a flow rate of 1 mL/min from 0-100% B. Here solvent A was 0.1% TFA aqueous solution and solvent B was 0.089% TFA/60% acetonitrile in water. This synthesis was conducted by Amanda Palumbo at Michigan

State University. The Genomics Technology Support Facility at Michigan State University determined the concentrations of aqueous stock solutions of the H_5 and D_5 peptides by amino acid analysis. Aliquots of the stock solutions were concentrated to 100 pmol and stored at -20° C until further use.

2.2.4 Fabrication of Polyelectrolyte/Metal Oxide Films

Gold-coated silicon wafers (1.1 x 2.4 cm) were UV/ozone-cleaned for 15 min and immersed in a 1 mM solution of 3-mercaptopropionic acid (MPA) in ethanol (0.87 μL MPA in 10 mL ethanol) for 1 h to give a self-assembled monolayer (SAM) of MPA on the gold surface. Wafers were rinsed with deionized water, followed by ethanol and dried in a stream of N_2 gas. The monolayer-modified wafers were then immersed for 2 min in a pH-4.5, 0.02 M poly(allylamine hydrochloride) (PAH, molarity is given with respect to the repeating unit) solution containing 0.5 M NaCl, (pH was adjusted using HCl). The films were rinsed with deionized water for 1 min, then dried in a stream of N_2 gas. Poly(4-styrene sulfonate) (PSS) was deposited on the films by immersing the wafers for 2 min in 3 mg/mL PSS containing 0.5 M NaCl (the pH of this solution was adjusted to 2.2 with HCl). Wafers were rinsed with water for 1 min and dried in a stream of N_2 gas. Aqueous suspensions of ZrO_2 were prepared with various concentrations, including 0.1 mg/mL, 0.2 mg/mL, and 1 mg/mL. The pH of the ZrO_2 suspension was lowered to ~1.5 using HCl so that the nanoparticles were positively charged, and the suspension was sonicated to ensure even distribution of the nanoparticles. Wafers were immersed in the ZrO_2 suspension for up to 20 min (Figure 2.1). They were then washed by placing them in a dilute HCl solution, pH ~1.5, for 1 min to remove any loosely bound ZrO_2. The wafers were then dried completely in a stream of N_2 gas. For thicker films, additional

bilayers of PSS/ZrO_2 can be deposited. However, only one bilayer of PSS/ZrO_2 was typically employed, as discussed below. Films containing TiO_2 were prepared in the same fashion, except PSS-terminated films were immersed in a 1 mg/mL TiO_2 suspension with a pH of ~1.5 for 20 min. Wafers were again washed in dilute HCl, pH ~1.5 for 1 min and dried in a stream of N_2 gas. Wafers were originally cut to fit the reflectance FTIR spectrophotometer sample holder (1.1 x 2.4 cm). To fit in the modified stainless steel MALDI plate, which was machined to hold standard microscope slides (1.7 x 7.7 x 0.1 cm), the wafers were cut to fit the width of the modified plate (1.7 cm). Sample wells were created on the modified wafers by lightly scratching circles (2 mm diameter) onto the wafer using a tungsten carbide-tipped pen. Typically six wells were scratched per wafer and each well is able to hold 2-3 μL of aqueous solution. Wafers were attached to the modified MALDI plate using double-sided tape.

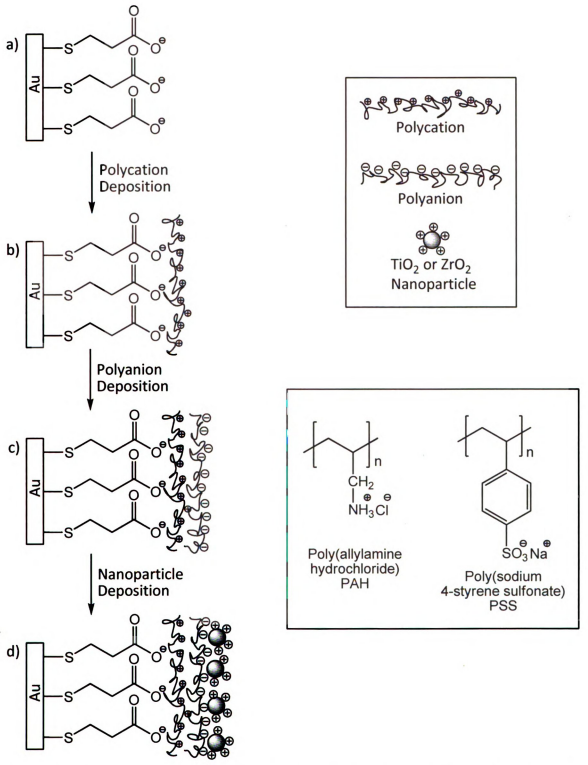

Figure 2.1: Schematic diagram showing the modification of a gold substrate with a) a SAM of MPA, followed by the deposition of b) the polycation PAH, c) the polyanion PSS, and finally d) the nanoparticles, either TiO_2 or ZrO_2. Additional bilayers can be formed by alternating steps c) and d). Inset shows the structures of the polyelectrolytes used.

2.2.5 Preparation of TiO_2-modified MALDI Plate

A second method of preparation of a TiO_2-modified MALDI plate was adapted from Qiao, et al.[22] In this case, 1 g of TiO_2 nanoparticles was first heated at 300 °C for 2 h and the nanoparticles were separated by grinding them for 2 h using a mortar and pestle. Throughout these two hours, a total of 1 mL of 10% acetic acid was added to the nanoparticles to keep them wet. A 100 mg/mL suspension was then prepared in 90% ethanol and sonicated for 1 h, and a 4 mg/mL suspension was prepared by diluting the 100 mg/mL TiO_2 suspension with water and sonicating for 15 min. Sample wells were machined into a magnetic plate (1.65 x 7.65 cm) which fits precisely into a stainless steel MALDI plate holder (this plate is the same size as a standard microscope slide and attaches to the MALDI plate holder which contains magnets) as shown in Figure 2.2. Both the plate and the holder were available through Thermo for the vMALDI LTQ XL mass spectrometer. The wells are 0.23 mm deep and have a diameter of either 2.4 mm or 3.2 mm. Either 1 or 2 μL of the 4 mg/mL TiO_2 suspension was spotted into the machined wells and allowed to dry in the air at room temperature. The plate was heated under nitrogen in a furnace which was ramped from room temperature to 400 °C in ~40 min and held at 400 °C for 1 h. The plate was then allowed to cool to room temperature and stored in a desiccator until further use.

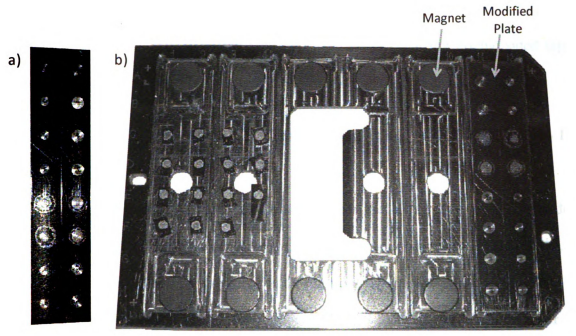

Figure 2.2: Photograph of a) TiO_2-modified magnetic MALDI plate with machined wells, and b) the MALDI sample plate holder, which contains magnets.

2.2.6 Enrichment Protocol for Plates Modified with Polyelectrolyte/Metal Oxide Films

For analysis of protein digests, 1 μL of digest solution was spotted in the 2 mm diameter wells that were scratched in the polyelectrolyte/metal oxide-modified gold wafers, as described above. Either 0.1 M acetic acid or 0.1% trifluoroacetic acid (TFA) was used as the solution from which digests were loaded on the plate. Samples were incubated for 1 h, and additional loading solution (0.5 or 1 μL without digest) was added to the wells as the sample solution evaporated throughout the incubation time. After 1 h, a modified wafer with six sample wells was rinsed with 5-10 mL of 66 mg/mL 2,5-dihydroxybenzoic acid (DHB) in 80% acetonitrile/0.1% TFA, followed by 5-10 mL of 80% acetonitrile/0.1% TFA solution, then dried under a stream of N_2 gas. After drying, 1 μL of 0.1% TFA was added to each well, followed immediately by 0.25 μL of 40 mg/mL

DHB solution (1:4 acetonitrile: 1% phosphoric acid). After crystallization of the DHB matrix, the wafer was affixed to the modified MALDI target using double-sided tape. The same protocol was followed for both TiO_2 and ZrO_2-modified plates.

2.2.7 Protocol for Enrichment of H_5 Peptide Using Plates Modified with TiO_2 by Heating

Stock solutions containing 100 pmol of either the H_5 or D_5 synthetic peptides were prepared in 200 μL of deionized water, and solutions containing 125, 62, 31, 16, 8 fmol/μL were prepared from the original stock solutions by serial dilutions with water. A calibration curve obtained through conventional MALDI analysis was prepared prior to enrichment to compare the signals due to the H_5 and D_5 peptides. The matrix solution used for conventional analysis was 1 μL of 10 mg/mL DHB solution (1:1 acetonitrile: 1% H_3PO_4). For the enrichment of the synthetic H_5 phosphopeptide using the plates modified with TiO_2 (Figure 2.3), 1 pmol of peptide mix, consisting of BSA, phosphorylase b, and esterase, in 0.1% TFA was spotted in the sample wells, followed immediately by 125 fmol of H_5 peptide. The H_5 peptide was incubated for 30 min and 0.1% TFA solution was periodically added as the solvent evaporated throughout the incubation time. The plate containing four wells was rinsed with 10 mL of 20 mg/mL DHB solution (1:1 acetonitrile: 0.2% TFA), followed by 10 mL of 1:1 acetonitrile: 0.2% TFA solution, then dried under a stream of N_2 gas. Phosphopeptides were desorbed using 1 μL of 1% phosphoric acid, and 125 fmol of the D_5 peptide was added as an internal standard just prior to addition of 0.25 μL of matrix solution, which contained 40 mg/mL DHB in 1:1 acetonitrile: 1% H_3PO_4). Upon crystallization of the matrix, the plate was easily fixed to the modified MALDI plate via the magnets in the plate.

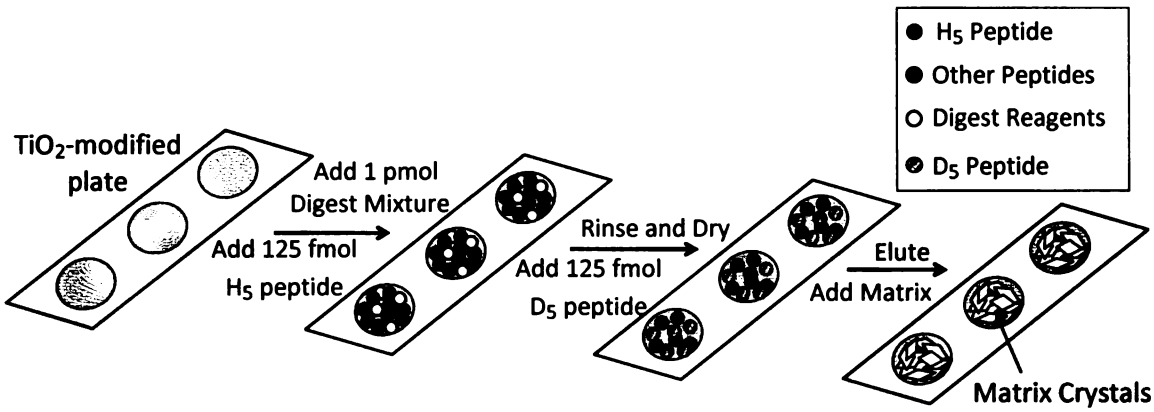

Figure 2.3: Schematic of the enrichment process used to determine the recovery of the H_5 peptide from a protein digest mixture using a TiO_2 modified plate. The D_5 peptide served as an internal standard.

2.2.8 Characterization and Instrumentation

The polyelectrolyte layers were characterized by reflectance FTIR spectrometry using a Nicolet Magna 560 spectrophotometer with a Pike grazing angle (80°) accessory. The thicknesses of the polyelectrolyte layers were determined using a rotating analyzer spectroscopic ellipsometer (J. A. Woollam, M-44), assuming a film refractive index of 1.5. Scanning Electron Microscopy (SEM) was used to characterize the TiO_2 nanoparticles deposited on PSS-terminated films. All SEM images shown here were taken by David Dotzauer of Michigan State University using a Hitachi S-4700-II field-emission electron microscope. Mass spectra were obtained using a MALDI linear ion trap mass spectrometer (Thermo vMALDI LTQ XL), and tandem MS was carried out using collision-induced dissociation (CID). For most samples, MS/MS, wideband MS/MS, and MS^3 were used for the identification of phosphopeptides. All spectra were obtained in positive ion mode.

2.3 Results and Discussion

2.3.1 Fabrication and Characterization of Polyelectrolyte/Metal Oxide-Modified Plates

The fabrication of the polyelectrolyte/metal oxide-modified plates (Figure 2.1) was characterized using reflectance FTIR spectroscopy, and the film thickness after each step was determined using ellipsometry. The reflectance FTIR spectra in Figure 2.4 confirm the deposition of the polyelectrolyte layers. The peak near 1730 cm^{-1} in spectrum a) is due to the acid carbonyl group of the MPA immobilized on the gold substrate. Spectrum b) which was taken after adsorption of positively charged PAH on the negatively charged MPA SAM contains a peak near 1570 cm^{-1}, which is probably due to the primary amine of PAH and the formation of the acid salt in the monolayer. Finally, spectrum c) in Figure 2.4 confirms the adsorption of the polyanion, PSS, onto the MPA-PAH film. The two sharp peaks at 1035 cm^{-1} and 1010 cm^{-1} are characteristic of the sulfonate group in PSS, as are the peaks at 1220 and 1174 cm^{-1}. These MPA-PAH-PSS films are approximately 30 Å thick, as determined by ellipsometry.

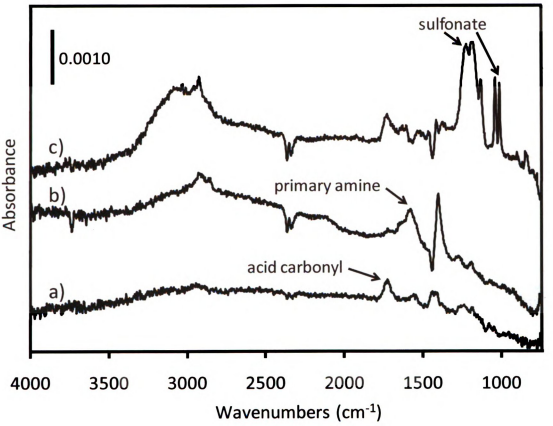

Figure 2.4: Reflectance FTIR spectra of a) a self-assembled monolayer of MPA on a gold substrate, and the same film after b) adsorption of the polycation, PAH, and finally c) adsorption of the polyanion, PSS.

Although reflectance FTIR spectroscopy and ellipsometry were used to characterize and confirm the growth of each of the polyelectrolyte layers, the deposition of either TiO_2 or ZrO_2 onto PSS could not be confirmed using these analytical tools. These metal oxides interfered with the IR signal, as well as the ellipsometric data, most likely due to a high surface roughness. Therefore the deposition of nanoparticles was examined using SEM. The image in Figure 2.5a shows a widespread distribution of TiO_2 nanoparticles on a PSS-terminated film, but the nanoparticles have aggregated (Figure 2.5b). These TiO_2 nanoparticle aggregates are approximately 2-3 μm in diameter.

Despite this aggregation, the metal oxide nanoparticles were still able to interact with and enrich the phosphopeptides from the protein digest, as discussed below.

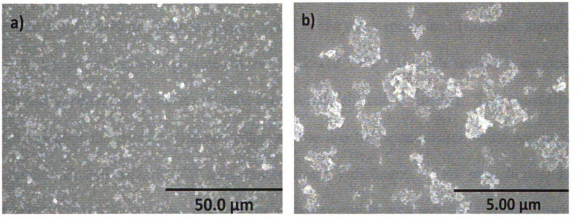

Figure 2.5: SEM images of a) TiO_2 adsorbed on an MPA-PAH-PSS modified gold substrate and b) a magnified image of the same film. TiO_2 was adsorbed from a 1 mg/mL suspension.

2.3.2 Analysis of Ovalbumin Digests Using MALDI-MS

Initial studies of the ability of polyelectrolyte/metal oxide-modified MALDI targets to enrich phosphopeptides focused on tryptic digests of ovalbumin, which has two phosphorylation sites and contains a disulfide bond (Figure 2.7). DTT and iodoacetamide were added to the ovalbumin digests for the cleavage of the disulfide bond and the carbamidomethylation of the resulting cysteine residues, respectively. Conventional MALDI-MS analysis of an ovalbumin digest (Figure 2.6a) shows the presence of three monophosphorylated peptides, which have $[M+H]^+$ m/z values of 2089 (EVVGpSAEAGVDAASVSEEFR), 2512 (LPGFGDpSIEAQCGTSVNVHSSLR), and 2903 (FDKLPGFGDpSIEAQCGTSVNVHSSLR). This third phosphopeptide at 2903 is the result of a miscleavage at lysine (K62). Although the conventional mass spectrum shows signals due to all three phosphorylated peptides, the use of ZrO_2-modified gold

plates to selectively enrich phosphopeptides greatly simplifies the mass spectrum by essentially eliminating signals due to nonphosphorylated peptides (Figure 2.6b). After enrichment on a gold plate modified with a PAH/PSS/TiO_2 film, the monophosphorylated peptide at *m/z* 2089 gives the dominant signal in the mass spectrum. However, signals due to the phosphorylated peptides at *m/z* 2512 and 2903 are much smaller compared with that at 2089; the signal at *m/z* 2903 is especially difficult to identify. This unusually high signal of the peptide with *m/z* 2089 may be due to the additional acidic residues, glutamic (E) and aspartic (D) acid, that enhance enrichment. This phosphopeptide contains five acidic residues, whereas the phosphopeptide with *m/z* 2512 contains two acidic residues and the third phosphopeptide with *m/z* 2903 contains three. The peptide with m/z 2089 may also ionize particularly well, as suggested by its relatively strong signal in the conventional MALDI mass spectrum. While there is minimal non-specific binding of nonphosphorylated peptides, the signal at *m/z* 1774 is likely due to the nonphosphorylated peptide ISQAVHAAHAEINEAGR, which contains two histidine and two glutamic acid residues. One study noted that these amino acid residues may have some affinity for metal oxides.[17] Glutamic acid, aspartic acid, and cysteine residues can be derivatized by *O*-methyl esterification to minimize non-specific binding,[15] but this additional step would take away from the advantages of rapid analysis using these modified plates. Incomplete esterification also complicates mass spectra. There is also a peak present at *m/z* 2132, which is 43 *m/z* units higher than the signal at 2089. This peak may be due to the carbamylation of the phosphopeptide at *m/z* 2089, which can result from heating protein digests containing urea. The peaks at *m/z* 697 and 1045 could not be identified, and neither peak was present in the conventional MALDI mass spectrum.

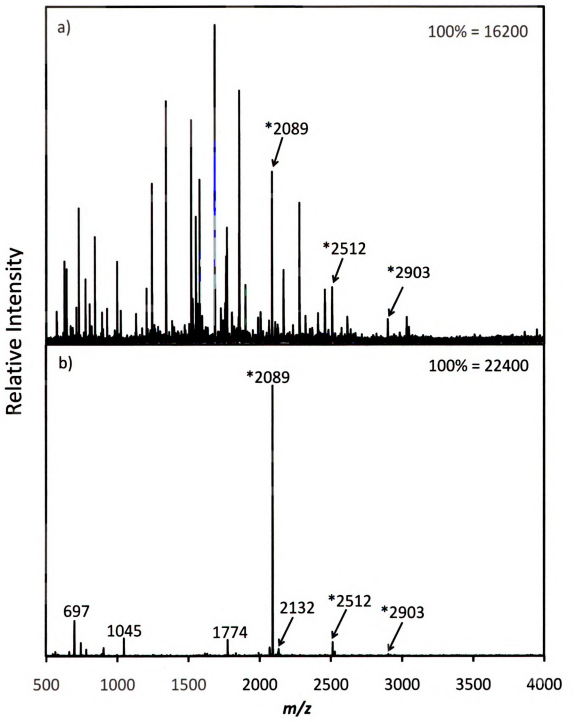

Figure 2.6: Positive ion MALDI mass spectra of 2 pmol of ovalbumin digest analyzed using a) conventional MALDI-MS, and b) a ZrO_2-PSS-PAH-MPA-modified gold plate with 0.1% TFA loading solution, rinsing with 66 mg/mL DHB (80% ACN/0.1% TFA) solution and 80% ACN/0.1% TFA solution, and addition of matrix prior to MALDI-MS. Asterisks (*) represent phosphorylated peptides.

```
  1  MGSIGAASME  FCFDVFKELK VHHANENIFY CPIAIMSALA MVYLGAKDST  RTQINKVVRF  60
 61  DKLPGFGDpSI EAQCGTSVNV HSSLRDILNQ ITKPNDVYSF SLASRLYAEE  RYPILPEYLQ 120
121  CVKELYRGGL  EPINFQTAAD QARELINSWV ESQTNGIIRN VLQPSSVDSQ  TAMVLVNAIV 180
181  FKGLWEKAFK  DEDTQAMPFR VTEQESKPVQ MMYQIGLFRV ASMASEKMKI  LELPFASGTM 240
241  SMLVLLPDEV  SGLEQLESII NFEKLTEWTS SNVMEERKIK VYLPRMKMEE  KYNLTSVLMA 300
301  MGITDVFSSS  ANLSGISSAE SLKISQAVHA AHAEINEAGR EVVGpSAEAGV  DAASVSEEFR 360
361  ADHPFLFCIK  HIATNAVLFF GRCVSP
```

Figure 2.7: Amino acid sequence for chicken egg ovalbumin (Swiss-Pro: P01012). Phosphorylation sites are designated by bold and italic type and a (*p*) label. Tryptic cleavage sites are labeled in bold.

Tandem mass spectrometry (MS/MS) is a useful tool for accurate identification of phosphopeptides present in mass spectra. Without MS/MS, it is possible to incorrectly assign *m/z* values to phosphorylated species, especially at larger *m/z* values. All MS/MS analysis was conducted using a vMALDI linear ion trap mass spectrometer with low energy collision-induced dissociation (CID). In Figure 2.8 the precursor ion selected was the monophosphorylated peptide EVVGpSAEAGVDAASVSEEFR, $[M+H]^+$ *m/z* 2089. The loss of water (18 Da) from this precursor ion, $[M+H-H_2O]^+$, yields the dominant peak in Figure 2.8a. Also present, although with much lesser intensity, is the signal due to loss of 98 Da from the precursor ion, at *m/z* 1991, and may be due to the loss of either phosphoric acid, $[M+H-H_3PO_4]^+$, or the loss of water and monophosphate, $[M+H-H_2O-HPO_3]^+$.[24] The signal at *m/z* 1973 is due to loss of both water and phosphoric acid (116 Da), $[M+H-H_2O-H_3PO_4]^+$. To confirm the identification of the $[M+H-H_2O-H_3PO_4]^+$ peak at *m/z* 1973, MS^3 was used to identify the amino acid residues present in this peak (Figure 2.8b). In general, $b_{(n\geq 2)}$ and y_n type ions are most commonly formed when a protonated peptide is fragmented using CID. Signals from several y_n type ions were present in the MS^3 spectrum in Figure 2.7b, confirming that the peak at *m/z* 2089 is the phosphorylated peptide.

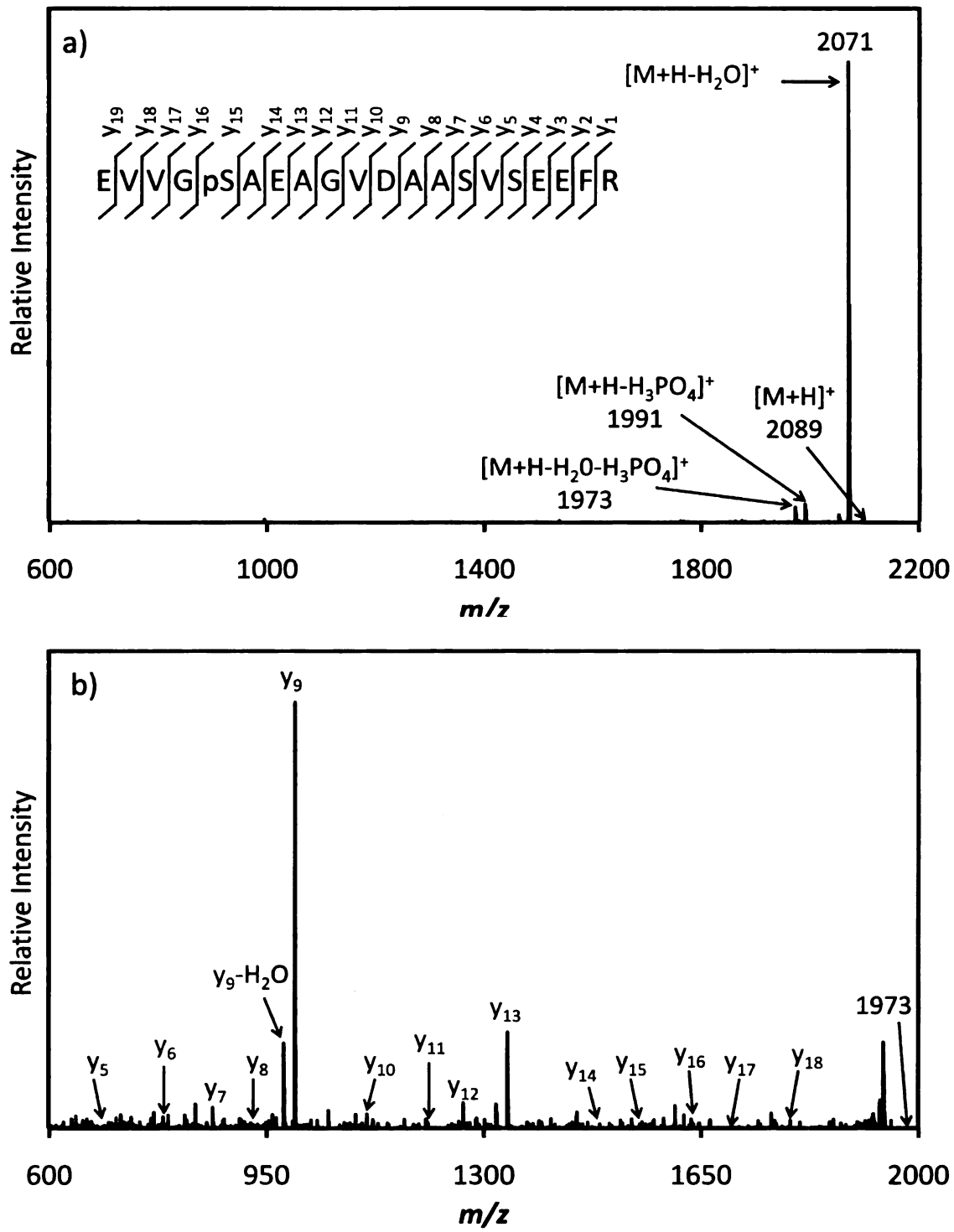

Figure 2.8: Multistage tandem mass spectrometry of a monophosphorylated peptide ion, *m/z* 2089, isolated from 2 pmol of ovalbumin digest enriched using a ZrO_2-PSS-PAH-MPA-modified gold plate: a) CID MS/MS of the *m/z* 2089 isolated $[M+H]^+$ precursor ion, and b) CID MS^3 of *m/z* 1973 isolated from the MS/MS product ion spectrum of *m/z* 2089 from spectrum a). In b) several y_n type ions were identified.

2.3.3 Calibration of H_5 and D_5 Signals for Recovery Analysis

A calibration curve for the synthetic H_5 and D_5 phosphopeptides, where the D_5 peptide serves as an internal standard, allowed quantitation of the enrichment efficiency for the H_5 peptide. Since these synthetic peptides differ only in the deuterated label on the D_5 peptide (Figure 2.9), an equimolar mixture of the H_5 and D_5 peptides should result in approximately equal ion intensities in the MALDI mass spectrum. The calibration curve was created by varying the amount of H_5 peptide (125, 62, 31, 16, and 8 fmol) in samples containing 125 fmol of D_5 peptide. These H_5 amounts were chosen in the MALDI-MS linear dynamic range for these synthetic phosphorylated peptides. Figure 2.10 shows the ratio of the peak intensities of the H_5 and D_5 peptides (I_{H5}/I_{D5}) versus the amount of H_5 peptide in the sample. The plot is linear, and the desorption and ionization efficiencies of the two peptides are similar, although signals from the H_5 peptide are as much as 20% less than expected for equal sensitivities for the two peptides.

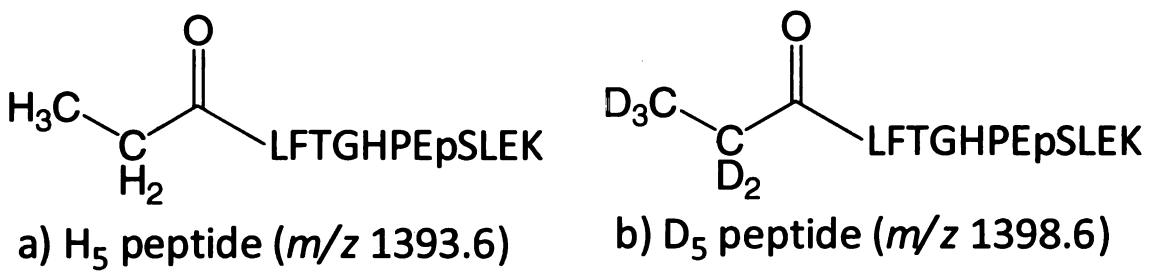

Figure 2.9: Sequence and *m/z* values of labeled synthetic phosphorylated peptides, a) H_5 peptide and b) D_5 peptide.

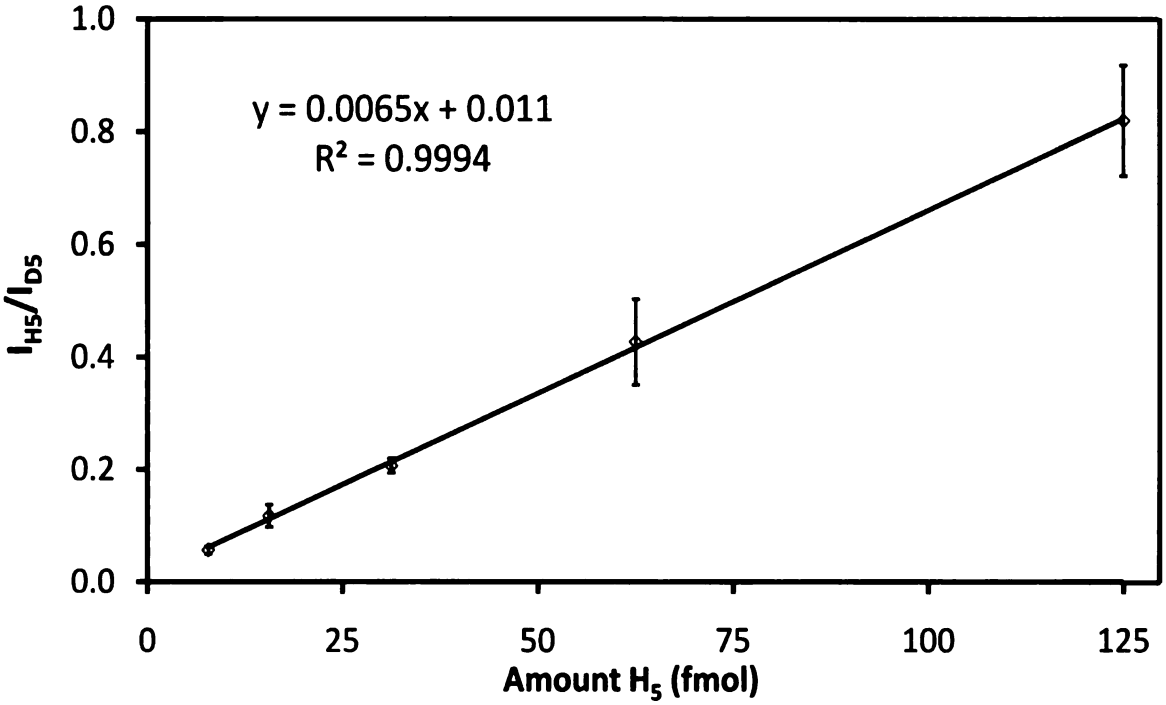

Figure 2.10: Calibration curve comparing the ratio of peak intensities (I_{H5}/I_{D5}) of synthetic phosphopeptides, H_5 and D_5, from MALDI-MS spectra as a function of the amount of H_5 peptide. 125 fmol of D_5 peptide was present in each sample as an internal standard.

2.3.4 Enrichment of H_5 Peptide from Peptide Mixtures Using Plate Modified by Heating of Nanoparticles.

Initial studies of the ability of the TiO_2-modified plates to enrich phosphopeptides examined the recovery of the H_5 peptide from a mixture containing digested BSA, esterase, and phosphorylase b. These studies utilized magnetic plates modified by simple heating of TiO_2 nanoparticles. One pmol of the digest mixture in 0.1% TFA was spotted within a TiO_2-modified well, followed by addition of 125 fmol of H_5 peptide in 0.1% TFA, and the mixture was incubated for 30 min. After rinsing with 10 mL of 20 mg/mL DHB (1/1 ACN/0.1% TFA), followed by 10 mL of 1/1 ACN/0.1% TFA, the plate was dried under N_2 gas. To desorb the H_5 phosphopeptide, 1 μL of 1% phosphoric acid was

added to the well, followed immediately by 125 fmol of the D_5 peptide as an internal standard. Finally, 0.25 μL of matrix solution (40 mg/mL DHB in 1/1 ACN/1% H_3PO_4) was added to the well. Figure 2.11a shows the mass spectrum of the H_5 peptide that was enriched from the peptide mixture, and Figure 2.11b shows an expanded region around the *m/z* values of the H_5 and D_5 peptides, 1393.6 and 1398.6, respectively.

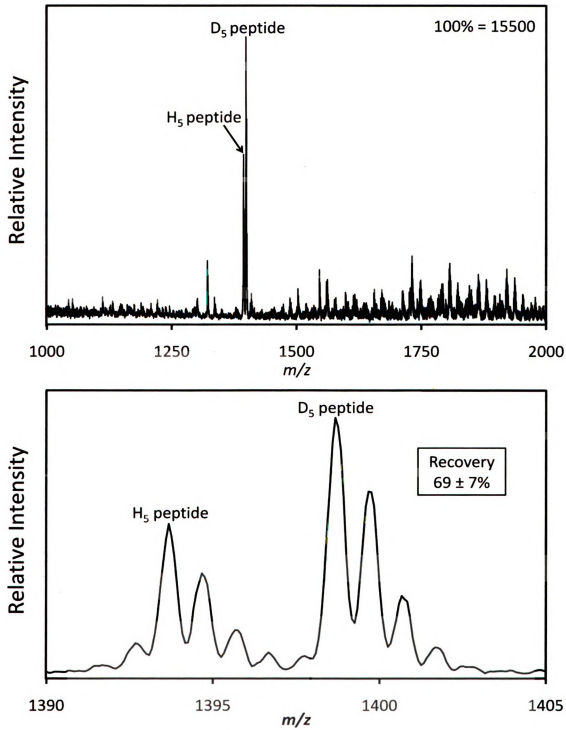

Figure 2.11: a) Positive ion MALDI mass spectrum of 125 fmol of H_5 peptide enriched from 1 pmol of a protein digest using a TiO_2-modified plate, and b) an enlarged region of the spectrum around peaks due to H_5 and D_5 peptides. 125 fmol of D_5 was added as an internal standard. The recovery of H_5 peptide from the mixture is 69 ± 7%. The modified plate was prepared by heating TiO_2 nanoparticles on a magnetic plate.

Although the full MALDI mass spectrum (Figure 2.11a) has a significant amount of noise, the recovery of the synthetic phosphopeptide, H_5, from the peptide mix containing digested BSA, esterase, and phosphorylase b, is 69 ± 7%, as determined from the ratio of the H_5 and D_5 signals and the calibration curve in Figure 2.9. Much of the noise present in Figure 2.11a is likely due to impurities found on the plate, due to the machining process. The plate was cleaned prior to modifying with TiO_2; however, this may not have removed all of the impurities from the machining process. Nevertheless, the 70% recovery is comparable to and even higher than for several commercially available IMAC and metal oxide materials, as described in Table 2.1. When analyzing the recovery of 125 fmol of this same H_5 peptide from 1 pmol of the same peptide mixture using the $ZipTip_{MC}$ pipette tips containing Fe (III) complexes, our group previously determined that this commercially available IMAC material has a recovery of only 12 ± 2%. Pipet tips with TiO_2 or ZrO_2 embedded into the tip walls (Glygen) exhibited recoveries of 22 ± 8% and 68 ± 5% for the ZrO_2 and TiO_2-containing tips, respectively.[23]

Table 2.1: Comparison of the ability of several commercially available enrichment materials and the TiO_2-modified plates to recover 125 fmol of H_5 peptide from 1 pmol of nonphosphorylated digest mixture.[23]

Enrichment Material	**Percent (%) Recovery of H_5 Peptide from Digest Mixture**
Fe(III)-NTA Monolayer	9 ± 2
Millipore $ZipTips_{MC}$	12 ± 2
Qiagen IMAC Chip	13 ± 3
Glygen ZrO_2 NuTips	22 ± 8
Glygen TiO_2 NuTips	68 ± 5
TiO_2 Plates by Heating	**69 ± 7**
Fe(III)-NTA-PHEMA	73 ± 12

2.4 Conclusions

Both types of metal oxide-modified plates allow separation and detection of phosphopeptides from protein digests without any additional purification prior to enrichment. Specifically, the PAH/PSS/ZrO_2 plates significantly improved the signal due to the monophosphorylated peptide with *m/z* 2089 from an ovalbumin digest. The other two phosphopeptides in the digest can also be detected using this enrichment method, but their signals are low. The use of this modified plate removed virtually all signal due to nonphosphorylated peptides initially present in the protein digest. While these PAH/PSS/ZrO_2-modified plates selectively captured phosphopeptides from an ovalbumin digest, the ZrO_2 nanoparticles aggregated on the surface (as seen by the SEM images), and it was often difficult to create a uniform surface. The second on-plate enrichment technique employing an array of TiO_2 nanoparticles on a MALDI plate by simple heating resulted in 69 ± 7% recovery of the synthetic H_5 peptide, which is comparable to, or even significantly better than, the recovery observed from various commercially available resins. Despite the reasonably high recovery using these plates, there was a significant amount of noise present in the mass spectra due to the inability to completely clean the surface of the plate. However, both of these modified plates allow for rapid, simple on-plate enrichment techniques, which allow the detection and analysis of phosphopeptides from protein digests by MALDI-MS.

2.5 References

[1] Nelson, D. L.; Cox, M. M. *Lehninger Principles of Biochemistry*. W. H. Freeman and Company: New York, NY, **2005**.

[2] Hunter, T. *Cell.* **2001** *100*, 113-127.

[3] Duronio, V. *Biochemical Journal* **2008**, *415*, 333-344.

[4] Palfrey, H. C.; Alper, S. L.; Greengard, P. *Journal of Experimental Biology* **1980**, *89*, 103-115.

[5] Sombroek, D.; Hofmann, T. G. *Cell Death and Differentiation* **2009**, *16*, 187-194.

[6] Stamm, S. *Journal of Biological Chemistry* **2008**, *283*, 1223-1227.

[7] Turner, K. M.; Burgoyne, R. D.; Morgan, A. *Trends in Neurosciences* **1999**, *22*, 459-464.

[8] Cohen, P. *European Journal of Biochemistry* **2001**, *268*, 5001-5010.

[9] Yu, L.; Issaq, H. J.; Veenstra, T. D. *Proteomic Clinical Applications* **2007**, *1*, 1042-1057.

[10] Kratzer, R.; Eckerstrom, C.; Karas, M.; Lottspeich, F. *Electrophoresis* **1998**, *19*, 1910-1919.

[11] Stensbalk, A.; Anderson, S.; Jensen, O. N. *Proteomics* **2001**, *1*, 207-222.

[12] Zeller, M.; Koenig, S. *Analytical and Bioanalytical Chemistry* **2004**, *378*, 898-909.

[13] Dunn, J. D.; Reid, G. E.; Bruening, M. L. *Mass Spectrometry Reviews* **2009**, DOI 10.1002/mas.20219.

[14] Thingholm, T. E.; Jensen, O. N.; Larsen, M. R. *Proteomics* **2009**, *9*, 1451-1468.

[15] Ficarro, S. B.; McCleland, M. L.; Stukenberg, P. T.; Burke, D. J.; Ross, M. M.; Shabanowitz, J.; Hunt, D. F.; White, F. M. *Nature Biotechnology* **2002**, *20*, 301-305.

[16] Larsen, M. R.; Thingholm, T. E.; Jensen, O. N.; Roepstorff, P.; Jorgensen, T. J. D. *Molecular & Cellular Proteomics* **2005**, *4*, 873-886.

[17] Pinske, M. W. H.; Uitto, P. M.; Hilhorst, M. J.; Ooms, B.; Heck, A. J. R. *Analytical Chemistry* **2004**, *76*, 3935-3943.

[18] Wilson-Grady, J. T.; Villen, J.; Gygi, S. P. *Journal of Proteome Research* **2008**, *7*, 1088-1097.

[19] Dotzauer, D; Dai, J.; Sun, L.; Bruening, M. L. *Nanoletters* **2006**, *6*, 2268-2272.

[20] Kommireddy, D. S.; Patel, A. A.; Shutava, T. G.; Mills, D. K.; Lvov, T. M. *Journal of Nanoscience and Nanotechnology* **2005**, *5*, 1081-1087.

[21] Burghard, Z.; Tucic, A.; Jeurgens, L. P. H.; Hoffmann, R. C.; Bill, J.; Aldinger, F. *Advanced Materials* **2007**, *19*, 970-974.

[22] Qiao, L.; Roussel, C.; Wan, J.; Yang, P; Girault, H. H.; Liu, B. *Journal of Proteome Research* **2007**, *6*, 4763-4769.

[23] Dunn, J. D.; Igrisan, E. A.; Palumbo, A. M.; Reid, G. E.; Bruening, M. L.; *Analytical Chemistry* **2008**, *80*, 5727-5735.

[24] Palumbo, A. M.; Reid, G. E. *Analytical Chemistry* **2008**, *80*, 9735-9747.

Chapter Three: Binding of Glutathione-S-Transferase to Glutathione-Functionalized Polymer Brushes for Protein Enrichment

3.1 Introduction

Glutathione-S-Transferase (GST) is a detoxification enzyme that defends the cell against reactive oxygen species.[1,2,3] This enzyme can also serve as a protein tag in fusion proteins,[4] which are created by joining two or more peptides or proteins together. In this case, a peptide or protein is fused to the C-terminus of GST, creating the recombinant GST-tagged protein. These fusion proteins are used in a variety of areas of research including vaccine development, immunodetecion, and analysis of protein-protein interactions.[5,6,7] Before any vaccination or immunological studies can be conducted, the GST-tagged protein must be purified from contaminants, including bacterial proteins. One domain of GST has a strong affinity for glutathione (GSH), specifically the γ-glutamic acid residue of glutathione.[8] Therefore, affinity chromatography using glutathione is one of the most commonly used purification techniques for GST-tagged proteins. Glutathione can be covalently immobilized on beads, such as agarose, and packed into a column to bind GST-tagged proteins.[9,10,11,12,13] After loading of the desired tagged protein, the beads are washed to remove any unbound species and contaminants. To elute the bound GST-tagged proteins, the column can be washed with a low pH buffer or free glutathione, which competitively displaces the GST-tagged proteins from the immobilized glutathione. The proteins can also be cleaved from the GST-tagged using a protease and then removed from the column.[14,15]

While GST-tagged proteins are typically purified using glutathione-affinity chromatography on a column, this method is relatively time consuming because the

analyte must be loaded onto the column, rinsed to remove unbound species, eluted to remove bound species, and then analyzed (Figure 3.1). This chapter discusses attempts to prepared glutathione-modified MALDI plates modified for rapid, on-probe capture of GST-tagged proteins. In principle, GST-tagged proteins can be bound to the glutathione immobilized on the modified-surface and directly analyzed on the plate, increasing throughput.

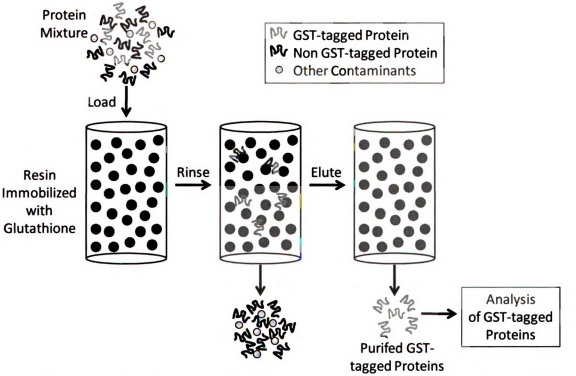

Figure 3.1: Schematic diagram showing the general procedure for separation of GST-tagged proteins using a column. The sample is loaded onto a column packed with glutathione-modified beads, rinsed to remove any non-GST-tagged proteins and contaminants, and finally the GST-tagged proteins bound to the resin are eluted and collected for further analysis. Figure adapted from Dunn et al.[16]

Reduced glutathione is a tripeptide consisting of glycine, cysteine, and γ-glutamic acid residues, where glutamic acid is bound to cysteine through its carboxyl group (Figure 3.2). This chapter describes immobilization of reduced glutathione on various polymer-modified films via reaction of the thiol group on the cysteine residue with

poly(acrylic acid) (PAA) and poly(hydroxyethyl methacrylate) (PHEMA) films. Additionally, initial studies of the binding of free GST to these plates were conducted to examine the feasibility of potentially binding GST fusion proteins.

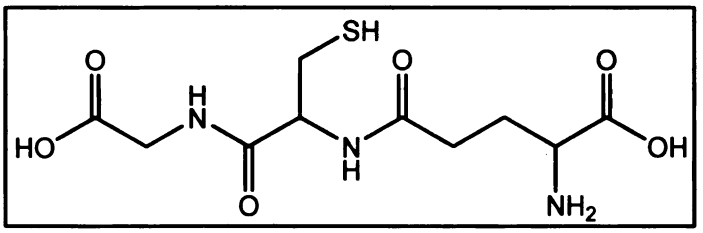

Figure 3.2: Structure of reduced L-glutathione, which consists of glycine, cysteine and γ-glutamic acid residues.

3.2 Experimental

3.2.1 Reagents and Materials

Silicon (100) wafers (Silicon Quest International) were sputter coated with 20 nm of chromium, followed by 200 nm of gold by Lance Goddard Associates (Foster City, CA). The reagents used for modifying the gold-coated plates include 11-mercaptoundecanoic acid (Aldrich), ethyl chloroformate (Aldrich), 4-methylmorpholine (Aldrich), methanesulfonic acid (Mallinckrodt), dichloromethane (Mallinckrodt), 11-mercaptoundecanol (Aldrich), 2-bromoisobutyryl bromide (Aldrich), triethylamine (Jade Scientific), 2-hydroxyethyl methacrylate (Aldrich), cupric bromide (Aldrich), cuprous chloride (Aldrich), 2,2'-bipyridine (Aldrich), succinic anhydride (J.T. Baker), 4-dimethylaminopyridine (Sigma), *N*-(3-dimethylaminopropyl)-*N'*-ethylcarbodiimide hydrochloride (Sigma), *N*-hydroxysuccinimde (Aldrich), bromoacetyl chloride (Aldrich), pyridine (Jade Scientific), *N*-(2-aminoethyl)maleimide trifluoroacetate (Fluka), tetrahydrofuran (Mallinckrodt), and reduced L-glutathione (GSH, Sigma). Glutathione-s-transferase from equine liver (Sigma) was used in studies of binding to substrates

modified with immobilized glutathione. Dimethylformamide (Spectrum) was dried using 3-Å molecular sieves (Spectrum), and deionized water was obtained from a Millipore purification system (Milli-Q, 18 MΩcm). HPLC grade methanol (Sigma), isopropyl alcohol (EMD), and ammonium hydroxide (Columbus Chemical Industries) were used to clean the conventional stainless steel MALDI plate according to Thermo Scientific's deep cleaning procedure, as described in Chapter 2. The plate was stored in a nitrogen-filled glove bag while not in use. The matrix used for all MALDI-MS experiments in this chapter was 1 μL of a 10 mg/mL 2,5-dihydroxybenzoic acid (DHB, Aldrich) in 1:1 HPLC grade acetonitrile (EMD): deionized water. This solution was applied directly to the protein sample on the conventional stainless steel MALDI plate. Slide-A-Lyzer Dialysis cassettes (Pierce Biotechnology Inc.) were used for the dialysis of glutathione-s-transferase. The reagents used for the purification of this protein through dialysis include glacial acetic acid (Spectrum), sodium acetate (Sigma), sodium phosphate dibasic (Spectrum), and potassium phosphate monobasic (Spectrum). Trifluoroacetic acid (Aldrich) was employed for desalting of Glutathione-S-Transferase using $ZipTip_{C18}$ pipette tips (Millipore).

3.2.2 Fabrication of Glutathione-Functionalized PAA Films

Gold-coated silicon wafers (1.1 x 2.4 cm) were UV/ozone-cleaned for 15 min and immersed in a 1 mM solution of 11-mercaptoundecanoic acid (MUA) in ethanol (2.2 mg MUA in 10 mL ethanol) for 1 h to form a self-assembled monolayer (SAM). Wafers were then rinsed with deionized water, followed by ethanol and dried under a stream of nitrogen gas. The MUA SAM was activated by immersing the wafers in 100 mM ethyl chloroformate, 90 mM 4-methylmorpholine in *N,N'*-dimethylformamide (DMF) (100 μL

of ethyl chloroformate and 100 μL of 4-methylmoropholine in 10 mL of DMF) for 10 min until the solution turned yellow. Activated films were rinsed with ethyl acetate and dried under a stream of N_2. Polymer was attached to the films by immersing wafers in a solution of amino-terminated poly(*tert*-butyl acrylate) (PTBA) (0.4 g PTBA in 10 mL of DMF) for 1 h. Amino-terminated PTBA was synthesized as described previously.[17] Polymer films were then rinsed with ethanol and dried with nitrogen gas. PTBA films were hydrolyzed to form poly(acrylic acid) (PAA) by immersing wafers in a solution of 0.15 M methanesulfonic acid in dichloromethane (100 μL of $MeSO_3H$ in 10 mL of CH_2Cl_2) for 10 min. Hydrolyzed films were rinsed with ethanol followed by deionized water and dried under a stream of nitrogen. To create thicker films, a second layer of PTBA was attached to the film by first activating the initial layer of PAA with ethyl chloroformate and 4-methylmoropholine in DMF as before. The second layer of polymer was then attached by immersing activated films in a solution of PTBA in DMF and hydrolyzing the polymer to form a bilayer of PAA. For glutathione attachment, this bilayer of PAA was first activated with 50 mM *N*-(3-dimethylaminopropyl)-*N*'-ethylcarbodiimide hydrochloride (EDC, 0.096 g) and 50 mM *N*-hydroxysuccinimide (NHS, 0.058 g) in 10 mL water for 30 min. The activated bilayer of PAA was rinsed with deionized water, followed by ethanol and dried under a stream of N_2 gas. Reduced glutathione was immobilized on the activated films (Figure 3.3) by immersing wafers in 33 mM glutathione (GSH) in deionized water (0.1 g glutathione in 10 mL water) for ~24 h at 37 °C. Wafers were finally rinsed with deionized water and dried under N_2. In an attempt to bind glutathione-S-transferase (GST) to the glutathione-functionalized films prior to GST purification by dialysis and desalting by ZipTips$_{TM}$, 100 μL of 1 mg/mL of

an aqueous undialyzed GST solution was dispensed on the polymer brush so that the entire gold-coated wafer was covered with the GST solution for 1 h. The film was rinsed with ethanol and dried under a stream of nitrogen gas.

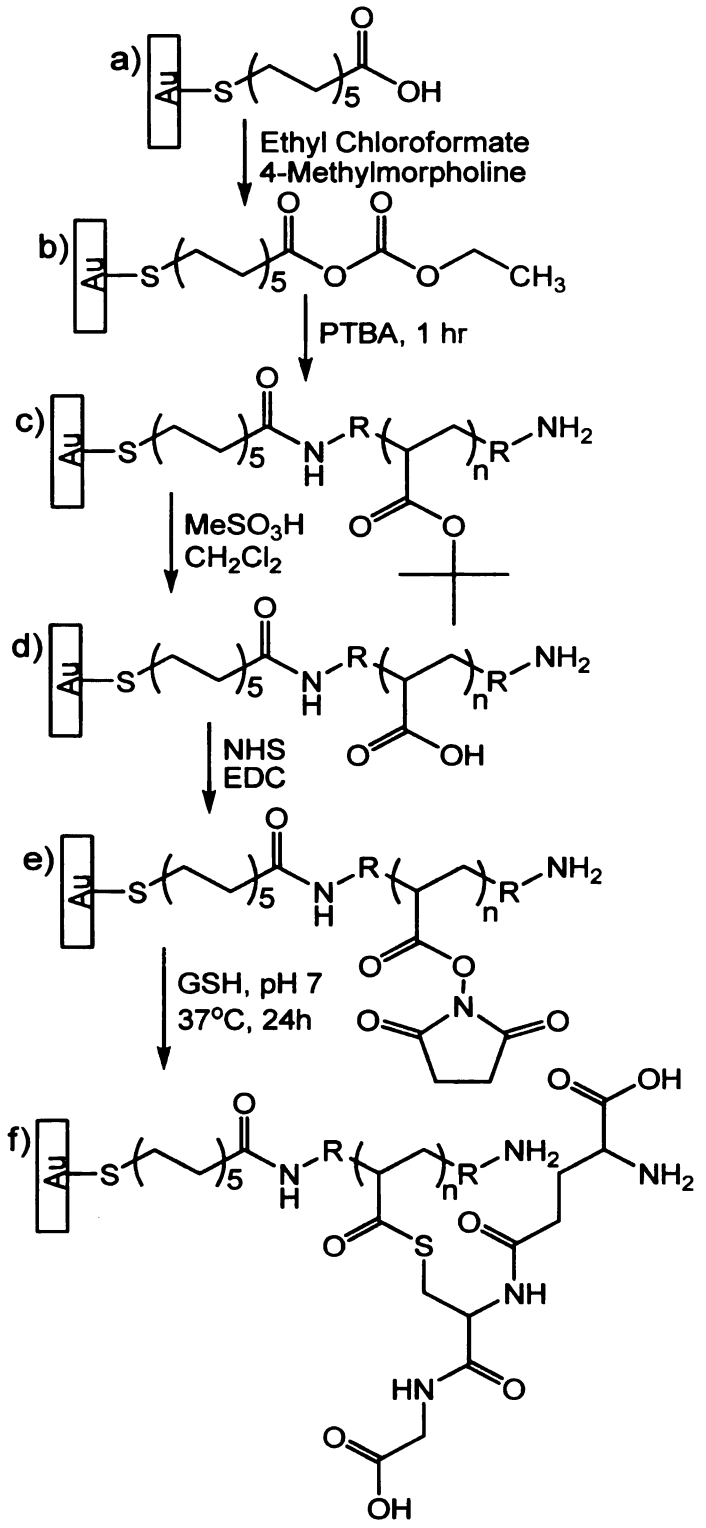

Figure 3.3: Schematic diagram showing a gold-coated substrate after a) formation of an MUA SAM, b) activation of the MUA SAM, c) attachment of PTBA, d) hydrolysis of PTBA to give immobilized PAA, e) activation of PAA with NHS/EDC, and f) immobilization of glutathione. In some cases, the PAA of step d was activated with ethyl chloroformate, and steps c, d, and e were repeated prior to immobilization of glutathione.

3.2.3 Fabrication of Glutathione-functionalized PHEMA Brushes Using Succinic Anhydride and NHS/EDC

Gold-coated silicon wafers (1.1 x 2.4 cm) were UV/ozone-cleaned for 15 min and immersed in a 1 mM solution of mercaptoundecanol (MUD) in ethanol (4.1 mg MUD in 20 mL ethanol) for ~16 h to form an MUD SAM. Wafers were rinsed with deionized water followed by ethanol and dried under a stream of N_2 gas. Gold wafers (typically 8 at a time) were arranged in a crystallizing dish and placed in a nitrogen-filled glove bag. Then 0.12 M triethylamine (TEA) (0.33 mL of TEA in 20 mL dry DMF) was added to the crystallizing dish, followed by 0.1 M 2-bromoisobutyryl bromide (BIBB, 0.25 mL in 20 mL DMF) that was added dropwise with swirling over the duration of 10 min. Wafers were removed from the solution and rinsed with DMF. After drying in the glove bag for 10 min, they were removed and rinsed with ethyl acetate, deionized water, and ethanol, and then dried under a stream of N_2 gas. Reflectance FTIR was used to identify the presence of the ester carbonyl peak (~1730 cm^{-1}) resulting from the attachment of the initiator to the MUD SAM. Using freeze-pump-thaw cycling, 30 mL of 2-hydroxyethyl methacrylate (HEMA) and 30 mL of deionized water were degassed in a Schlenk flask. During the third cycle, 165 mg CuCl, 108 mg $CuBr_2$, and 640 mg 2,2'-bipyridine were added to the frozen mixture of HEMA and deionized water. The catalyst dissolved in mixture of HEMA and deionized water as it thawed. The freeze-pump-thaw cycle was completed, followed by two additional cycles. The flask was transferred to the nitrogen-filled glove bag, and the HEMA solution was distributed equally among four 20-mL scintillation vials, each containing two wafers with initiator attached to the MUD SAM. Wafers were typically immersed in the HEMA solution for 2 h, giving 45-50 nm thick

PHEMA films. The PHEMA films were removed from the vials and rinsed with DMF, deionized water, and acetone and were then characterized using reflectance FTIR spectroscopy. To convert the hydroxyl groups of the PHEMA brushes to carboxylic acid groups, the films were then immersed in a 10 mL of DMF containing 0.1 g succinic anhydride (SA) and 0.2 g 4-dimethylaminopyridine (DMAP) and heated at 55 ^{o}C for 3 h. These films were rinsed with DMF, deionized water, and ethanol and were dried under a stream of N_2 gas. The carboxylic acid groups were then activated using 50 mM *N*-(3-dimethylaminopropyl)-*N*'-ethylcarbodiimide hydrochloride (EDC, 0.096 g) and 50 mM *N*-hydroxysuccinimide (NHS, 0.058 g) in 10 mL water for 30 min. Activated films were rinsed with water and ethanol, and then dried under N_2 gas. Reduced glutathione was immobilized onto these polymer brushes (Figure 3.4) by immersing the films in a pH 6.7, 33 mM glutathione solution containing 10 mM Na_2HPO_4, 0.15 M NaCl, and 1 mM EDTA (0.1 g glutathione in 10 mL of buffer). Films were incubated for ~16 h at room temperature and were rinsed with buffer solution, followed by ethanol and dried under nitrogen. In an attempt to bind glutathione-S-transferase (GST) to the glutathione-functionalized films prior to GST purification by dialysis or desalting by ZipTips$_{TM}$, 100 μL of 1 mg/mL undialyzed GST in phosphate buffer solution (PBS, 80 mM Na_2HPO_4, 2 mM KH_2PO_4, 140 NaCl, 10 mM KCl, pH 7.4) was dispensed on the polymer brush so that the entire gold-coated wafer was covered with the GST solution for 1 h. The wafer was rinsed with buffer solution, followed by ethanol and dried under a stream of N_2 gas.

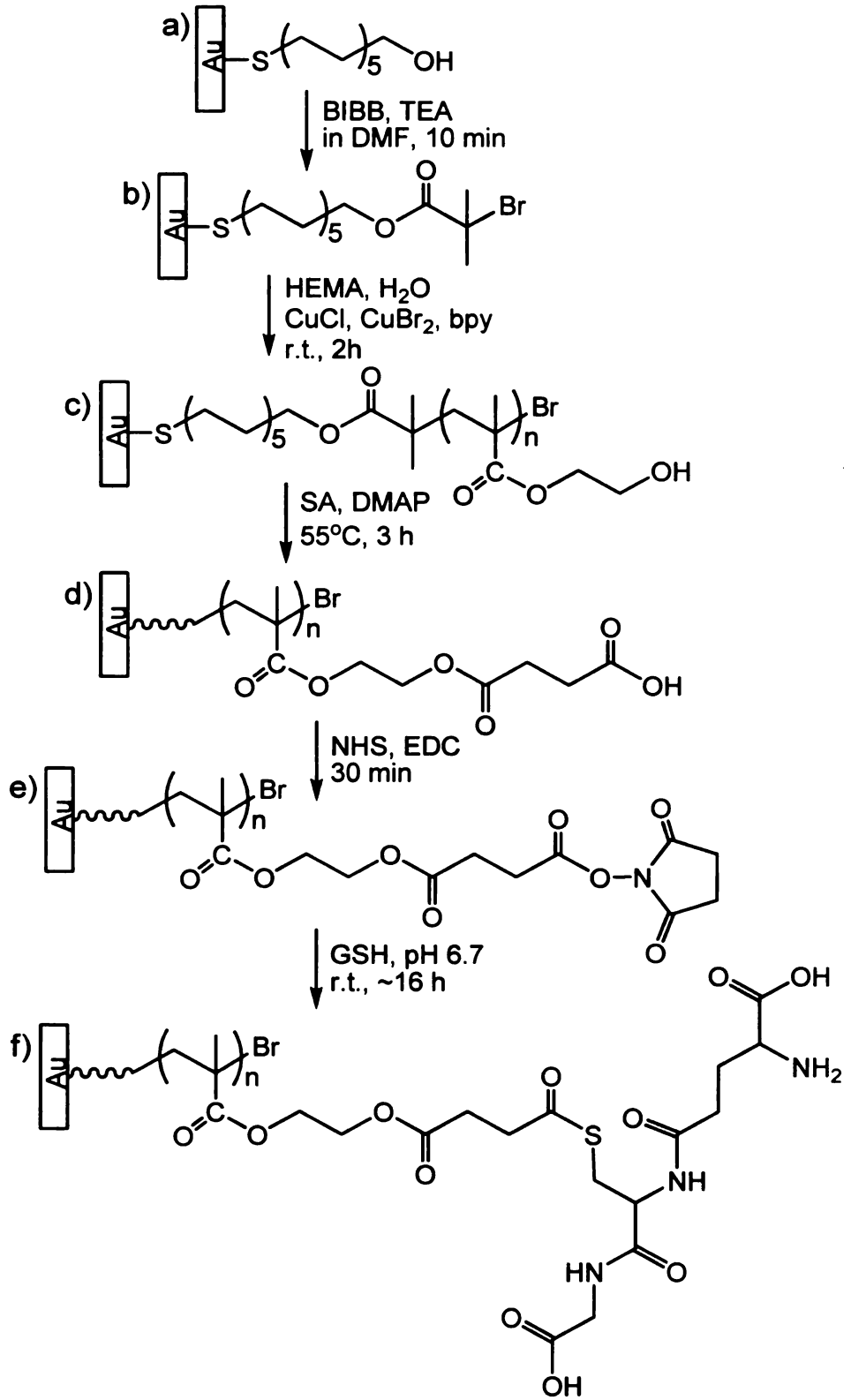

Figure 3.4: Schematic diagram of a gold-coated substrate after a) formation of an MUD SAM, b) initiator attachment to the MUD SAM, c) polymerization of HEMA, d) derivatization of PHEMA with SA, e) activation with NHS, and f) immobilization of glutathione onto PHEMA-SA films.

3.2.4 Binding of Glutathione to Brominated-PHEMA Brushes

PHEMA films were prepared on gold-coated wafers as described above. Instead of functionalizing these brushes with succinic anhydride and activating them with EDC and NHS, the films were brominated by immersing films for 1 h under N_2 in a 10 mL *N,N'*-dimethylformamide solution containing 100 μL of bromoacetyl chloride (BAC) and 100 μL of pyridine. The wafers were rinsed with DMF followed by ethyl acetate and dried under a stream of N_2 gas. Glutathione was bound to the polymer brushes (Figure 3.5) by immersing the brominated films in a pH 7.8, 33 mM aqueous glutathione solution for ~16 h. Wafers were rinsed with deionized water and dried under a stream of N_2 gas. Finally, 100 μL of 1 mg/mL GST in phosphate buffer solution (80 mM Na_2HPO_4, 2 mM KH_2PO_4, 140 NaCl, 10 mM KCl, pH 7.4) was dispensed on the glutathione-functionalized polymer brushes, completely covering the gold-coated substrate with the solution, in an attempt to bind GST to the glutathione-derivatized films prior to GST purification by dialysis or desalting by $ZipTips_{C18}$. This solution was allowed to incubate for 1 h, and the wafer was then rinsed with PBS followed by ethanol and dried under nitrogen gas.

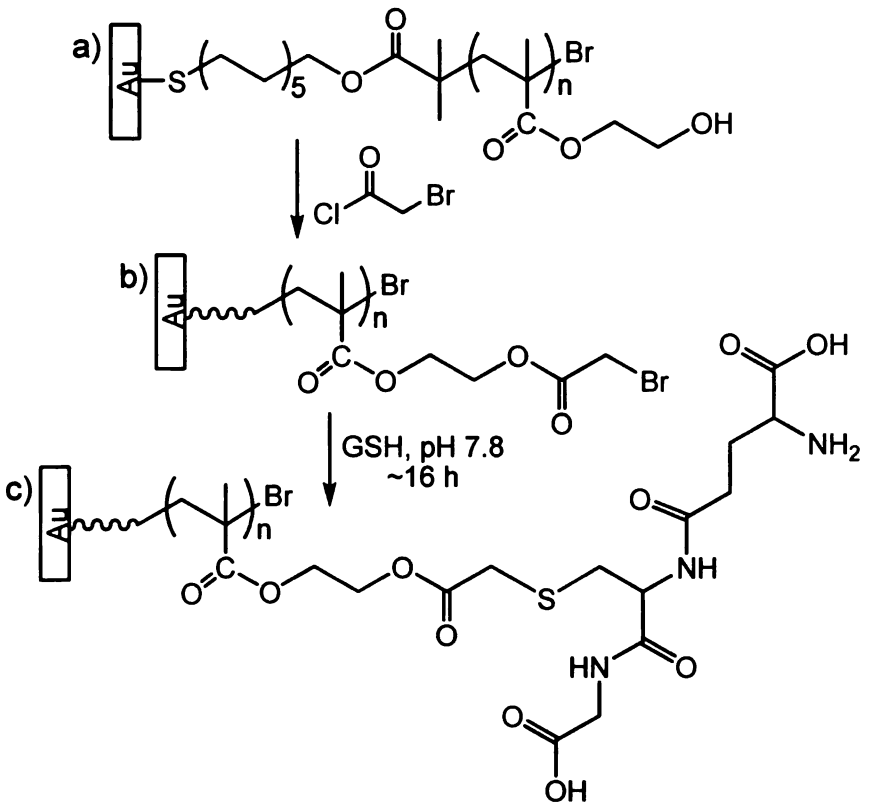

Figure 3.5: Schematic diagram of the modification of a gold-coated substrate with a) PHEMA, b) brominated-PHEMA, and c) glutathione immobilized on the PHEMA film.

3.2.5 Binding of Glutathione to Maleimide-Derivatized PHEMA Brushes

PHEMA brushes were prepared on gold-coated wafers and were derivatized with succinic anhydride and activated with EDC and NHS, as described above. Activated PHEMA-SA films were derivatized with a maleimide by immersing the films in a 10 mg/mL solution of *N*-(2-aminoethyl)maleimide trifluoroacetate in tetrahydrofuran (THF) (0.05 g maleimide in 5 mL of THF) solution, containing 100 μL of triethylamine (TEA) for ~21 h. Wafers were sonicated in DMF, then rinsed with DMF followed by ethyl acetate and dried under a stream of N_2 gas. Glutathione was immobilized on the film (Figure 3.6) by immersing the brushes in 100 mM of reduced glutathione in phosphate buffer solution (0.3 g glutathione in 10 mL of buffer solution) for 24 h. The PBS contained 80 mM Na_2HPO_4, 2 mM KH_2PO_4, 140 mM NaCl, and 10 mM KCl, at a pH of

7.4. Wafers were rinsed with PBS, followed by ethanol and dried with N_2. GST solution was dispensed onto the glutathione-immobilized PHEMA brushes as described above, in an attempt to bind GST to the film prior to GST purification by dialysis or desalting by ZipTips$_{TM}$. After incubating for 1 h, the wafer was rinsed with buffer solution followed by ethanol and was dried under a stream of nitrogen gas.

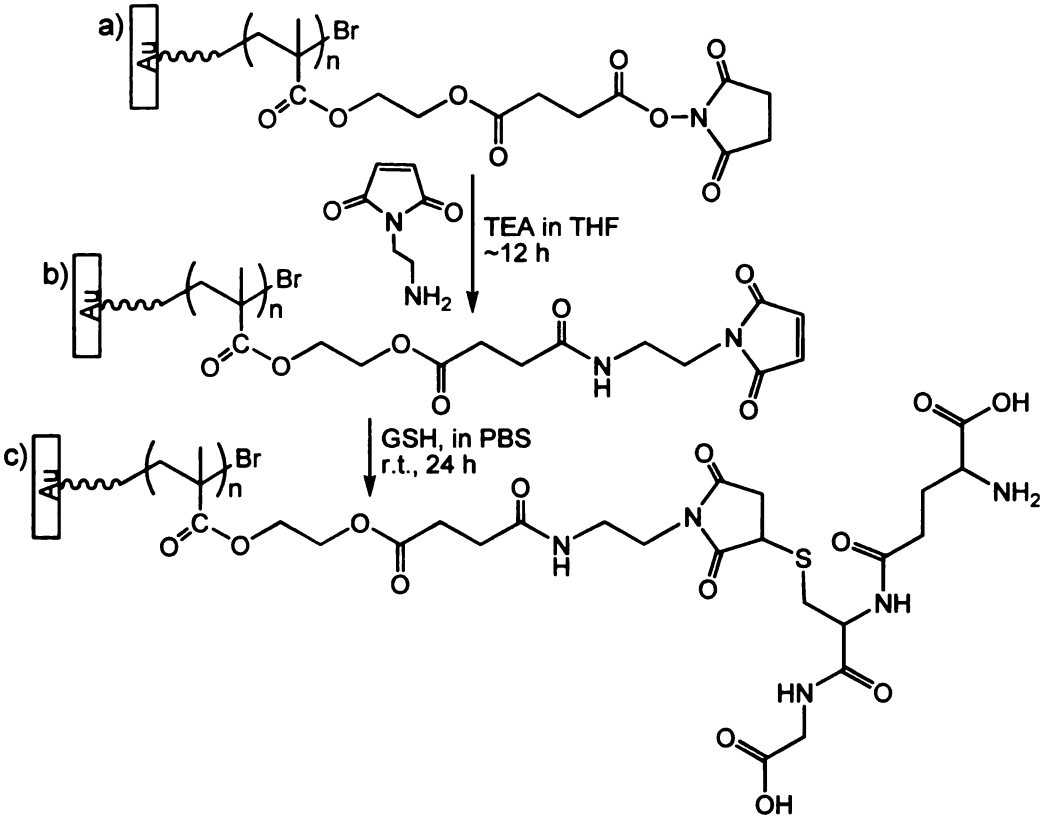

Figure 3.6: Schematic diagram of the modification of a gold-coated substrate after a) formation of a PHEMA-SA film activated with NHS/EDC, b) attachment of maleimide, and c) immobilization of glutathione on the PHEMA film.

3.2.6 Dialysis of Glutathione-S-Transferase

A Slide-A-Lyzer Dialysis cassette (Pierce Biotechnology Inc., MWCO 10 kDa) was used to remove impurities, specifically reduced glutathione, from Glutathione-S-Transferase according to the procedure provide by Pierce. The presence of free glutathione could interfere with the binding of GST to the glutathione immobilized on the

polymer brushes. Briefly, 500 mL of buffer solution containing 100 mM acetic acid and 100 mM sodium acetate in deionized water (2.85 mL of acetic acid, 0.038 g of sodium acetate) was prepared. The dialysis cassette was immersed in the buffer for 30 sec to hydrate the membrane of the cassette. Using a syringe, 1 mL of deionized water was carefully injected into the cassette to ensure that the membrane was fully sealed and that no water leaked out. The water was removed, and 1 mL of 0.5 mg/mL GST in 5% acetic acid was injected into the cassette. Any air remaining in between the membranes was removed to maximize the surface area exposed to the sample buffer solutions. A buoy was slipped onto the Slide-A-Lyzer cassette so that it would float in the buffer solution. The acetic acid/sodium acetate buffer solution was replaced with fresh buffer solution every 2 h for the first 6 h, and the protein was dialyzed for ~16 h. A syringe was used to remove the GST solution from the cassette, being careful not to puncture the membrane with the syringe. The protein sample was dried down and analyzed by MALDI-MS.

A second GST sample was dialyzed using the Slide-A-Lyzer Dialysis cassette with a different buffer solution, which was previously used by Chen and coworkers.[18] In this case, a phosphate buffer solution (PBS) containing 10 mM Na_2HPO_4, 1.8 mM KH_2PO_4, 140 mM NaCl, and 2.7 mM KCl (5.4 g Na_2HPO_4, 0.49 g KH_2PO_4, 16.4 g NaCl, 0.40 g KCl in 2 L water, pH 7.4) was employed in place of the acetic acid/sodium acetate buffer. The membrane was hydrated by immersing it in the PBS for 30 sec, and the absence of leaks was ensured by injecting 1 mL of deionized water into the cassette prior to sample injection. A syringe was used to inject 1 mL of GST solution into the cassette, which was then placed in the PBS. The PBS was replaced with fresh solution every 2 h for the first 6 h and was then replaced with deionized water, which was replaced only

once after 2 h. The sample was dialyzed for a total of 20 h. The GST sample was removed from the cassette using a syringe and was dried down and analyzed by MALDI-MS.

3.2.7 Purification of Glutathione-S-Transferase Using ZipTip$_{C18}$ Pipette Tips

The dried down GST sample from the second dialysis (~50 μg) was resuspended in 167 μL of deionized water. Two μL of this 0.3 mg/mL GST solution were desalted using 10 μL ZipTip$_{C18}$ pipette tips (Millipore). Briefly, the tips were equilibrated by wetting with acetonitrile twice, followed by aspirating 0.1% trifluoroacetic acid (TFA) and dispensing the solution two times. The sample was bound to the ZipTip pipette tip by aspirating and dispensing the GST solution 10 times. The 0.1% TFA wash solution was aspirated and dispensed three times to remove any unbound species. The protein was finally eluted by aspirating with 0.1% TFA/50% ACN and dispensing the solution three times. The eluent was spotted onto a conventional stainless steel MALDI plate, and 1 μL of 10 mg/mL 2,5-dihydroxybenzoic acid (DHB) in 1:1 ACN:H_2O was added directly to the sample on the MALDI plate as the matrix. In addition to desalting this purified GST sample, an unpurified GST sample was also desalted in the same fashion and was then analyzed by MALDI-MS.

3.2.8 Characterization and Instrumentation

Polymer brushes were characterized by reflectance FTIR spectroscopy using a Nicolet Magna 560 spectrophotometer with a Pike grazing angle (80°) accessory. The thicknesses of the functionalized polymer brushes were determined using a rotating analyzer spectroscopic ellipsometer (J. A. Woollam, M-44), assuming a film refractive index of 1.5. Mass spectra were obtained using a MALDI linear ion trap mass

spectrometer (Thermo vMALDI LTQ XL), and tandem MS was carried out using low energy collision-induced dissociation (CID). All spectra were obtained in positive ion mode. The mass spectra in this chapter were collected by Jamie Dunn of Michigan State University.

3.3 Results and Discussion

3.3.1 Fabrication and Characterization of Glutathione-Functionalized PAA Films

The fabrication of glutathione-derivatized PAA films (Figure 3.3) was characterized using reflectance FTIR spectroscopy, and film thicknesses after each step were determined using ellipsometry. The reflectance FTIR spectra in Figure 3.7 confirm the functionalization of the PAA brushes. The peak at 1730 cm^{-1} in spectrum a) of Figure 3.7 is due to the acid carbonyl group of the PAA immobilized on the gold-coated substrate. These PAA films, which are prepared using two PTBA deposition and hydrolysis steps, have a thickness of approximately 50 Å. After activation of PAA with NHS, the IR spectrum of the film contains succinimide ester peaks at 1790 and 1760 cm^{-1} (Figure 3.7b). The asymmetric stretch due to succinimide at 1743 cm^{-1} overlaps with the carbonyl stretch (1730 cm^{-1}) of the previously formed acid carbonyl, forming a broad peak with an absorbance more than double that of the acid carbonyl of PAA. Upon immobilization of glutathione on the PAA films, a broad peak appears around 3300 cm^{-1} probably due to the presence of two amine groups in GSH (Figure 3.7c). Additionally, the very strong shoulder at 1690 cm^{-1} is due to the amide I band, which partly overlaps with the carbonyl stretch, resulting in a much broader peak. The second amide band appears at 1520 cm^{-1}. Figure 3.7d shows the same glutathione-functionalized film after exposure to GST for 1 h. The absorbance of the amide I band decreases, as does the

carbonyl stretch, perhaps indicating that some of the PAA desorbed from the surface. While it is appears that glutathione was immobilized on the PAA, it is not clear that GST was bound to the immobilized glutathione. There is no peak present in the GST spectrum that positively identifies the binding of this protein to the glutathione-functionalized PAA films.

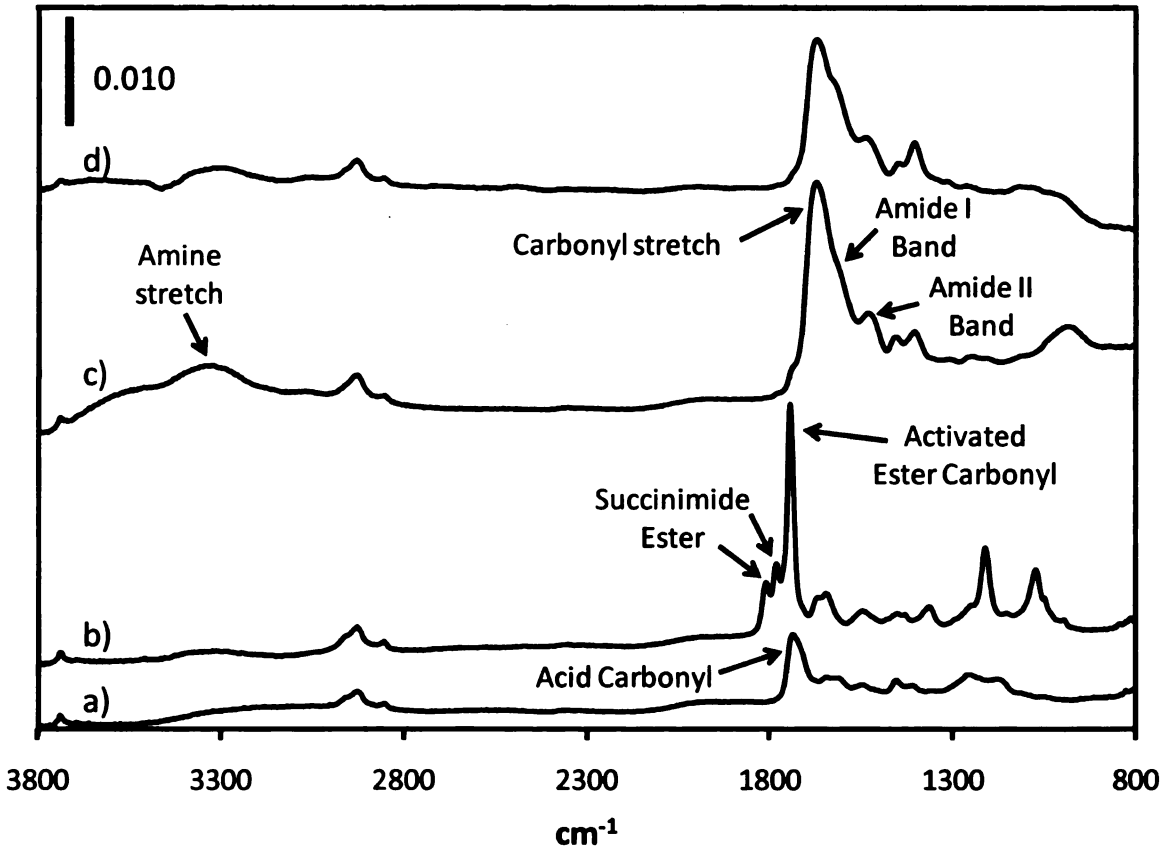

Figure 3.7: Reflectance FTIR spectra of a gold-coated Si wafer after a) deposition of a PAA film, b) activation of the PAA with NHS, c) reaction of glutathione with the activated PAA bilayer, and d) exposure of the glutathione-containing film to GST. The initial PAA film was deposited using two activation, PTBA deposition, and hydrolysis steps.

3.3.2 Fabrication and Characterization of Glutathione-Functionalized PHEMA Brushes

PHEMA brushes grown from immobilized initators are much thicker than grafted PAA films, so derivatized PHEMA may bind more GST than derivatized PAA. Figure 3.4 shows the procedure for preparing PHEMA films and one method for derivatizing them with glutathione to bind GST. The reflectance FTIR spectra in Figure 3.8 confirm the synthesis and derivatization of PHEMA. The strong ester carbonyl absorbance at 1730 cm^{-1} (spectrum a) and the hydroxyl stretch at 3650 – 3100 cm^{-1} (not shown here) are characteristic of PHEMA films. After reaction of PHEMA with succinic anhydride (SA), the absorbance of the ester carbonyl doubles due to an additional ester group formed on each repeating unit of the polymer chain (spectrum b, Figure 3.8). The hydroxyl stretch disappears (not shown here) as a result of the complete derivatization of the polymer chains. The reaction with succinic anhydride results in an increase in film thickness from 50 nm to approximately 75 nm. Spectrum c) is consistent with the activation of the polymer brush with NHS, as it shows the succinimide ester peaks at 1813 and 1784 cm^{-1} and the asymmetric stretch of succinimide at 1750 cm^{-1}, which overlaps with the carbonyl stretch. Figure 3.8d presents the spectra of the film after reaction with glutathione. The peak at about 1580 cm^{-1} may be due to the amide II band, althouth the absence of the amide I band suggests that immobilization may not have been successful. The peak at 1580 cm^{-1} could also be due to deprotonated carboxylic acid groups. Finally, spectrum e) in Figure 3.8 shows the spectrum of the glutathione-derivatized film after exposure to "impure" GST. Spectra d) and e) are very similar, and thus it appears that GST did not bind to the immobilized glutathione.

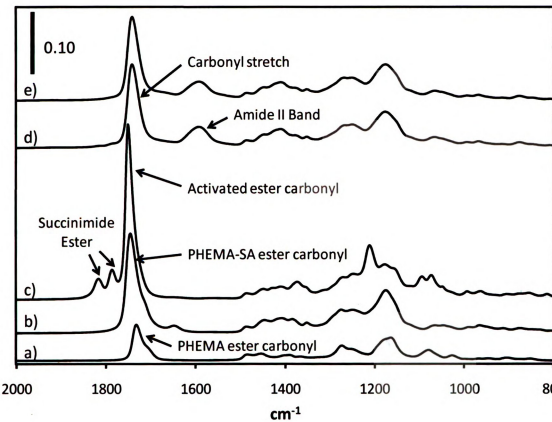

Figure 3.8: Reflectance FTIR spectra of a) a PHEMA brush immobilized on a gold-coated substrate, b) functionalization of PHEMA with succinic anhydride, c) activation of PHEMA-SA with NHS, d) immobilization of glutathione onto PHEMA-SA, and e) binding of GST to glutathione-immobilized polymer brushes.

3.3.3 Immobilization of Glutathione on Brominated-PHEMA Brushes

To determine whether the glutathione immobilization method might be limiting GST binding, we also immobilized glutathione via reaction with PHEMA brushes that were activated with bromoacetyl chloride (Figure 3.5). When immersed in a solution of glutathione, the reactive bromine is replaced via the formation of the thiol ether from the reduced glutathione. This derivatization was again characterized using reflectance FTIR spectroscopy (Figure 3.9). Spectrum a) in the figure shows the presence of stretches typical of PHEMA, and the increase in absorbance of the peaks present at 1270 and 1200

cm^{-1} (spectrum b) may be due to the presence of the alkyl bromide. The absence of a hydroxyl peak in spectrum b suggests that the reaction of PHEMA with the acid chloride is complete. The peak due to the ester carbonyl stretch shows a high energy shoulder due to the electronegativity of bromine, which withdraws electrons from the newly formed carbonyl ester. Attempts to immobilize reduced glutathione on the brominated-PHEMA film involved immersing the gold-coated substrate in an aqueous glutathione solution. However, this reaction was not successful as the spectrum of the film did not change significantly after immersion in the glutathione (compare spectra 3.9b and 3.9c).

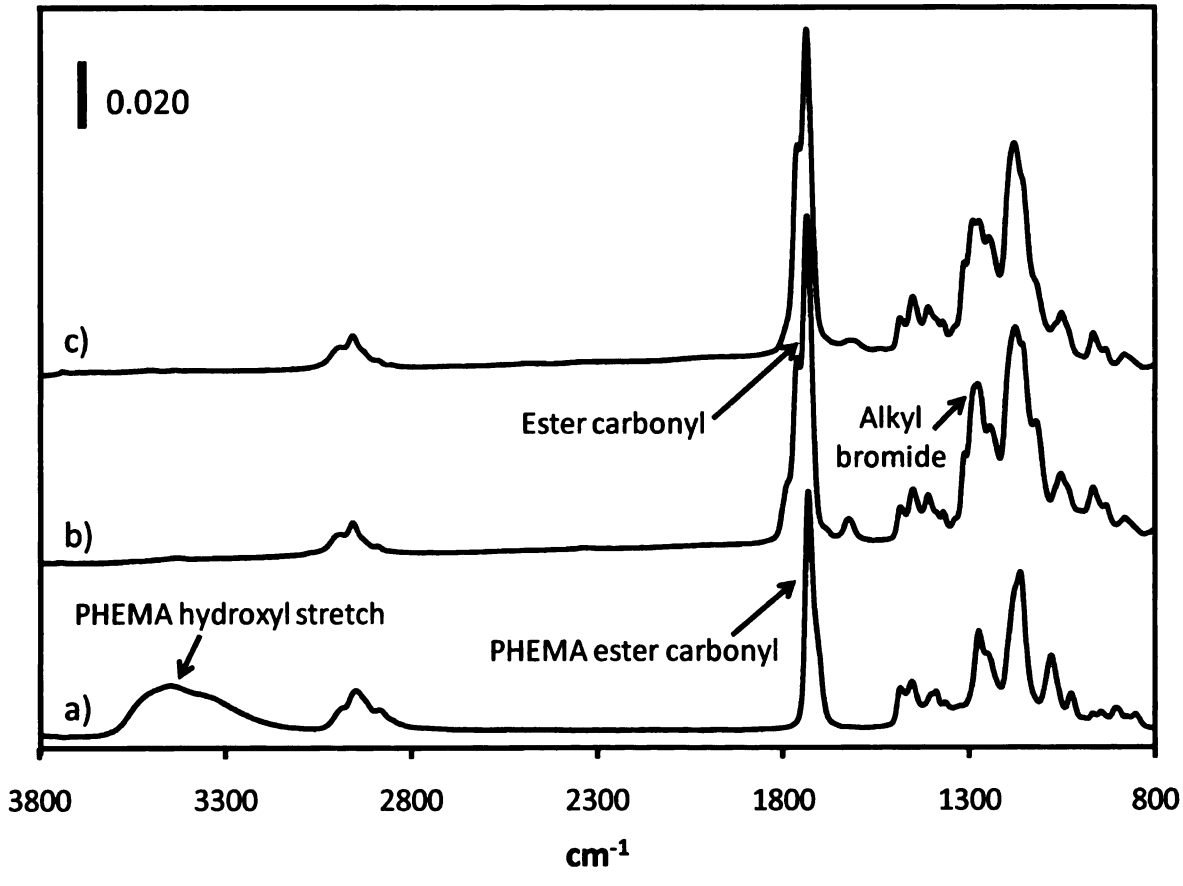

Figure 3.9: Reflectance FTIR of a) PHEMA immobilized on a gold-substrate, b) PHEMA brominated with bromoacetyl chloride, and c) immobilization of glutathione on PHEMA film.

3.3.4 Fabrication and Characterization of Glutathione Immobilized on Maleimide-PHEMA Brushes

In another method for immobilizing glutathione, PHEMA brushes were first derivatized with a maleimide (Figure 3.6). For optimal GST binding, not only does glutathione need to be attached to the modified substrate, it should be immobilized through its thiol group and not through the amine. Immobilized maleimides have been used to anchor thiol-terminated molecules in a variety of applications,[19,20,21] and this reaction should ensure the covalent attachment of glutathione to the polymer film through its thiol group. Functionalization of the PHEMA brush with maleimide occurred via reaction of the succinimidyl ester of PHEMA with *N*-(2-aminoethyl)maleimide trifluoroacetate. Comparison of spectra a) and b) in figure 3.10 confirms the attachment of the maleimide. The peak at 1714 cm^{-1} is due to the carbonyl stretch of the maleimide immobilized on a PHEMA-SA film. Figure 3.11 is the subtraction spectrum of PHEMA-SA (spectrum a in Figure 3.10) from PHEMA-SA-maleimide (spectrum b in Figure 3.10). This subtraction more clearly shows the asymmetric carbonyl stretching of the maleimide at 1714 cm^{-1} and the amine stretch between 3410 and 3240 cm^{-1}. The asymmetric aromatic C-C stretching is present at 1525 cm^{-1}, as well as the symmetric stretching at 1404 cm^{-1} due to C-N-C in the maleimide.[21] After reaction of glutathione with maleimide-functionalized brushes (Figure 3.10c), the amine stretch broadens and amide bands appear near 1660 cm^{-1} and1530 cm^{-1}.

Unfortunately, the spectrum of the film after exposure to GST (spectrum d in Figure 3.10) is very similar to the spectrum after immobilization of glutathione. Moreover the ellipsometric thickness of the film (~90 nm) changed by < 2 nm after

exposure to GST. Since GST is a large protein (M_w = 45-50 kDa), the thickness of the film should have increased more than 20 nm if the protein was actually bound throughout the polymer brush. Figure 3.12 shows the subtraction of the PHEMA-SA-maleimide-GSH spectrum (Figure 3.10c) from the PHEMA-SA-maleimide-GSH after exposure to GST (Figure 3.10d). This subtraction results in a spectrum with negative absorbances and no clear evidence of GST binding.

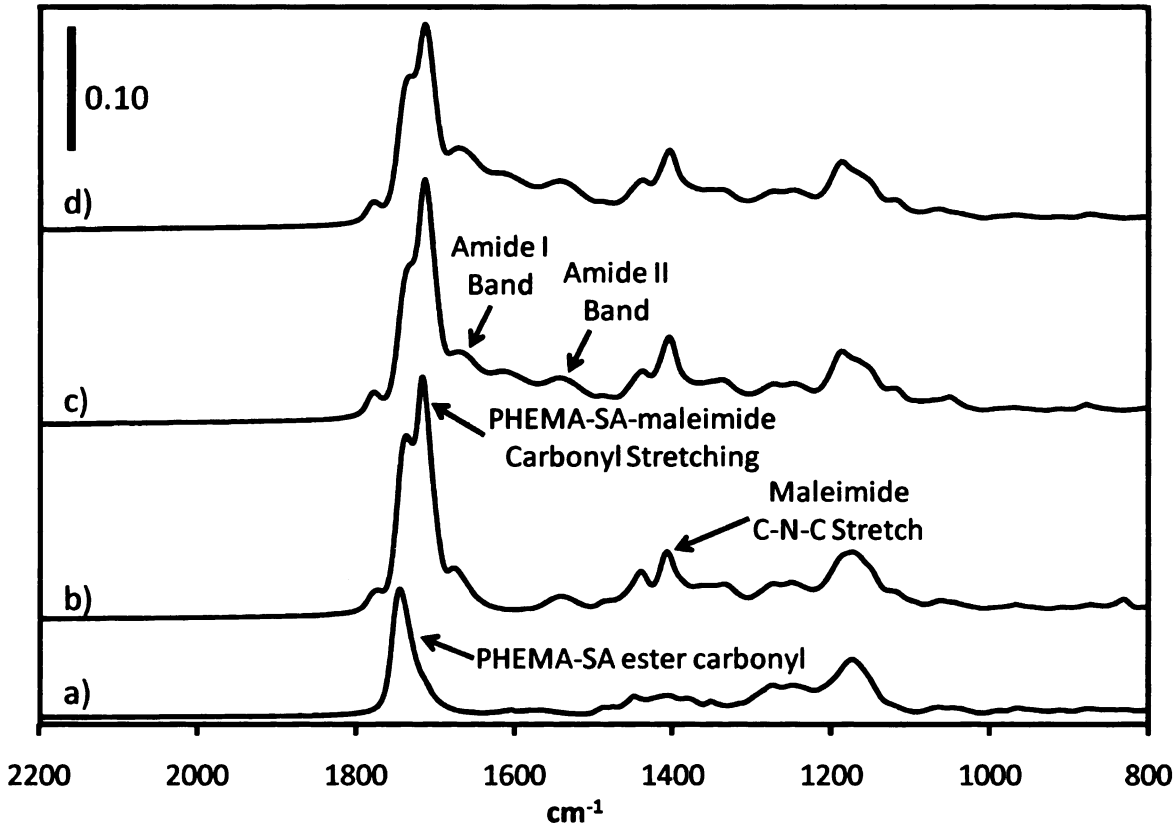

Figure 3.10: Reflectance FTIR spectra of PHEMA-SA a) before and after b) derivatization of with *N*-(2-aminoethyl)maleimide trifluoroacetate, c) immobilization of reduced glutathione through the maleimide, and d) exposure of GST to the glutathione-functionalized film.

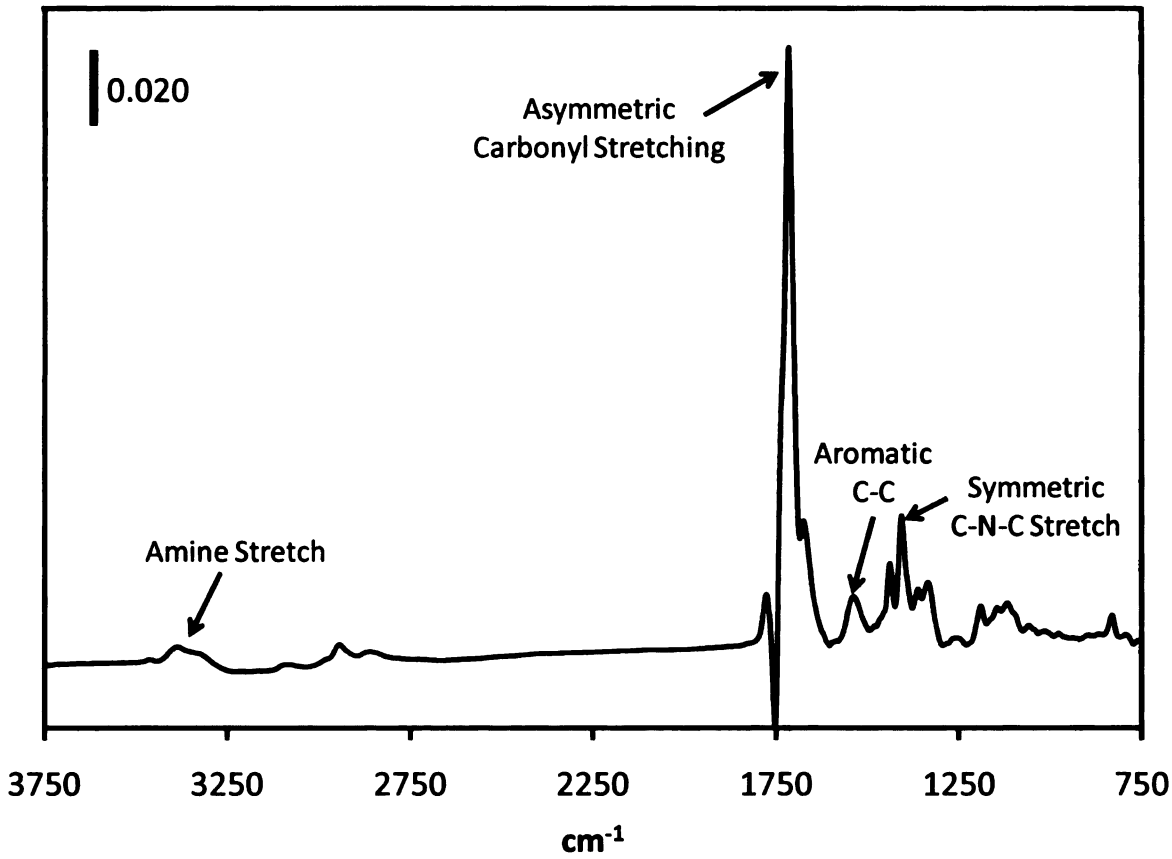

Figure 3.11: Spectrum resulting from subtraction of the PHEMA-SA spectrum (Figure 3.10a) from the PHEMA-SA-maleimide spectrum (Figure 3.10b) showing the immobilization of the maleimide to the film.

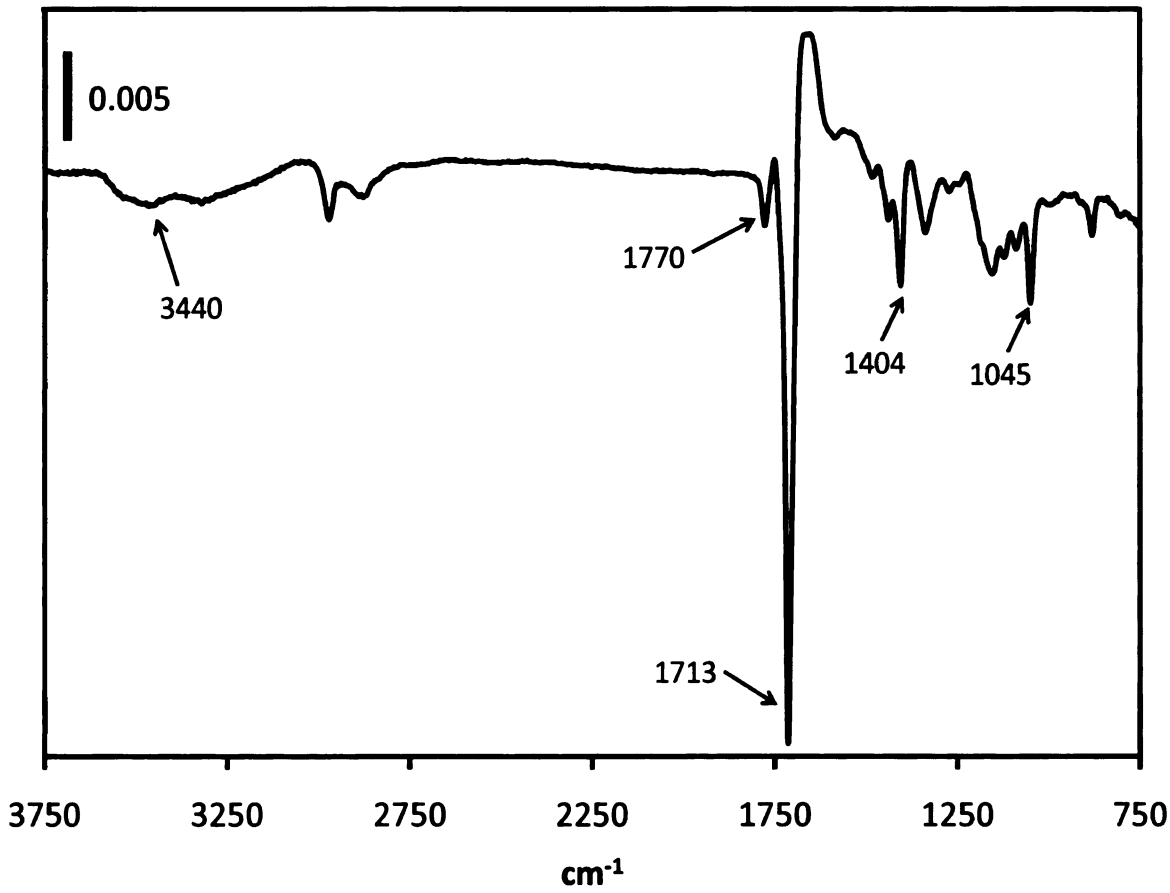

Figure 3.12: Spectrum resulting from subtraction of the PHEMA-SA-maleimide-GSH spectrum (Figure 3.10c) from the PHEMA-SA-maleimide-GSH spectrum after exposure to GST (Figure 3.10d) showing that there is essentially no GST bound to the film.

3.3.5 Attempts to Purify Glutathione-S-Transferase to Increase Binding

According to the manufacturer, the GST used in binding experiments has glutathione present as an impurity, which may inhibit the binding of GST to the immobilized glutathione. Both dialysis and ZipTip$_{C18}$ pipette tips were employed in efforts to purify the GST and remove unwanted glutathione. However, matrix-assisted laser desorption/ionization-mass spectrometry (MALDI-MS) shows that these methods do not completely remove glutathione (Figure 3.13). The GST sample analyzed here was dialyzed for 16 h in the acetic acid/sodium acetate buffer using a Slide-A-Lyzer cassette, and the buffer solution was replaced with fresh solution every two hours for the first six

hours. Reduced glutathione has an $[M + H]^+$ *m/z* value of 308.3, and the conventional MALDI mass spectrum of the Glutathione-S-Transferase sample after dialysis suggests that glutathione is still present (Figure 3.13). Tandem mass spectrometry (MS/MS) confirmed the assignment of glutathione to the peak with an *m/z* value of 308 (Figure 3.14). Reduced glutathione is a tripeptide, containing glycine (G), cysteine (C), and glutamic acid (E) residues (Figure 3.2). The MS/MS spectrum of this molecule (Figure 3.14) shows the loss of either water or one of these residues, confirming the assignment of the glutathione to the peak present at $[M+H]^+$ *m/z* 308. The peak found at $[M+H]^+$ *m/z* of 262 (Figure 3.14) which is a loss of 46 *m/z* units and may be due to the loss of water and the loss of a carbonyl group (CO).

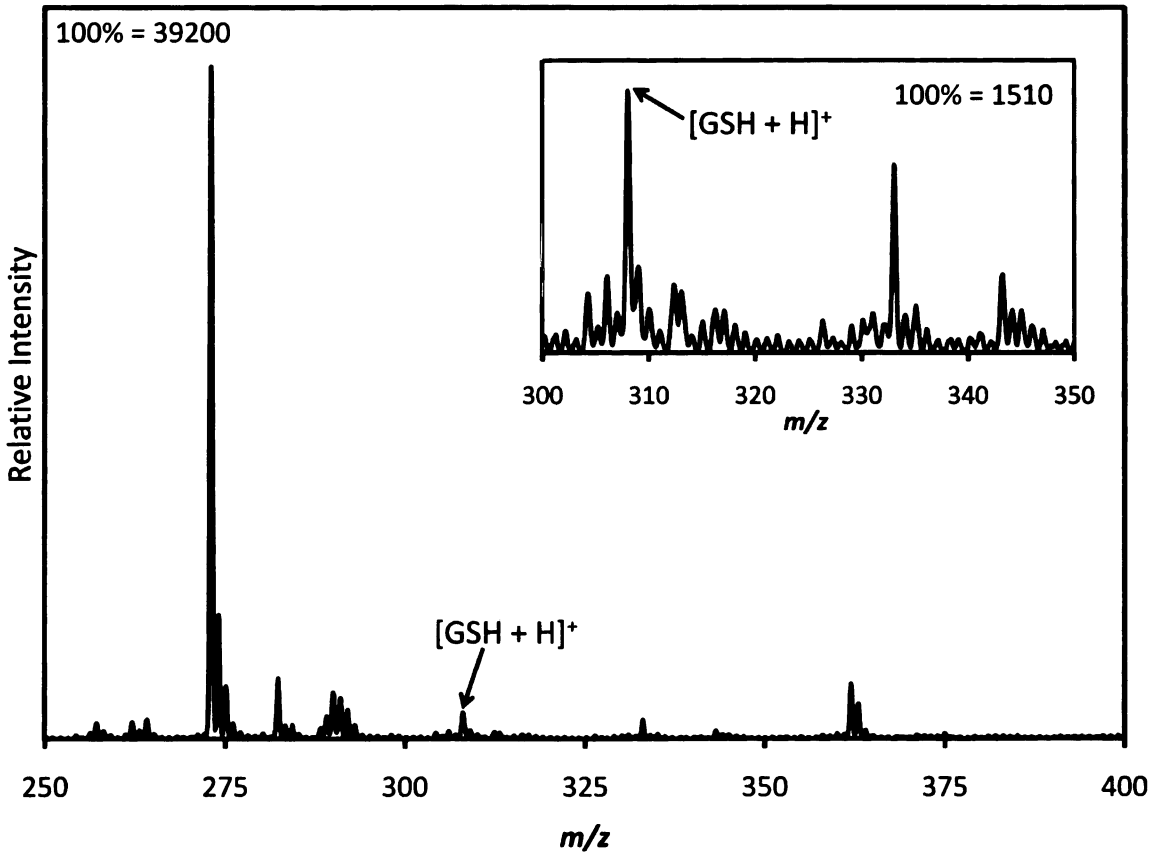

Figure 3.13: Positive-ion conventional MALDI mass spectra of 20 pmol of GST that was purified using dialysis. The signal for the $[M+H]^+$ ion of glutathione (GSH) has an *m/z* value of 308. The inset shows an expanded region of the mass spectrum.

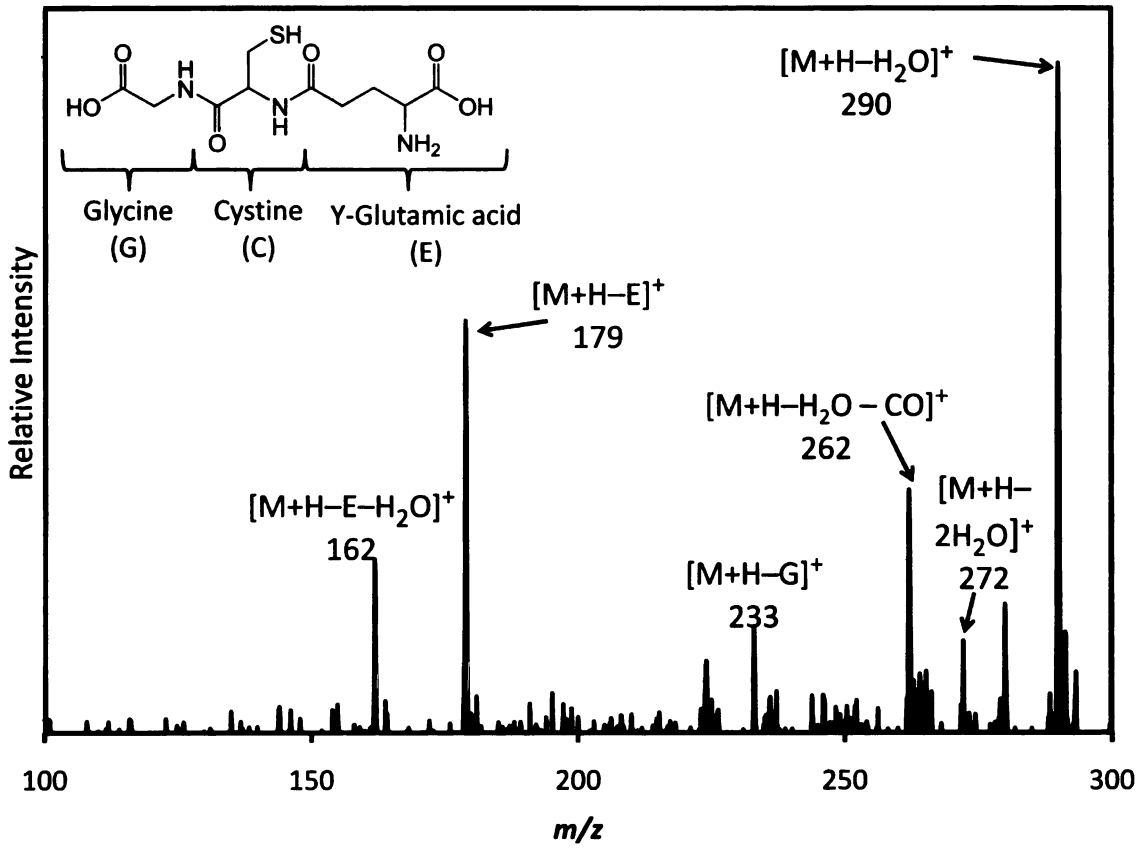

Figure 3.14: CID MS/MS spectrum of glutathione (*m/z* 308) isolated from 20 pmol of GST purified by dialysis. Losses of water as well as glycine (G) and glutamic acid (E) residues are labeled, as well as the loss of a carbonyl group (CO).

Upon discovering that glutathione was still present in the protein sample, a second GST sample was dialyzed in a phosphate buffer solution using a Slide-A-Lyzer cassette, as described in Section 3.2.6. The PBS was replaced with fresh solution every two hours for the first six hours and was then replaced with deionized water, which was replaced once after two hours; the GST sample was dialyzed for 20 h in total. This same GST sample was also purified using ZipTip$_{C18}$ pipette tips to remove any unwanted impurities. MALDI-MS was used to analyze the purified GST and to determine whether any glutathione remained in the sample. Figure 3.15 shows the conventional MALDI mass spectrum of GST, again revealing the presence of a peak at *m/z* 308, which suggests that glutathione is still present in the protein sample. MS/MS was used to confirm the identity

of this signal and several product ions generated by CID tandem mass spectrometry are the same as those identified previously (Figure 3.14). Unfortunately, reduced glutathione is still present in the GST sample, despite multiple purification methods.

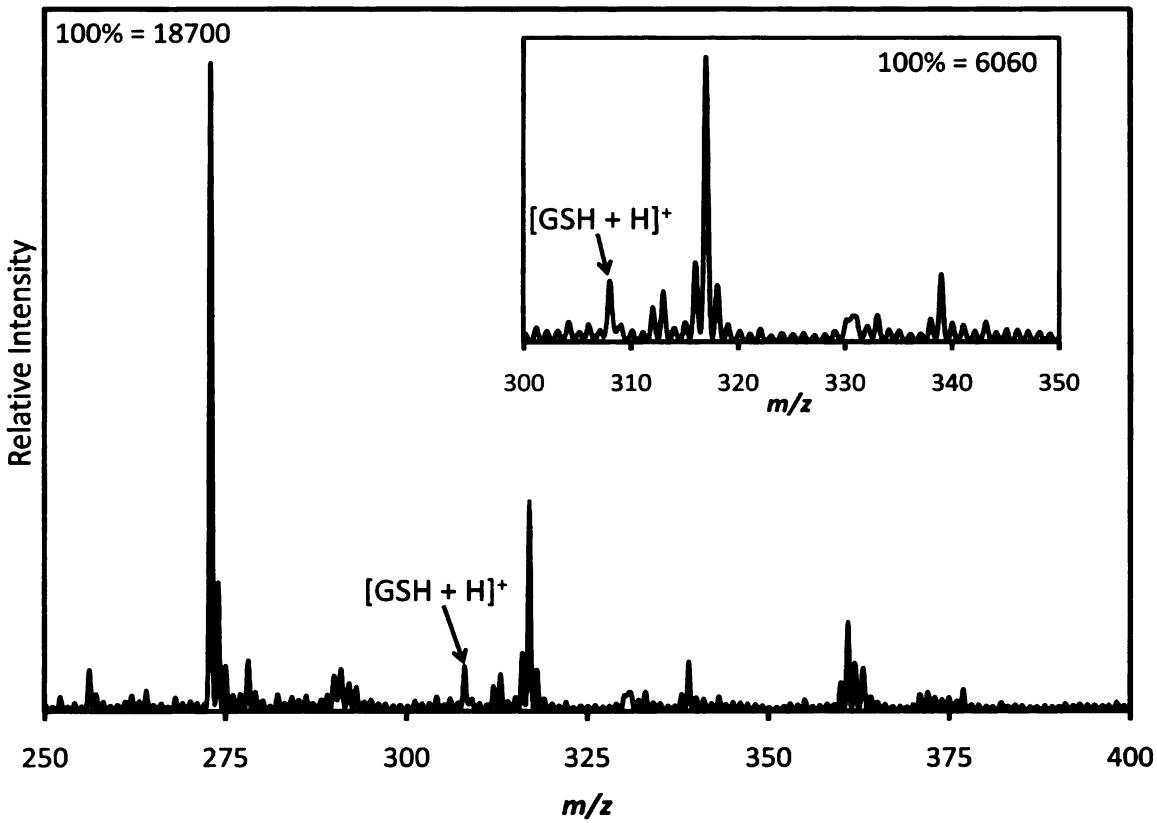

Figure 3.15: Positive-ion MALDI mass spectra, obtained by conventional analysis, of 12 pmol of GST purified according to the dialysis with phosphate buffer and by adsorption and elution from ZipTip$_{C18}$ pipette tips. Reduced glutathione is present at *m/z* 308. The inset shows an enlarged region of the mass spectrum.

3.3.6 Binding Purified GST to GSH-Maleimide-PHEMA Films

Although reduced glutathione was present in the GST sample after dialysis and desalting, a wafer with glutathione immobilized on a maleimide-functionalized PHEMA film was immersed in an aqueous solution of the "purified" GST for 1 h and rinsed with buffer solution. Figure 3.16 compares the reflectance FTIR spectrum of films exposed to (a) as-received and the (b) purified GST. The inset in Figure 3.16 shows the subtraction of these spectra. While there is a difference between the spectra, most of the differences

are due to the underlying films. The two spectra were obtained from different wafers, which had slightly different thicknesses, and the subtraction spectrum largely resembles a spectrum of PHEMA-maleimide. From these data, the dialysis and desalting of GST do not appear to have enabled this protein to bind to the glutathione-modified surface. It is also possible that the GST sample was not eluted from the ZipTip$_{C18}$ column following desalting, which would also inhibit its binding.

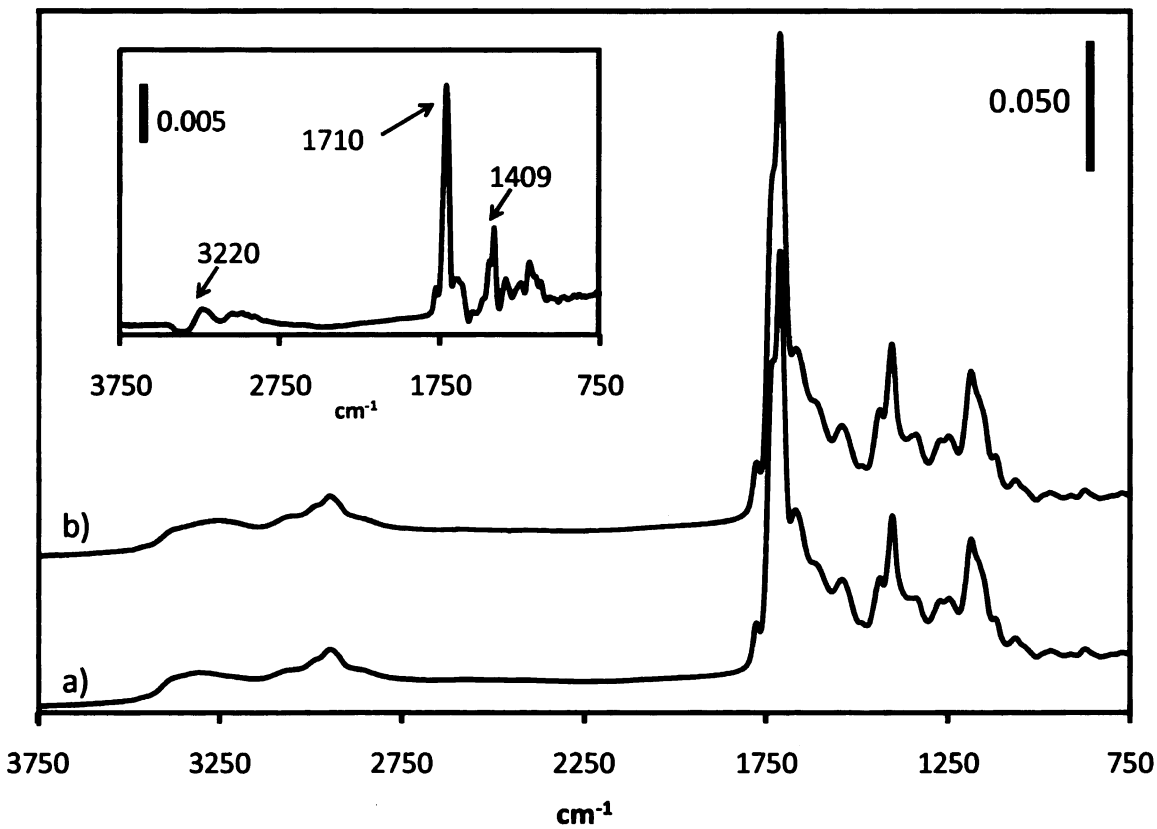

Figure 3.16: Reflectance FTIR spectra of PHEMA-maleimide-glutathione films after immersion in a) as received GST and b) GST purified by dialysis with PBS and desalting with ZipTips$_{TM}$. The inset shows the subtraction of these spectra.

3.4 Conclusions

Reduced glutathione was immobilized on both poly(acrylic acid) and poly(hydroxyethyl methacrylate) films. While several methods of attaching glutathione

to these polymer brushes were explored, PHEMA films derivatized with a maleimide are perhaps most promising because glutathione should be immobilized through the thiol group of the cysteine residue, instead of through the amine group. Immobilization through the amine group of glutathione may decrease the ability to bind GST. Unfortunately, the question of whether immobilized glutathione binds Glutathione-S-Transferase is still open. Glutathione is present as an impurity in the GST sample even after dialysis and desalting using $ZipTip_{C18}$ pipette tips. The presence of glutathione in the protein may inhibit binding of GST to the immobilized glutathione. The reflectance FTIR spectra of films exposed to GST show no signs of protein binding. Perhaps GST was not eluted from the $ZipTip_{C18}$ packing material, also preventing binding to the film. The GST sample analyzed here (Sigma) consists of only 60% protein. Other Glutathione-S-Transferases have a significantly higher purity, which may allow more efficient binding to immobilized glutathione. Further studies of GST binding in the absence of glutathione are needed to show whether immobilized glutathione could be useful in binding GST-tagged proteins.

3.5 References

[1] Mezzetti, A. D.; Ilio, C.; Calafiore, A. M.; Aceto, A.; Marzio, L.; Frederici, G.; Cuccurullo, F. *Journal of Molecular and Cellular Cardiology*, **1990**, *22*, 935-938.

[2] Oesch, F.; Gath, I.; Igarashi, T.; Glatt, H.; Thomas, H. *NATO ASI Series, Series A: Lifesciences*, **1991**, *202*, 447-461.

[3] Rietjens, I. M.; Lemmink, H. H.; Alink, G. M.; van Bladeren, P. J. *Chemico-Biological Interactions*, **1987**, *62*, 3-14.

[4] Kaplan, W.; Husler, P.; Klump, H.; Erhardt, J.; Sluis-Cremer, N.; Dirr, H. *Protein Science*, **1997**, *6*, 399-406.

[5] Kursula, I.; Heape, A. M.; Kursula, P. *Protein and Peptide Letters*, **2005**, *12*, 709-712.

[6] Smith, D. B. *Methods in Enzymology*, **2000**, *326*, 254-270.

[7] Smyth, D. R.; Mrozkiewicz, M. K.; McGrath, W. J.; Listwan, P.; Kobe, B. *Protein Science*, **2003**, *12*, 1313-1322.

[8] Wilce, M. C. J.; Parker, M. W. *Biochimica et Biophysica Acta*, **1994**, *1205*, 1-18.

[9] Lipin, D. I.; Lua, L. H. L.; Middelberg, A. P. J. *Journal of Chromatography A*, **2008**, *1190*, 204-214.

[10] Murray, A. M.; Kelly, C. D.; Nussey, S. S.; Johnstone, A. P. *Journal of Immunological Methods*, **1998**, *218*, 133-139.

[11] Sadilkova, L.; Osicka, R.; Sulc, M.; Linhartova, I.; Novak, P.; Sebo, P. *Protein Science*, **2008**, *17*, 1834-1843.

[12] Scheich, C.; Sievert, V.; Büssow, K. *BMC Biotechnology*, **2003**, *3*, 1-8.

[13] Smith, D. B.; Johnson, K. S. *Gene*, **1988**, *67*, 31-40.

[14] Simons, P. C.; Vander Jagt, D. L. *Analytical Biochemistry*, **1977**, *82*, 334-341.

[15] Thermo Fisher Scientific Inc. "Reusable Glutathione Agarose Resin for Purifying GST Fusion Proteins," **2009**, http://www.piercenet.com/products/

[16] Dunn, J. D.; Reid, G. E.; Bruening, M. L. *Mass Spectrometry Reviews* **2009**, DOI 10.1002/mas.20219.

[17] Bruening, M. L.; Zhou, Y. F.; Aguilar, G.; Agee, R.; Bergbreiter, D. E.; Crooks, R. M. *Langmuir*, **1997**, *13*, 770-778.

[18] Chen, H.; Luo, S.; Chen, K.; Lii, C. *Journal of Chromatography A*, **1999**, *852*, 151-159.

[19] Houseman, B. T.; Gawalt, E. S.; Mrksich, M. *Langmuir*, **2003**, *19*, 1522-1531.

[20] Jin, L.; Horgan, A.; Levicky, R. *Langmuir*, **2003**, *19*, 6968-6975.

[21] Xia, B.; Xiao, S.; Guo, D.; Wang, J.; Chao, J.; Liu, H.; Pei, J.; Chen, Y.; Tang, Y.; Liu, J. *Journal of Materials Chemistry*, **2006**, *16*, 570-578.

Chapter Four: Enrichment of Glycopeptides Using Aminophenylboronic Acid-Derivatized Polymer Brushes

4.1 Introduction

Protein glycosylation is one of the most common, as well as complex, post-translational modifications (PTMs) in the cell. The core oligosaccharides of the glycan moiety are attached to the polypeptide chain and processed by enzymatic reactions in the endoplasmic reticulum (ER), and the glycoprotein is subsequently transported to the Golgi complex for further trimming and processing.[1,2] The carbohydrate moiety of the glycoprotein aids in the folding and conformational stability of the protein, and the entire glycoprotein plays a key role in protein recognition, the immune system, and cell-to-cell recognition.[1,2,3,4,5] Unlike the polypeptide chain, whose composition is controlled genetically, the carbohydrate group on a glycoprotein is controlled by enzymatic reactions. Thus, the glycan moiety may change if the enzyme or reactant concentration varies, and these glycan variants sometimes alter protein activity and function, which can lead to disease.[1,2] In fact, abnormal glycosylation of proteins is either the cause or consequence of numerous hereditary and acquired diseases.[6,7] Abnormal glycosylation patterns were first associated with cancer in the late 1970s,[8] and subsequent studies showed that changes in glycosylation and in levels of glycosylated proteins play a role in liver disease, diabetes, and various forms of cancer.[9,10,11,12] Therefore, the identification of glycosylation sites, as well as the quantification of glycosylated species, is necessary to understand and identify biochemical processes and diseases.

Due to the development of electrospray ionization (ESI) and matrix-assisted laser desorption/ionization (MALDI) over the last two decades, mass spectrometry (MS) has

become the premier tool for the analysis of carbohydrates and glycoproteins.[13,14,15,16,17] Despite the ability of these soft ionization MS techniques to identify intact biomolecules, however, the low abundance of glycosylated peptides and proteins makes their detection challenging.[18] Glycosylation sites are also diverse and may contain a range of different carbohydrates at each site, which also makes their analysis more challenging. Nevertheless, a number of recently developed techniques that isolate glycosylated peptides from nonglycosylated species make detection by mass spectrometry more feasible. The most common method to separate glycoproteins and glycopeptides from a complex mixture is lectin affinity chromatography. Lectins are proteins, such as concanavalin A (Con A) and wheat-germ agglutinin (WGA), that have a high affinity for specific carbohydrates.[19,20,21,22] Lectin affinity chromatography separates glycoproteins based on their glycan moiety, and the lectins are typically bound to beads, such as agarose, that are packed into a column. Unfortunately, column-based methods often decrease throughput, as the sample must be loaded onto the column, rinsed to remove any unbound species, and then eluted to collect the analyte. The column eluate is finally either analyzed by ESI-MS or mixed with matrix and spotted on a target and analyzed by MALDI-MS.

More recently, hydrazide- and boronic acid-functionalized magnetic beads have been used for enrichment of glycoproteins and peptides.[23,24,25,26,27] These beads covalently bind glycosylated proteins and peptides and have the ability to enrich a wider range of glycoproteins and peptides than lectins, which may be necessary, depending on the aim of the separation. Typically the magnetic beads must be loaded with analyte and then collected prior to rinsing to remove contaminants. Finally, the analyte is eluted, the

beads are collected, and the eluate is analyzed by ESI-MS or MALDI-MS (after addition of matrix in the latter case). This is a tedious process, as collection of beads can be difficult, and sample loss is also a concern using this enrichment technique.

This chapter describes attempts to develop an on-plate enrichment technique, where an unpurified glycopeptide sample is spotted on a modified MALDI plate that covalently binds glycopeptides. After rinsing to remove any impurities and nonglycopeptides, matrix is added prior to analysis by MALDI-MS. This on-plate enrichment technique should, in principle, exhibit minimal sample loss because the enriched glycoopeptides are analyzed directly on the modified plate with no sample handling steps.

Specifically, the on-plate enrichment technique employs gold-coated substrates modified with polymer brushes that are functionalized with 3-aminophenylboronic acid (APBA). APBA covalently binds *cis*-diol groups, which are present in essentially all carbohydrate groups. The derivatized brushes are significantly thicker than the monolayer films that were used to cover the magnetic beads discussed above. Because of their greater thickness, polymer brushes have a higher binding capacity than monolayer films and should, therefore, have a greater capability to enrich glycopeptides, as illustrated in Figure 4.1.

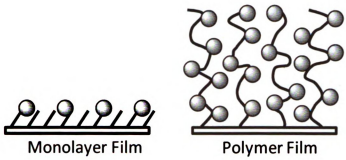

Figure 4.1: Comparison of the binding capacity of a thin monolayer film and a thicker polymer brush. Spheres represent either a protein or peptide.

4.2 Experimental

4.2.1 Materials

Peroxidase from Horseradish (HRP) was purchased from Sigma and digested using sequencing grade modified trypsin from Promega. Other digest reagents include Tris-HCl (Invitrogen), urea (J. T. Baker), 1,4-dithio-DL-threitol (BioChemika), ammonium bicarbonate (Columbus Chemical Industries), and iodoacetamide (Sigma). Silicon wafers (Addison Engineering) were sputter coated with 20 nm of chromium, followed by 200 nm of gold (Lance Goddard Associates, Santa Clara, CA). The reagents used for the preparation of surface-modified gold-coated plates include 11-mercaptoundecanol (Aldrich), 2-bromoisobutyryl bromide (Aldrich), triethylamine (Jade Scientific), 2-hydroxyethyl methacrylate (Aldrich), cupric bromide (Aldrich), cuprous chloride (Aldrich), 2,2'-bipyridine (Aldrich), succinic anhydride (J.T. Baker), 4-dimethylaminopyridine (Sigma), *N*-(3-dimethylaminopropyl)-*N'*-ethylcarbodiimide hydrochloride (Sigma), *N*-hydroxysuccinimde (Aldrich), and 3-aminophenylboronic acid monohydrate (Aldrich). Fructose (Aldrich) was bound to the surface-modified plates. Dimethylformamide (Spectrum) was dried using 3-Å molecular sieves (Spectrum), and deionized water was obtained through a Millipore purification system (Milli-Q, 18

MΩcm). HPLC grade methanol (Sigma), isopropyl alcohol (EMD), and ammonium hydroxide (Columbus Chemical Industries) were used to clean the conventional stainless steel MALDI plate according to Thermo Scientific's deep cleaning procedure as described in Chapter 2. The plate was in a nitrogen-filled glove bag while not in use. Ammonium bicarbonate (Columbus Chemical Industries) was used as the loading solution for some protein samples. The matrix used for all MALDI-MS experiments in this chapter was 0.25 μL of a 40 mg/mL solution of 2,5-dihydroxybenzoic acid (DHB, Aldrich) in 1:1 HPLC grade acetonitrile (EMD): 0.1% trifluoroacetic acid (Aldrich), which was applied directly to the protein sample on the conventional stainless steel MALDI plate or within a well scratched on the modified gold-coated MALDI plates.

4.2.2 Protein Digestion

For the tryptic digestion of horseradish peroxidase samples (MW ~44 kDa), twenty 100 μg samples of protein were separately dissolved in 20 μL of 6 M urea containing 50 mM tris-HCl as discussed in Chapter 2. To reduce any disulfide linkages present, 5 μL of 10 mM 1,4-dithio-DL-threitol (DTT) was added to each sample, and the protein solutions were heated in a water bath at ~65°C for 1 h. After cooling the sample to room temperature, 160 μL of 50 mM ammonium bicarbonate and 10 μL of 100 mM iodoacetamide were added to each protein solution, and the samples were placed in the dark for 1 h. Finally, 10 μL of 0.5 μg/μL modified trypsin was added to each sample, and they were incubated for ~16 hours at 37 °C. The digestion reaction was quenched with the addition of 11 μL of glacial acetic acid, which lowered the pH to ~3. Samples were dispensed into Eppendorf tubes in 22 μL aliquots and stored in a -70 °C freezer until further use.

4.2.3 Fabrication of APBA-PHEMA Brushes

Gold-coated silicon wafers (1.1 x 2.4 cm) were UV/ozone-cleaned for 15 min and immersed in a 1 mM solution of mercaptoundecanol (MUD) in ethanol (4.1 mg in 20 mL ethanol) for ~16 h to form a self-assembled monolayer (SAM). Wafers were rinsed with deionized water, followed by ethanol and dried under a stream of N_2 gas. Gold wafers (typically 8 at a time) were arranged in a crystallizing dish and placed in a nitrogen-filled glove bag. Then 0.12 M triethylamine (TEA) (0.33 mL of TEA in 20 mL dry DMF) was added to the crystallizing dish, followed by dropwise addition of 0.1 M 2-bromoisobutyryl bromide (BIBB, 0.25 mL in 20 mL DMF) with swirling over a 10 min period. Wafers were removed from the crystallizing dish and rinsed with DMF. After drying in the glove bag for 10 min, they were removed and rinsed with ethyl acetate, deionized water, and ethanol, and then dried under a stream of N_2 gas. Reflectance FTIR spectroscopy was used to identify the presence of the ester carbonyl peak (1730 cm^{-1}) due to the attachment of the initiator to the MUD SAM. Using freeze-pump-thaw cycling, 30 mL of 2-hydroxyethyl methacrylate (HEMA) and 30 mL of deionized water were degassed in a Schlenk flask. During the third cycle, 165 mg CuCl, 108 mg $CuBr_2$, and 640 mg 2,2'-bipyridine were added to the frozen mixture of HEMA and deionized water. The catalyst dissolved once the mixture of HEMA and deionized water thawed. The freeze-pump-thaw cycle was completed, followed by two additional cycles. The flask was transferred to the nitrogen-filled glove bag and was distributed equally among four 20-mL scintillation vials, each containing two wafers modified with initiators attached to the MUD SAM. Typically wafers were immersed in the HEMA solution for 2 h, which gave film thicknesses of 45-50 nm. Thicknesses of the PHEMA films were varied by

either shortening or lengthening the polymerization time. The PHEMA films were removed from the vials and rinsed with DMF, deionized water, and acetone, and were characterized using reflectance FTIR spectroscopy. To convert the hydroxyl groups of the PHEMA brushes to carboxylic acid groups, the films were immersed in 10 mL of DMF containing 0.1 g succinic anhydride (SA) and 0.2 g 4-dimethylaminopyridine (DMAP) and heated at 55 °C for 3 h. These films were rinsed with DMF, water, and ethanol and dried under a stream of N_2 gas. The carboxylic acid groups were then activated using 50 mM *N*-(3-dimethylaminopropyl)-*N'*-ethylcarbodiimide hydrochloride (EDC, 0.096 g) and 50 mM *N*-hydroxysuccinimide (NHS, 0.058 g) in 10 mL water for 30 min. Activated films were rinsed with water and ethanol, and then dried under N_2 gas. Finally, the PHEMA brushes were functionalized with 3-aminophenylboronic acid (APBA) (Figure 4.2) by immersing films for ~16 h in 10 mL of DMF containing 0.031 g APBA and 0.06 g DMAP. These APBA-PHEMA brushes were rinsed with DMF, followed by ethanol and dried using N_2 gas. All steps of the fabrication process were characterized by reflectance FTIR spectroscopy, and wafers were initially cut to fit the FTIR sample holder (1.1 x 2.4 cm). To fit the modified stainless steel MALDI plate, wafers were cut to a width of 1.7 cm. Circular sample wells, with a diameter of 2 mm, were scratched onto the wafers using a tungsten carbide-tipped pen. Typically six wells were created on each wafer. The modified wafers were then secured to the modified stainless steel MALDI plate using double-sided tape.

4.2.4 Binding of Fructose to APBA-PHEMA Brushes

Fructose was bound to APBA-derivatized PHEMA brushes (Figure 4.4) by immersing wafers for 15 or 30 min in a 0.01 M aqueous solution of fructose (0.018 g

fructose in 10 mL deionized water) at pH 10.6 (pH was adjusted with 0.125 M NaOH, final NaOH concentration was ~1mM). Wafers were briefly rinsed with ethanol (~10 s) and dried under a stream of nitrogen gas. Films with bound fructose were characterized using reflectance FTIR spectroscopy and ellipsometry.

4.2.5 Protocol for Enrichment of Glycopeptides Using APBA-PHEMA Brushes

For analysis of tryptic protein digests, 1 μL of digest solution was spotted in the 2 mm diameter wells that were scratched in the APBA-PHEMA-modified gold wafers. Protein digest stock solutions were diluted in loading solution, either deionized water or 0.1 M ammonium bicarbonate, and samples were then spotted directly on the modified wafer. Samples were incubated for 15 min, and additional loading solution (0.5 or 1 μL of loading solution without digest) was added to the wells as the sample solution evaporated throughout the incubation time. After 15 min, samples in deionized water were rinsed with ~5 mL of ethanol and samples in 0.1 M NH_4HCO_3 were rinsed with ~5 mL of loading solution, followed by ~5 mL of ethanol, and then dried under a stream of N_2 gas. After drying, 1 μL of 0.1% TFA was added to each well to elute the glycopeptides, followed immediately by addition of 0.25 μL of 40 mg/mL DHB solution (1:1 acetonitrile: 0.1% trifluoroacetic acid) to deposit the matrix. After crystallization of the solution, the gold-coated wafer was secured to the modified MALDI target using double-sided tape.

4.2.6 Characterization and Instrumentation

The polymer brushes were characterized by reflectance FTIR spectrometry using a Nicolet Magna 560 spectrophotometer with a Pike grazing angle (80°) accessory. The thicknesses of the polymer films were determined using a rotating analyzer spectroscopic

ellipsometer (J. A. Woollam, M-44), assuming a film refractive index of 1.5. Mass spectra were obtained with a MALDI linear ion trap mass spectrometer (Thermo vMALDI LTQ XL) in positive ion mode.

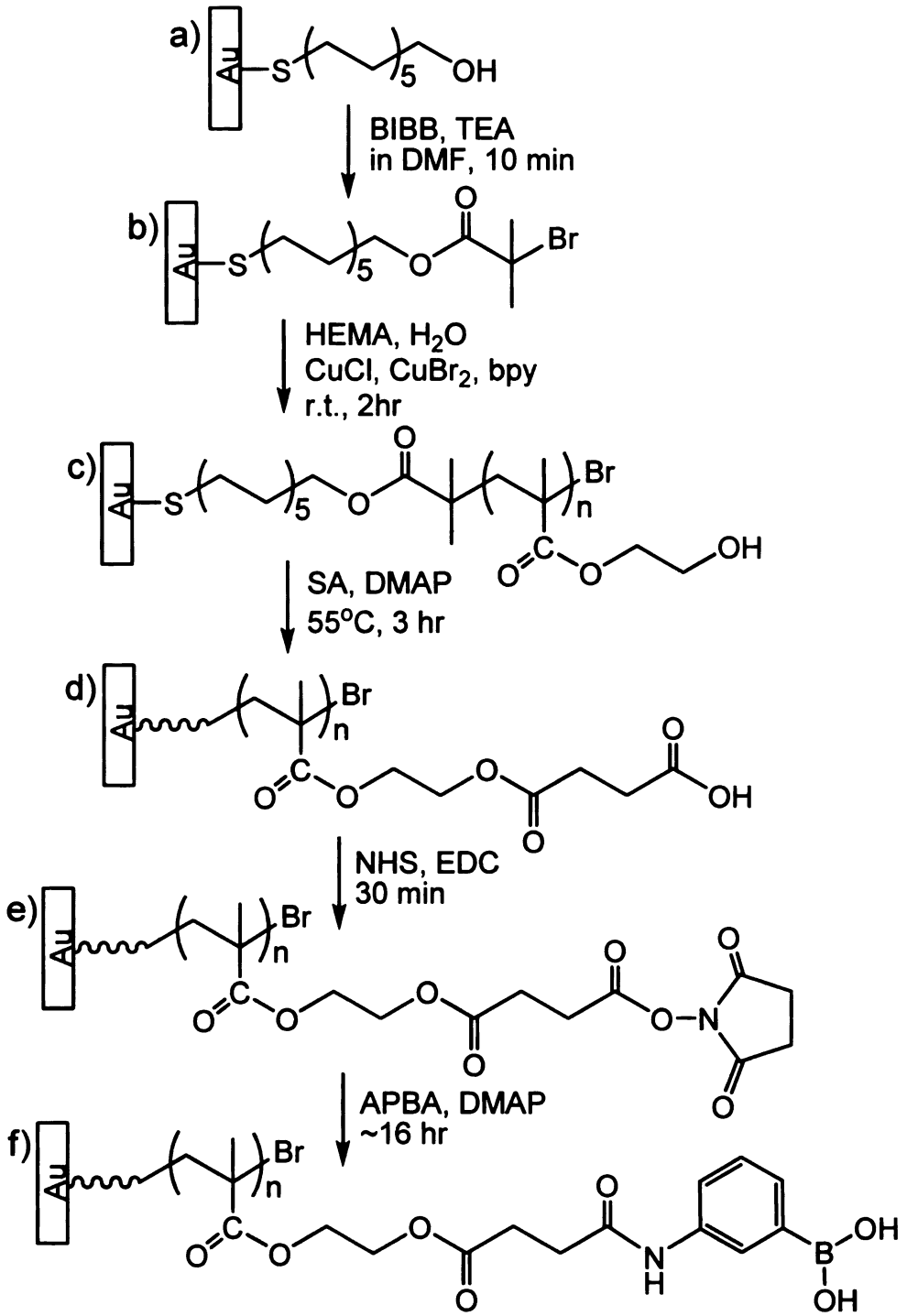

Figure 4.2: Schematic diagram showing modified gold-coated substrates after a) adsorption of an MUD SAM, b) attachment of initiator to MUD, c) polymerization of HEMA, d) derivatization of PHEMA with succinic anhydride (SA), e) activation of PHEMA-SA with NHS, and f) derivatization of PHEMA-SA with 3-aminophenylboronic acid (APBA).

4.3 Results and Discussion

4.3.1 Characterization of PHEMA-APBA Brushes

The fabrication and derivatization of PHEMA brushes (Figure 4.2) were characterized using reflectance FTIR spectroscopy, and film thicknesses were determined after each step using ellipsometry. The reflectance FTIR spectra in Figure 4.3 confirm the growth and derivatization of PHEMA on a gold-coated surface. After growth of PHEMA, the spectrum of the 50 nm-thick films contains the expected ester carbonyl (1730 cm^{-1}, spectrum 4.3a) and hydroxyl stretches (3650 – 3100 cm^{-1}, not shown). Functionalization of PHEMA with succinic anhydride results in a doubling of the ester carbonyl absorbance (compare spectra 4.3a and 4.3b) due to an additional ester group in each repeating unit of the polymer chain (Figure 4.1). The hydroxyl stretch also disappears as a result of the essentially complete derivatization of the hydroxyl groups. After functionalization with succinic anhydride, the polymer brushes increase in thickness to approximately 75 nm. Spectrum 4.3c shows that the activation of the polymer brush with NHS gives rise to succinimide ester peaks at 1813 and 1784 cm^{-1} and an asymmetric stretch of succinimide at 1750 cm^{-1} that overlaps with the carbonyl stretch. Attachment of APBA to the PHEMA-SA film occurs through the amine group (Figure 4.2). After derivatization with APBA, the FTIR spectrum of the film contains a hydroxyl stretch at 3550 – 3250 cm^{-1} that may overlap with the N–H stretch of the amide. The amide I band exists as a shoulder around 1664 cm^{-1}, and vibrations due to the phenyl group of APBA appear at 1600, 1575, 1540, and 1483 cm^{-1}. The amide II band should also contribute to the absorbance around 1550. Vibrations due to the boronic acid occur around 1362 and 1342 cm^{-1}. After derivatization with 3-aminophenylboronic acid, the

polymer film thickness increases to approximately 100 nm, suggesting widespread derivatization.

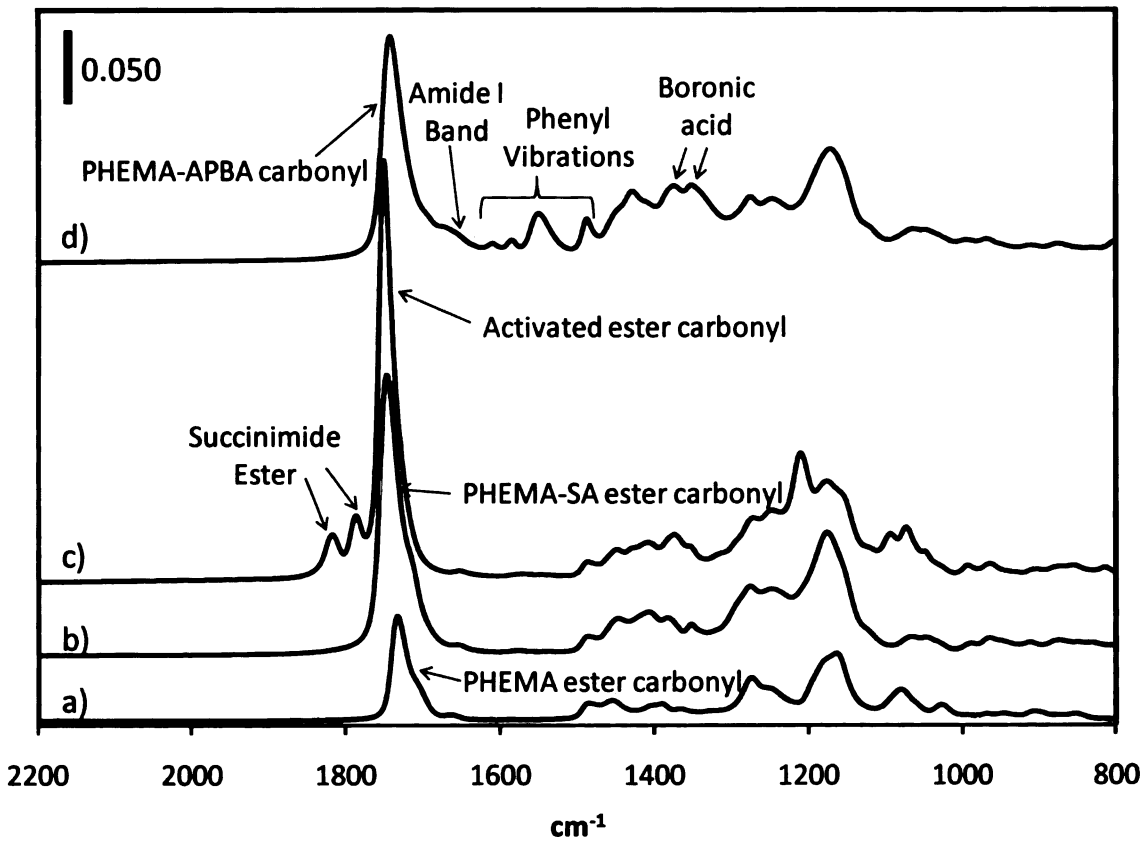

Figure 4.3: Reflectance FTIR spectra of a PHEMA brush immobilized on a gold-coated substrate before a) and after b) functionalization with succinic anhydride, c) activation of PHEMA-SA with NHS, and d) attachment of APBA to the PHEMA-SA film.

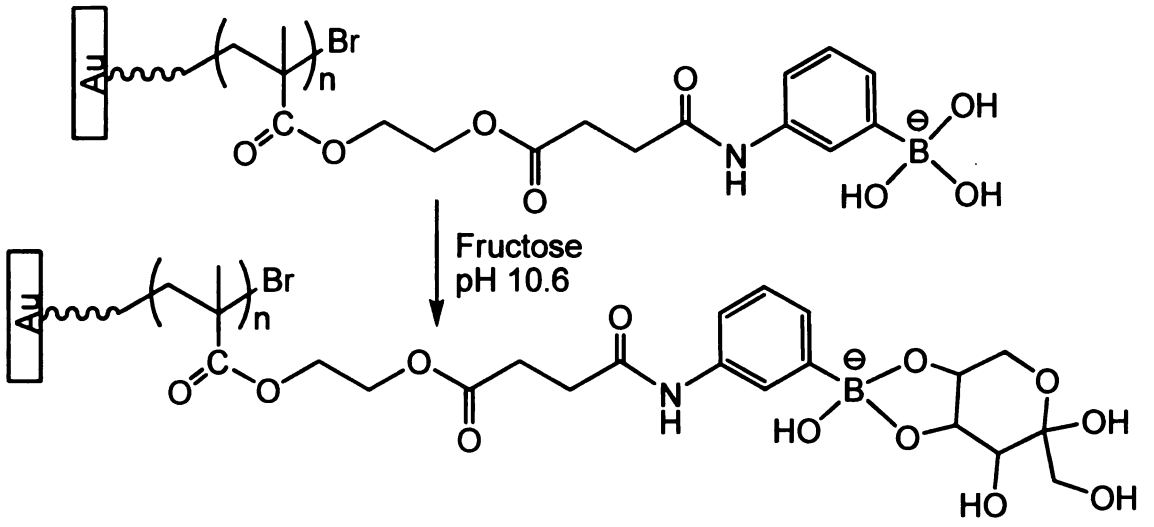

Figure 4.4: Schematic diagram showing fructose binding, under basic conditions, to a gold-coated substrate modified with an APBA-PHEMA film.

4.3.2 Characterization of Fructose Bound to APBA-PHEMA Brushes

Before enriching any glycopeptides using the APBA-PHEMA brushes, fructose, a simple carbohydrate, was bound to the APBA-derivatized polymer film under basic conditions (Figure 4.4) to ensure that these modified plates were able to bind a compound containing *cis*-diols. Substrates modified with APBA-PHEMA brushes were first immersed in a pH 10.6 solution (pH adjusted with 0.125 M NaOH, where the final NaOH concentration is ~1mM) without fructose for 15 min (Figure 4.5a), then rinsed with ethanol and dried under a stream of N_2 prior to obtaining a reflectance FTIR spectrum and an ellipsometric thickness of the film. Subsequently, the films were immersed in a 0.01 M fructose solution, pH 10.6 for 15 min (Figure 4.5b) and rinsed with ethanol before again obtaining an IR spectrum and ellipsometric thickness. This procedure was employed to ensure that the reflectance FTIR spectra and film thicknesses before and after fructose binding were being compared under the same conditions. The inset of Figure 4.5 shows the FTIR difference spectrum between APBA-PHEMA films before

and after exposure to fructose. There is an increased absorbance in the region from 3550 – 3000 cm^{-1}, which may be due to the increase in hydroxyl groups present in fructose. Sharp peaks in the subtraction spectrum at 1174 and 1066 cm^{-1} may also stem from C-O-C stretches in fructose. The thickness of the APBA-PHEMA film, initially 82 nm, increased 5 nm after immersion in the fructose solution. Taken together, these results provide evidence for fructose binding, but the amount of binding is not extensive. The high density of the polymer brushes may limit the ability of fructose to diffuse to boronic acid sites, thus decreasing the binding of the *cis*-diol-containing carbohydrate. Longer incubation times did not appear to increase fructose binding.

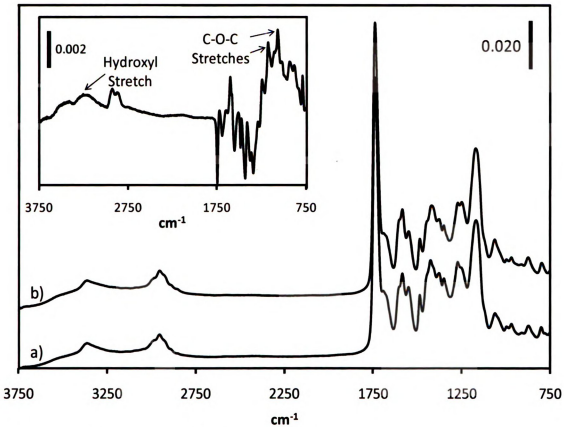

Figure 4.5: Reflectance FTIR spectra of a) a gold-coated substrate modified with APBA-PHEMA (the substrate was immersed in a pH 10.6 solution for 15 min prior to taking the spectrum), and b) fructose bound to the same APBA-PHEMA-modified substrate in pH 10.6 solution. The inset shows the subtraction of the spectrum of APBA-PHEMA film (a) from the spectrum of the fructose-bound film (b).

4.3.3 Analysis of Horseradish Peroxidase Digests Using MALDI-MS

Initial attempts to enrich glycopeptides on APBA-PHEMA-modified MALDI plates focused on tryptic digests of horseradish peroxidase (HRP), which contains nine *N*-linked glycosylation sites (Figure 4.6). However, only eight glycopeptides result from tryptic digestion because one peptide contains two glycosylation sites. This protein also contains four disulfide bonds, which were reduced using DTT and iodoacetamide. Table 4.1 lists the sequences of the eight *N*-linked glycopeptides, the composition of their oligosaccharide chains, and their experimental *m/z* values, $[M+H]^+$, as reported

previously by Wuhrer et al.[28] Unfortunately, two glycopeptides (69-92 and 214-236) cannot be detected using the vMALDI LTQ XL because their $[M+H]^+$ *m/z* values (4058.4 and 4986.2, respectively) exceed the upper mass limit of the mass analyzer of this instrument (4000). However, this should not affect the enrichment or analysis of the other glycopeptides using the APBA-PHEMA-modified MALDI plates.

```
 31   QLTPTFYDNS   CPN#VSNIVRD   TIVNELRSDP    60
 61   RIAASILRLH   FHDCFVNGCD   ASILLDN#TTS    90
 91   FRTEKDAFGN   ANSARGFPVI   DRMKAAVESA   120
121   CPRTVSCADL   LTIAAQQSVT   LAGGPSWRVP   150
151   LGRRDSLQAF   LDLANANLPA   PFFTLPQLKD   180
181   SFRNVGLN#RS  SDLVALSGGH   TFGKNQCRFI   210
211   MDRLYN#FSNT  GLPDPTLN#TT  YLQTLRGLCP   240
241   LNGN#LSALVD  FDLRTPTIFD   NKYYVNLEEQ   270
271   KGLIQSDQEL   FSSPN#ATDTI  PLVRSFAN#ST  300
301   QTFFNAFVEA   MDRMGN#ITPL  TGTQGQIRLN   330
331   CRVVNSNS
```

Figure 4.6: Amino acid sequence of horseradish peroxidase.[28] *N*-glycosylation sites are labeled with bold and italic type and with a pound (#) sign. Cysteine residues involved in disulfide bonds are underlined and tryptic cleavage sites are in bold.

The conventional MALDI mass spectrum (Figure 4.7a) of 5 pmol of HRP digest in H_2O shows the presence of five glycosylated peptides with $[M+H]^+$ *m/z* values of 1843, 3355, 3607, 3673, and 3896. While not listed in Table 4.1, the peak at *m/z* 3896 is due to the peptide sequence LHFHDCFVNGCDASILLDN#TTSFR, but the glycan has only three hexose units instead of four.[28] Although the conventional mass spectrum shows signals due to several of the glycopeptides in the HRP digest, enrichment of the HRP digest using an APBA-PHEMA-modified MALDI plate aids in increasing signal-to-noise ratio (S/N) of these glycopeptides, as well as decreasing the presence of some nonglycosylated peptides and other contaminants (Figure 4.7b). Unfortunately, the mass spectrum in Figure 4.7b has a relatively low signal-to-noise ratio and several signals due

to nonglycopeptides are still present. Relative to the conventional MALDI mass spectrum, the S/N increased for the glycopeptides at *m/z* of 3355, 3673, and 3896, and remained the same for the other two glycopeptides identified in the mass spectrum, at *m/z* values of 1843 and 3607. Figure 4.7 gives the S/N values for these five glycopeptides. The relatively short HRP incubation time (15 min) may account for the absence of the other glycopeptides described in Table 4.1, as well as the low S/N ratio. Following incubation, the modified MALDI plates were briefly rinsed with ethanol and then dried before eluting with 0.1% TFA and addition of the matrix. Perhaps a more thorough rinsing would result in the removal of the nonglycosylated species seen in Figure 4.6b. It should also be noted that conventional MALDI analysis of 1 pmol of digested HRP in H_2O yielded a mass spectrum with an S/N of 31.4 for the most intense peak; whereas the most intense peak in the conventional MALDI mass spectrum of 5 pmol of HRP in H_2O (Figure 4.7) has an S/N of 24. This suggests that the increased amount of digest reagents and salt present in a 5 pmol of HRP digest sample may decrease the S/N of the mass spectra, as well as interfere with the enrichment of glycopeptides from the digest.

Table 4.1: *N*-linked glycopeptides present in a tryptic HRP digest. The oligosaccharide structure of each glycopepdide is shown, along with its $[M+H]^+$ *m/z* value. $N^{\#}$ represents the *N*-linked glycosylation site on asparagine residues. Hex stands for hexose, HexNAc for *N*-acetylhexosamine, dHex for deoxyhexose, and Pent for pentose.

Sequence Number	Peptide Sequence	Glycan Structure[28]	*m/z*
31-49	QLTPTFYDNSCPN$^{\#}$VSNIVR	$Hex_3HexNAc_2dHex_1Pent_1$	3323
69-92	LHFHDCFVNGCDASILLDN$^{\#}$TTSFR	$Hex_4HexNAc_2dHex_1Pent_1$	4058
184-189	NVGLN$^{\#}$R	$Hex_3HexNAc_2dHex_1Pent_1$	1844
214-236	LYN$^{\#}$FSNTGLPDPTLN$^{\#}$TTYLQTLR	$Hex_3HexNAc_2dHex_1Pent_1$	4986
237-254	GLCPLNGN$^{\#}$LSALVDFDLR	$Hex_3HexNAc_2dHex_1Pent_1$	3607
272-294	GLIQSDQELFSSPN$^{\#}$ATDTIPLVR	$Hex_3HexNAc_2dHex_1Pent_1$	3674
295-313	SFAN$^{\#}$STQTFFNAFVEAMDR	$Hex_3HexNAc_2dHex_1Pent_1$	3355
314-328	MGN$^{\#}$ITPLTGTQGQIR	$Hex_3HexNAc_2dHex_1Pent_1$	2612

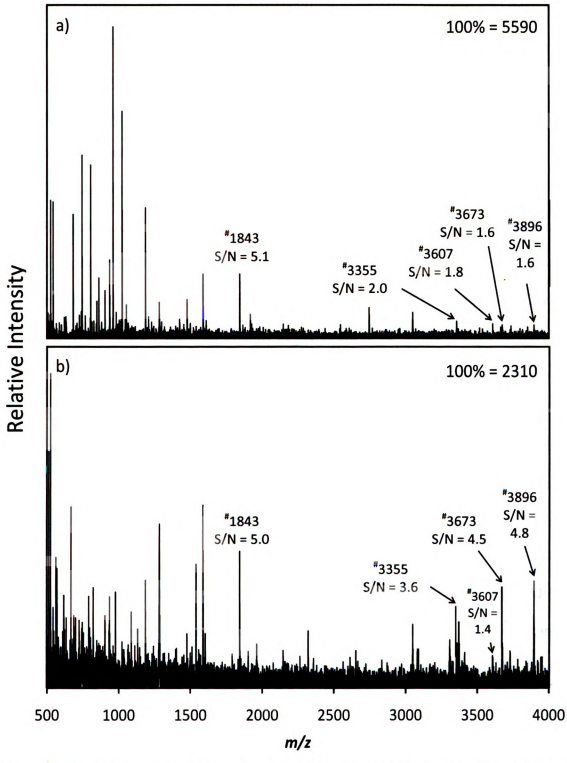

Figure 4.7: Positive ion MALDI mass spectra of 5 pmol of HRP digest analyzed using a) conventional MALDI-MS, and b) an APBA-PHEMA-modified plate with H_2O as the loading solution and rinsing with ethanol. In b), glycopeptides were eluted with 1 μL of 0.1% TFA, followed by addition of matrix prior to analysis. Pound signs (#) represent signals due to glycopeptides.

Most studies of enrichment of glycopeptides using phenylboronic acid have been performed under basic conditions. Under alkaline conditions phenylboronic acid exists in a tetrahedral form, instead of its trigonal form, and while *cis*-diol-containing compounds may bind to phenylboronic acid in either of its forms, they are more likely to bind to phenylboronic acid in the tetrahedral form.[29,30] Figure 4.8a shows the conventional MALDI mass spectrum of 2 pmol of HRP digest in 0.1 M ammonium bicarbonate, where 43 μL of digest stock solution (pH ~3) was diluted in 184 μL of 0.1 M NH_4HCO_3 to raise the pH. Figure 4.8b displays the mass spectrum of the same digest/NH_4HCO_3 solution that was enriched on the APBA-PHEMA plate. While the higher pH of the NH_4HCO_3 solution should aid in the covalent binding of glycopeptides to aminophenylboronic acid-functionalized polymer brushes, these basic conditions result in no signals due to glycopeptides. Conventional MALDI analysis of 2 pmol of HRP in 0.1 M ammonium bicarbonate shows significantly greater noise than the conventional mass spectrum of HRP diluted in deionized water (Figure 4.7a), and this noise may mask the signals due to several glycosylated and nonglycosylated peptides. The high salt content likely suppresses signals.[31] Unfortunately, Figure 4.8b suggests that the tryptic HRP glycopeptides were not enriched from the ammonium bicarbonate solution using APBA-PHEMA brushes, as no signals from any of the peptides listed in Table 4.1 can be identified. Perhaps a lower concentration of ammonium bicarbonate in the loading solution would decrease noise present in the conventional analysis and not interfere as much with the enrichment process. Xu and coworkers used a 50 mM NH_4HCO_3 solution for enrichment of glycopeptides using their APBA-functionalized mesoporous silica beads.[24] Other works use a phosphate buffer as the loading solution at a pH of either 7.4

or 9,[27] which could be better because the binding conditions would be less harsh than in a basic solution. Recently, Laštovičková and coworkers determined that when a 1 mg/mL solution of ribonuclease B, a common glycoprotein, is diluted in a 20 mM ammonium bicarbonate solution and is analyzed by MALDI-MS, the intensity and resolution of this protein peak decreases significantly.[32] This decrease in intensity and resolution occurs with a number of different matrices: 2,5-dihydroxybenzoic acid (DHB), 2,4,6-trihydroxyacetophenoe (THAP), α-cyano-4-hydroxycinnamic acid (α-CHCA), or sinapinic acid as the matrix. However, the authors show that the use of binary matrices helps to alleviate this problem, specifically the combination of DHB/α-CHCA, DHB/THAP, and DHB/sinapinic acid.[32] It would be worthwhile to compare the mass spectra of the enrichment of HRP in NH_4HCO_3 with DHB as the matrix, as shown above, with the same enrichment, only using one of these binary matrices.

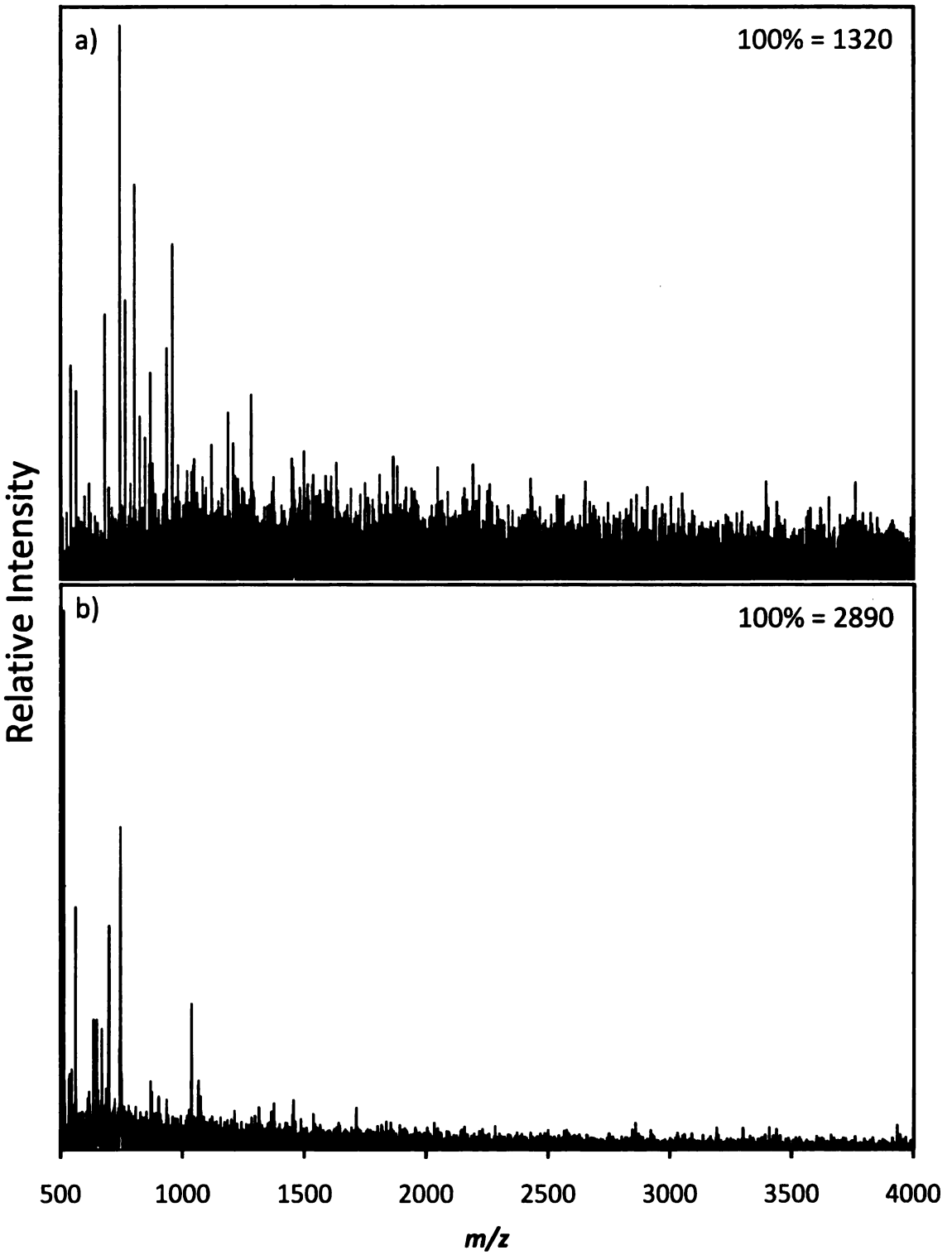

Figure 4.8: Positive ion MALDI mass spectra of 2 pmol of HRP digest in 0.1 M ammonium bicarbonate obtained using a) conventional analysis, and b) binding to APBA-PHEMA-modified gold-coated plates that were rinsed with 0.1 M NH_4HCO_3, followed by ethanol, prior to elution of glycopeptides by deposition of 1 µL 0.1% TFA, addition of matrix solution, and MALDI-MS.

4.4 Conclusions

Poly(2-hydroxyethyl methacrylate) brushes were successfully derivatized with 3-aminophenylboronic acid to yield APBA-PHEMA-modified gold-coated substrates. These polymer films bind at least small amounts of fructose, a simple *cis*-diol-containing carbohydrate. When used as MALDI substrates for on-plate enrichment of glycopeptides from a protein digest, the APBA-PHEMA films marginally improved the signal-to-noise ratios of some of the glycopeptides from an HRP digest in water, although a large number of peaks due to nonglycosylated species are still present in the MALDI mass spectra. Even though phenylboronic acids bind *cis*-diol-containing compounds more completely under basic conditions, enrichment of glycopeptides from an HRP digest in ammonium bicarbonate resulted in no signals due to glycosylated peptides. If the optimal binding and matrix conditions can be determined, APBA-PHEMA-modified MALDI plates have the potential for rapid and simple on-plate enrichment of glycopeptides.

4.5 References

[1] Helenius, A.; Aebi, M. *Carbohydrates and Glycobiology*, **2001**, *291*, 2364-2369.

[2] Rudd, P. M.; Dwek, R. A. *Critical Reviews in Biochemistry and Molecular Biology*, **1997**, *32*, 1-100.

[3] Durand, G.; Seta, N. *Clinical Chemistry*, **2000**, *46*, 795-805.

[4] Paulson, J. C. *Trends in Biochemical Sciences*, **1989**, *14*, 272-276.

[5] Varki, A. *Glycobiology*, **1993**, *3*, 97-130.

[6] Jaeken, J.; Matthijs, G. *Annual Review of Genomics and Human Genetics*, **2001**, *2*, 129-151.

[7] Freeze, H. H. *Encyclopedia of Biological Chemistry*, **2004**, *2*, 302-307.

[8] Rostenberg, I.; Guizar-Vazquez, J.; Suarez, P.; Rico, R.; Nungaray, L.; Dominguez, C. *Journal of the National Cancer Institute*, **1978**, *60*, 83-87.

[9] Coffman, F. D. *Critical Reviews in Clinical Laboratory Sciences*, **2008**, *45*, 531-562.

[10] Dias, W. B.; Hart, G. W. *Molecular Biosystems*, **2007**, *3*, 766-772.

[11] Saldova, R.; Wormald, M. R.; Dwek, R. A.; Rudd, P. M. *Disease Markers*, **2008**, *25*, 219-232.

[12] Turner, G. A. *Clinica Chimica Acta*, **1992**, *208*, 149-171.

[13] Dell, A.; Morris, H. R. *Carbohydrates and Glycobiology*, **2001**, *291*, 2351-2356.

[14] Hagglund, P.; Larsen, M. R. *Spectral Techniques in Proteomics*, **2007**, 81-100.

[15] Hernández-Borges, J.; Neusüess, C.; Cifuentes, A.; Pelzing, M. *Electrophoresis*, **2004**, *25*, 2257-2281.

[16] Kurogochi, M.; Nishimura, S. *Analytical Chemistry*, **2004**, *76*, 6097-6101.

[17] Zaia, J. *Mass Spectrometry Reviews*, **2004**, *23*, 161-227.

[18] Ullmer, R.; Plematl, A.; Rizzi, A. *Rapic Communications in Mass Spectrometry*, **2006**, *20*, 1469-1479.

[19] Endo, T. *Journal of Chromatography A*, **1996**, *720*, 251-261.

[20] Hirabayashi, J. *Journal of Biochemistry*, **2008**, *144*, 139-147.

[21] Monzo, A.; Bonn, G. K.; Guttman, A. *Trends in Analytical Chemistry*, **2007**, *26*, 423-432.

[22] Satish, P. R.; Surolia, A. *Journal of Biochemical and Biophysical Methods*, **2001**, *49*, 625-640.

[23] Sparbier, K.; Wenzel, T.; Kostrzewa, M. *Journal of Chromatography B*, **2006**, *840*, 29-36.

[24] Xu, Y.; Wu. Z.; Zhang, L.; Lu, H.; Yang, P.; Webley, P. A.; Zhao, D. *Analytical Chemistry*, **2009**, *81*, 503-508.

[25] Yeap, W. S.; Tan, Y. Y.; Loh, K. P. *Analytical Chemistry*, **2008**, *80*, 4659-4665.

[26] Zhang, H.; Li, X.; Martin, D. B.; Aebersold, R. *Nature Biotechnology*, **2003**, *21*, 660-666.

[27] Zhou, W.; Yao, N.; Yao, G.; Deng, C.; Zhang, X.; Yang, P. *Chemical Communications*, **2008**, 5577-5579.

[28] Wuhrer, M.; Hokke, C. H.; Deelder, A. M. *Rapid Communications in Mass Spectrometry* **2004**, *18*, 1741-1748.

[29] James, T. D. *Topics in Current Chemistry* **2007**, *277*, 107-152.

[30] Yan, J.; Springsteen, G.; Deeter, S.; Wang, B. *Tetrahedron* **2004**, *60*, 11205-11209.

[31] Xu, Y.; Bruening, M. L.; Watson, J. T. *Mass Spectrometry Reviews* **2003**, *22*, 429-440.

[32] Laštovičková, M.; Chmelik, J.; Bobalova, J. *International Journal of Mass Spectrometry* **2009**, *281*, 82-88.

Chapter Five: Conclusions and Future Work

The use of ZrO_2-PSS-PAH-modified plates for phosphopeptide enrichment and subsequent identification of phosphorylation sites shows great potential. These metal oxide-modified plates can separate phosphorylated peptides from an unpurified protein digest and are fully capable of phosphopeptide enrichment at the picomolar level. After enrichment using ZrO_2-PSS-PAH-modified plates, the intensity of the phosphorylated peptide peaks from a 2 pmol ovalbumin digest significantly improved, compared with the intensity of these peaks from the conventional MALDI mass spectrum. Additionally, there was little nonspecific binding when using these plates modified with metal oxides. Plates prepared by heating an array of TiO_2 nanoparticles also appear to be promising for enrichment and analysis of phosphopeptides and their phosphorylation sites. These TiO_2-modified plates selectively enriched 125 fmol of a synthetic H_5 phosphopeptide in the presence of 1 pmol of a nonphosphopeptide mixture with a recovery of 69%. Both techniques provide rapid and selective on-plate enrichment of phosphorylated peptides. Further work regarding the ZrO_2-PSS-PAH-modified plates should include examining whether they can enrich phosphopeptides at the low fmol level. It would also be interesting to compare these ZrO_2 plates with other metal oxides such as aluminum oxide. The only samples studied here were synthetic peptides and simple protein digests. For modified plates to have true significance in the area of cancer research or in the study of cellular regulatory mechanisms, they must be capable of enriching phosphopeptides from biological samples, and this merits further investigation.

In an effort to expand the utility of on-plate enrichment, gold substrates modified with poly(acrylic acid) or poly(2-hydroxyethyl methacrylate) films were derivatized with

reduced glutathione in a variety of methods. Unfortunately these glutathione-immobilized films did not bind free GST, perhaps because of the presence of glutathione in the GST sample. Despite desalting and purification of free GST by dialysis, MALDI mass spectra confirmed that some glutathione remained in the sample. The GST initially contained only 60% protein, and purer samples are needed to determine if the presence of glutathione is truly preventing GST from binding to the films. Much work still needs to be completed in this area.

Poly(2-hydroxyethyl methacrylate) brushes were also functionalized with 3-aminophenylboronic acid to provide gold-coated substrates for on-plate enrichment of glycopeptides prior to analysis by MALDI-MS. These modified films bind small amounts of simple *cis*-diol-containing carbohydrates, specifically fructose. Initial studies of the utility of these APBA-PHEMA-modified surfaces involved the enrichment of either 2 or 5 pmol of glycoproteins from digested HRP. While these derivatized polymer brushes improved the signal-to-noise ratio for some glycopeptides in an HRP digest in water, a significant amount of nonspecific binding of nonglycosylated species was apparent in the MALDI mass spectra. Even though phenylboronic acids bind *cis*-diol-containing compounds more completely under alkaline conditions, enrichment of glycopeptides from an HRP digest in ammonium bicarbonate resulted in no detectable signals due to glycosylated peptides. Loading and rinsing solutions as well as incubation times need to be optimized for the covalent binding between *cis*-diol-containing glycopeptides and APBA-functionalized brushes. The use of binary matrices may improve the intensity and resolution of glycopeptides peaks in the presence of salts and other contaminants. With optimal binding conditions, the APBA-PHEMA-modified

MALDI plates might provide a useful method for rapid and simple on-plate glycopeptides enrichment.